REDESIGN OF THE STANDARD MACINTOSH LARYNGOSCOPE TO IMPROVE GLOTTIC VISUALIZATION DURING ENDOTRACHEAL INTUBATION

A THESIS
SUBMITTED TO THE FACULTY OF
UNIVERSITY OF MINNESOTA
BY

YASHOVARDHAN SAND

IN PARTIAL FULFILLMENT OF THE REQUIREMENTS
FOR THE DEGREE OF
[MASTER OF SCIENCE]

ARTHUR G. ERDMAN

AUGUST 2016

ACKNOWLEDGEMENTS

This thesis was only possible because of the perfect support structure I had throughout my time as a graduate student, and caffeine. I would like to thank Dr. Arthur Erdman who guided me through this long arduous journey and motivated me at the necessary times. I have learned a lot from him; I hope his wisdom has rubbed off on me. This project would not have been possible without Dr. Mojca Konia. Her guidance and insight have been invaluable. She was a major part of the entire process and I am truly indebted to her. I would also like to thank Jack Stubbs who took me on as a graduate student and believed in my engineering abilities, and gave me the opportunity to work on this project. His practical outlook through his advisement was refreshing beneficial. I would also like to acknowledge CREST and SimPORTAL for their resources and funding.

My roommates and friends through the years have been a major part of my graduate school experience. A special mention goes out to Arjun Dubhashi who pushed me through the roughest of patches; his invaluable inputs on my research and belief in my project helped me greatly. Kshitiz Thapa gave me company throughout the final phase of the project and spent the long days and late nights keeping me motivated to finish the project. Anshul Gupta and Indrajith Premanath get special mentions for their inputs and unorthodox methods of motivating me. Countless hours were spent on the phone with Shruti Sharma; thank you for being there and believing in me.

My parents have been the most significant part of my life. I would like to thank them for their support, love, and for never giving up on me. They have helped me fight through the low points and encouraged me during the high points. My sister's unique words of wisdom guided me through this process and she taught me to never give up.

DEDICATION

This thesis is dedicated to those who were, are, and will be.

ABSTRACT

Direct laryngoscopy is a procedure which allows for the visualization of the glottis during the process of endotracheal intubation (placement of the endotracheal tube into the trachea). The primary device used for this procedure is called the laryngoscope. The laryngoscope consists of a handle and a blade. During insertion of the blade, the curvature of the tongue is followed and the tip of the blade is inserted into the vallecula. In the vallecula resides the hyoepiglottic ligament, which connects the anterior surface of the epiglottis and the body of the hyoid bone. Different types of laryngoscopes exist, with the two most frequently used being the Macintosh and the Miller laryngoscope. The two laryngoscopes differ in the shape of the blade, one being curved (mac) and the other one straight (miller). During laryngoscopy with the Macintosh laryngoscope, the tip of the blade is used to push on the hyoepiglottic ligament, which lifts the epiglottis up and allows for exposure of glottis. In this procedure, the forces exerted on tissues can be significant (up to 50 N) and there can be complications as a result of the forces exerted on the soft tissues of the oropharynx and larynx. These complications can be esophageal intubation, hypoxia, and nerve damage. Furthermore, difficult intubations result in increased intubation time and a higher number of intubation attempts. The most common hurdle is the inability to successfully complete the endotracheal intubation. One of the reasons why the endotracheal intubation may not be successful is the inability to visualize the glottic opening. The level of intubation difficulty is based on the extent of the view of the glottis obtained during intubation and is classified into four grade views.

A new type of laryngoscope blade, which looks like the Macintosh blade, but adds features that would allow to mitigate the aforementioned factors, was designed. The primary goal of the design was to provide a mechanism which could deliver a more anterior direct laryngoscopy view and allow for an enhanced lift of the epiglottis. This would be accomplished by adding a feature which would compress the body of the tongue and also lift the tip of the epiglottis more than the conventional Macintosh blade. The new design, unlike current blades, consists of three blade segments—one fixed and two movable. The

fixed blade segment is the largest, with one end fixed to the laryngoscope handle and the other hinged to the first movable segment. The first movable segment is the second largest segment of the blade, and at one end is hinged to the fixed segment and at the other it is hinged to the third segment. The middle segment is designed to compress the tongue and push it out of the way to improve vocal cord visualization. The third (smallest) segment is the blade tip which is hinged at one end to the middle second segment. This is used to enter the vallecula and push against the hyoepiglottic ligament to lift the epiglottis. The design is purely mechanical with no electrical or electronic components.

A prototype was built and tested on manikins by anesthesiologists to primarily assess the change in the grade view of intubation by the flexible design. To evaluate the efficacy of the blade, a poor intubation grade view was forced and then without applying any incremental lifting forces, the mechanism was engaged to produce a final grade view. A qualitative pressure distribution was mapped for each attempt, and was compared to that obtained by a Macintosh blade. The improvement in the view with the flexible design was significant ($p=0.000038$). The pressures applied on the manikin airway by the flexible laryngoscope was less than that applied by the Macintosh laryngoscope to successfully intubate.

The design of the flexible laryngoscope allowed for an improvement in the grade view of intubation and reduced the lifting forces applied on the airway. The built device proved that a flexible design can assist in difficult intubations.

TABLE OF CONTENTS

1. INTRODUCTION 1
1.1 UPPER AIRWAY ANATOMY 1
1.2 ENDOTRACHEAL INTUBATION 3
1.3 PROCESS OF ENDOTRACHEAL INTUBATION 5
1.4 OBJECTIVE OF THE THESIS 8

2. ENDOTRACHEAL INTUBATION DEVICES 10
2.1 CONVENTIONAL LARYNGOSCOPES 10
2.1.1 Laryngoscope Blade Features 10
2.2 CURVED LARYNGOSCOPES 11
2.2.1 Macintosh Laryngoscope 11
2.3. STRAIGHT BLADES 13
2.3.1 Miller Laryngoscope 13
2.3.2 Other Straight Blade Laryngoscopes 14
2.4 BELSCOPE 15
2.5 LEVERING TIP LARYNGOSCOPE 16
2.6 FLEXIBLADE™ 17
2.7 MISCELLANEOUS BLADES 18
2.8 PEDIATRIC BLADES 19
2.9 LARYNGOSCOPE LIGHTING SOURCES 20
2.10 LARYNGOSCOPE DISPOABILITY 21
2.11 VIDEO-LARYNGOSCOPES 22

3. LITERATURE REVIEW 24
3.1 CORMACK LEHANE VIEWS 24
3.2 LARYNGEAL EXPOSURE AND INTUBATION FORCES 26
3.3 DENTAL AND SOFT TISSUE DAMAGE 27
3.4 MACINTOSH LARYNGOSCOPE VS. OTHER INTUBATION DEVICES 28
3.5 REPEATED INTUBATION ATTEMPTS 33
3.6 ANATOMY MAPPING 34

4. PRELIMINARY TESTING 36
4.1 FORCE AND MANIKIN STUDY 36
4.2 REENGINEERING OF THE LARYNGOSCOPE 40
4.2.1 Design Rev. 1 41
4.2.2 Design Rev. 2 42
4.2.3 Pressure Film—A qualitative force distribution experiment 44
4.3 CONCLUSION 51

5. THEORY AND DEVICE DESIGN 52
5.1 DESIGN THEORIES 52
5.2 CURRENT DESIGN THEORY—MULTILOOP SYNTHESIS 55
5.2.1 Design Synthesis 56
5.2.2 Mechanism synthesis 58
5.2.3 Triggering Mechanism 67
5.2.4 Mechanism Analysis 69
5.3 DESIGN EVOLUTION 73
5.3.1 Design 1.0 73

5.3.2 Design 2.0 75
5.3.3 Design 2.1 79
5.4 DESIGN 3.0 82
5.4.1 Design 3.1 89
5.4.2 Design 3.1.1 93
5.5 DESIGN 4.0 [FINAL DESIGN] 96

6. DEVICE VALIDATION 99
6.1 EXPERIMENTAL SET-UP 99
6.2 PROCEDURE 100
6.3 RESULTS AND DISCUSSION 102
6.3.1 Cormack-Lehane Grade Views 102
6.3.2 Force/Pressure (Preliminary) 105
6.3.3 Post intubation survey 108
6.4 LIMITATIONS OF THE STUDY 109

7. CONCLUSION AND FUTURE WORK 110

BIBLIOGRAPHY 111

LIST OF TABLES

Table 1. Airway dimensions [52] 35
Table 2. t-Test Results for Force and Torque on Macintosh Blade 38
Table 3. Dimensions and rotations for design 1.1 77
Table 4. Pins and fasteners used in device 78
Table 5. Dimension for design 3.0 84
Table 6. Tip deflections 97
Table 7. Demographics of participating experts 101
Table 8. Anesthesiologist 1 102
Table 9. Anesthesiologist 2 102
Table 10. Anesthesiologist 3 103
Table 11. Anesthesiologist 4 103
Table 12. Anesthesiologist 5 103
Table 13. Anesthesiologist 6 104
Table 14. Survey outcome 108

LIST OF FIGURES

Figure 1. Upper airway anatomy [46] 1
Figure 2. Sagittal view (left), posterior view (right) [45] 2
Figure 3. Vocal cords [47] 3
Figure 4. Tracheostomy tube inserted [47] 4
Figure 5. Endotracheal tube (A), cuff inflation tube (B), trachea (C), esophagus (D) [48] 4
Figure 6. Head positions [5] 6
Figure 7. Laryngoscopy using a curved blade (left), straight blade (right) [49] 7
Figure 8. Endotracheal tube (ETT), with the stylet inserted [45] 8
Figure 9. Standard Laryngoscope Design [45] 11
Figure 10. American 4 vs. German 4 Macintosh Blades [50] 12
Figure 11. English vs. Standard Macintosh Laryngoscope [45] 12
Figure 12. Improved Vision Laryngoscope (left); Improved Vision vs. Macintosh (right) [45] 13
Figure 13. Miller Laryngoscope [51] 13
Figure 14. Flagg blade [45] 14
Figure 15. Snow blade [45] 14
Figure 16. Phillips blade [45] Figure 17. Henderson blade [45] 15
Figure 18. Belscope (left), Belscope during intubation (right) [45] 16
Figure 19. Levering tip laryngoscope [52] 17
Figure 20. Degree of articulation of the McCoy laryngoscope (levering tip) [34] 17
Figure 21. Flexiblade, BC=Flexible intermediate section, R=rod, T=triggering lever, P=pusher [12] 18
Figure 22. Patil handle with a Macintosh blade in multiple configurations [53] 19
Figure 23. The Diaz pediatric laryngoscope [43] 20
Figure 24. Modified CL grade views [19] 25
Figure 25. Modified CL Grade Views Developed by Cook [20] 26
Figure 26. A demonstrates the correct use of a laryngoscope; B shows a case there the upper incisors are used as a fulcrum during intubation (incorrect technique) [26] 28
Figure 27. The laryngoscopes mounted with the pressure films [27] 29
Figure 28. Normal airway (left), Difficult airway (right) [31] 31
Figure 29. Airway dimensions [35] 34
Figure 30. Instrumented Laryngoscope (left), Force resistive sensor (right) [57] 36
Figure 31. Arduino Uno [58]
Figure 32. Voltage divider circuit set up for one sensor; schematic developed using Frtizing 37
Figure 33. TruCorp AirSim Standard (left), Laerdal Airway Management Trainer (middle), and VBM Air Management Simulator Bill I (right) 37
Figure 34. Toque applied on each Simulator 39

Figure 35. Subjective Force Applied 39
Figure 36. First revision of the 3D printed laryngoscope 41
Figure 37. Design rev. 2 with slots for compliant sensors 42
Figure 38. Arduino Mega with a shield. Voltage divider circuits for five sensors soldered onto the shield. 43
Figure 39. Macintosh laryngoscope blade mounted with Pressurex-micro pressure films 44
Figure 40. Top view of blade with pressure film 46
Figure 41. Original image and Gaussian blurred of the top film 46
Figure 42. Contour plot of top surface film 46
Figure 43. Bottom view of blade with pressure film 47
Figure 44. Original image and Gaussian blurred of the bottom film 47
Figure 45. Contour plot of top surface film 48
Figure 46. Top view of blade with pressure film (CREST manikin) 48
Figure 47. Original and Gaussian blurred version of the top film (CREST manikin) 49
Figure 48. Contour plot of top film (CREST manikin) 49
Figure 49. Bottom view of blade with pressure film (CREST manikin) 49
Figure 50. Original and Gaussian blurred version of bottom film (CREST manikin) 50
Figure 51. Contour plot of bottom film (CREST manikin) 50
Figure 52. Sagittal view of the upper airway during laryngoscopy [36] 53
Figure 53. Hyoid bone movement angle MIT (left), eye-line displacement angle EIT (right) [36] 54
Figure 54. Schematics of the inversions of the Watt and Stephenson six-bar topologies 57
Figure 55. Schematic of the six bar mechanism with links. Angles labelled represent the rotations of the respective links 59
Figure 56. Ground pivots and precision points 60
Figure 57. Six-bar chain wireframe at precision position 1 and precision position 3 67
Figure 58. Schematic of a four-bar crank slider chain 68
Figure 59. Schematic of the complete mechanism 68
Figure 60. Wireframe of entire mechanism in the initial and final state; mechanism is to scale 69
Figure 61. Transmission angles in a Stephenson I mechanism 70
Figure 62. Transmission angle for a crank slider mechanism 71
Figure 63. Design revision one of the flexible laryngoscope show in the standard state (left), at precision point 1 (center), and at precision point 3 (right) 73
Figure 64. 3D printed model. Right view (left), left view (center), maximum input angle orientation (right) 74
Figure 65. Two channel handle 75
Figure 66. (a) Precision point 1, (b) Precision point 2, (c) Precision point 3, (d) Isometric view 76

Figure 67. All numbered links and coordinate system used for mechanism synthesis. Refer to figure 59 for schematic drawing 76
Figure 68. Laryngoscope blade with pivots numbered 77
Figure 69. Machine screw (left), dowel pin (right) [64] 78
Figure 70. (a) Blade in initial state, (b) Blade in final state 80
Figure 71. 3D printed model at precision position 1 and precision position 3 81
Figure 72. Broken laryngoscope (left), 3D printed model with failure locations highlighted 81
Figure 73. Approximate length of the blade middle segment [35] 84
Figure 74. Blade in initial state (left), blade completely engaged (center), blade in collapsed state (right) . 86
Figure 75. Transmission angles through the motion of the mechanism 86
Figure 76. Mechanical advantage of the mechanism 87
Figure 77. Joint forces for all 8 joints in the mechanism. Refer to figure 68 for joint location 88
Figure 78. Failure locations highlighted in both tested devices 89
Figure 79. Design 3.1 with the fixed blade segment fixed to the handle 90
Figure 80. Pressure film on device 90
Figure 81. Failure region 91
Figure 82. (a) Stress distribution, (b) Critical stress location at junction between main body and the middle blade segment, (c) Stress on higher order joint, (d) blade deformation 92
Figure 83. Reinforced middle blade segment 93
Figure 84. AirSim manikin used for testing 93
Figure 85. Blade 1 failure location 94
Figure 86. Blade 2 failure location 94
Figure 87. (a) Stress distribution, (b) critical stress location at pivot between main blade body and middle segment, (c) stress on higher order joint, (d) deformation 95
Figure 88. Final blade design with pivots hidden 97
Figure 89. (a) Stress distribution, (b) reduced stress at pivot, (c) stress on input link, (d) total deflection ... 98
Figure 90. Experimental set-up 99
Figure 91. Initial and Final grade view 104
Figure 92. (Top) Coordinate system on the pressure film for the Macintosh laryngoscope; (bottom) coordinate system for pressure film for the flexible laryngoscope 106
Figure 93. (Top) Average pressure distribution for all Macintosh blade intubations, (bottom) average pressure distribution for flexible blade intubations 107
Figure 94. Pressure distribution on the flexible blade 107

1. INTRODUCTION

Endotracheal intubation is the placement of a flexible tube (endotracheal tube) into the trachea through the mouth. This is generally done post anesthesia for lung ventilation, administration of drugs, and prevention of airway obstruction. A mechanical ventilator is then attached to the open end of the endotracheal tube to regulate the breathing of a patient and to maintain appropriate vitals during a procedure. The endotracheal tube is inserted in the trachea as soon as possible, after the anesthesia is administered. The process of clearing out the upper airway to gain sight of the vocal chords to insert the tube is known as laryngoscopy. Laryngoscopy primarily is performed using a laryngoscope; a conventional laryngoscope consists of a rigid blade with a light and handle with a battery to power the light.

1.1 UPPER AIRWAY ANATOMY

The airway starts from the nose and ends in the bronchioles in the lungs. The upper airway is the primary region of focus in endotracheal intubation. The upper airway consists of the nose, pharynx, and larynx. The upper airway anatomy is depicted in the figure below.

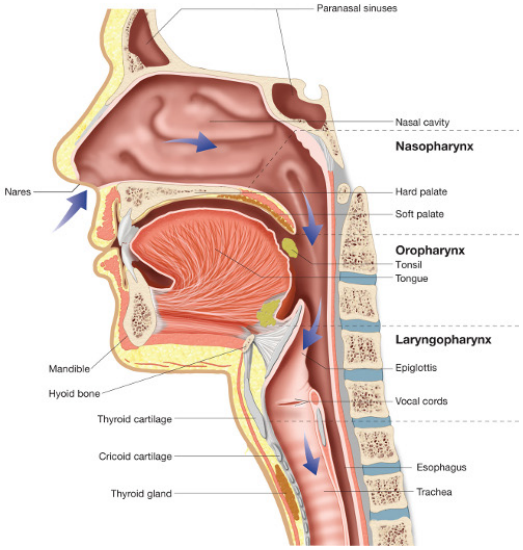

Figure 1. Upper airway anatomy [46]

The nose is used in respiration, humidification, olfaction, and filtration. There is no specific function of the nose in endotracheal intubation since the endotracheal tube is inserted through the mouth. The pharynx is the 12-15 cm long passage starting from the base of the skull to the level of the cricoid cartilage. It is further divided into three regions namely, nasopharynx, oropharynx, and laryngopharynx. Nasopharynx is the primary area for respiration and starts from the opening of the Eustachian tubes and extends down to the edge of the soft palate. The oropharynx's function is digestion—it extends from below the soft palate till the superior edge of the epiglottis. The laryngopharynx ranges from the superior edge of the epiglottis till the sixth cervical vertebrae, where it becomes continuous with the esophagus. The most critical area in intubation is the larynx; it consists of the epiglottis, arytenoids, the vocal chords, and the glottis.

The larynx lies between the third and sixth vertebrae opposite the neck and is at the intersection of the opening of the trachea and esophagus. It functions as the organ of phonation and only allows air to enter the trachea. The hyoid bone is a U-shaped bone that anchors the larynx during respiratory movement.

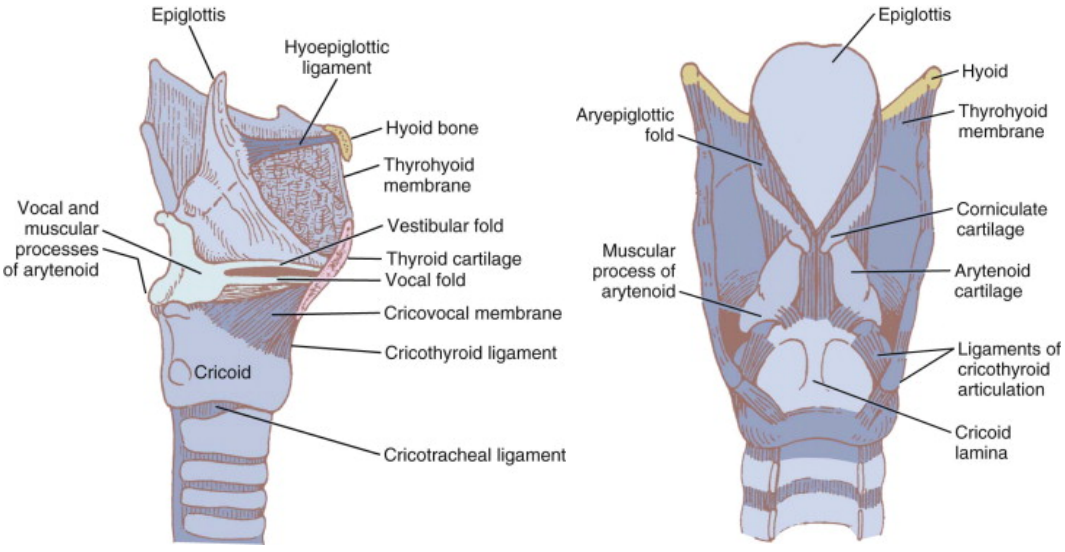

Figure 2. Sagittal view (left), posterior view (right) [45]

The epiglottis is leaf-shaped and primarily composed of cartilage; it is between the base of the tongue and the larynx. The concave anterior surface of the epiglottis, in combination with its elevation protects the airway during swallowing. It is attached to the thyroid through the thyroepiglottic ligament and to the hyoid bone through the hyoepiglottic ligament. The membrane covering the anterior surface of the epiglottis extends to the tongue as median glossoepiglottic folds and to the pharynx as the paired lateral pharyngoepiglottic folds. The pouch-like area formed between these folds is known as the vallecula. This is a common area of impaction foreign bodies in the airway.

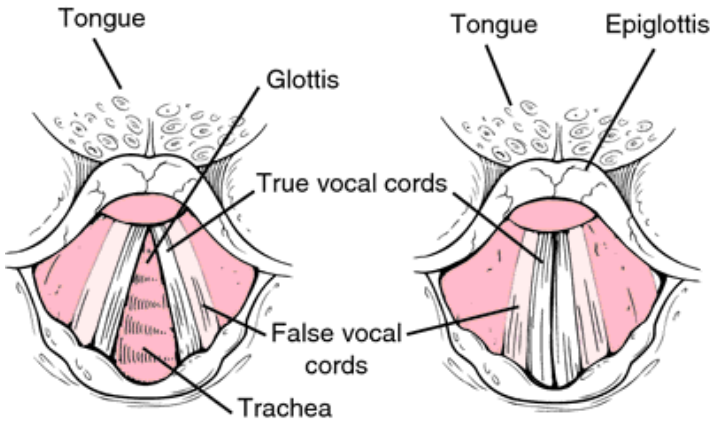

Figure 3. Vocal cords [47]

There are two arytenoid cartilages and are shaped like three-sided pyramids. They are located in the posterior region of the larynx. The vocal cords are attached to the arytenoids. This pair of cartilage aids in vocal cord movement. The vocal cords are responsible for phonation.

1.2 ENDOTRACHEAL INTUBATION

Historically intubation was a means of resuscitation by a tracheostomy. It later progressed with the development of the endotracheal tube—the endotracheal tube is a means of prevention of aspiration from the lungs. Tracheostomy is a surgical procedure where a surgical incision is made in the trachea to establish an airway.

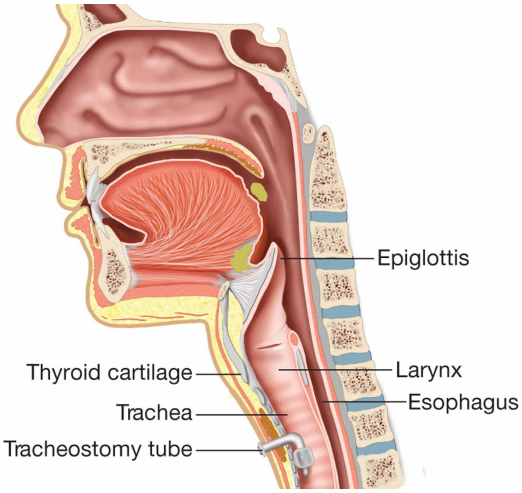

Figure 4. Tracheostomy tube inserted [47]

Endotracheal intubation is now primarily done for resuscitation, pre-hospital care, emergency medicine, intensive care, and for anesthesia. The primary benefits of intubation are controlled ventilation with 100% oxygen, ventilation with elevated airway pressures, lung isolation, administration of medication through anesthetic gases, and the creation of airways by oral, nasal, or tracheal pathways. Endotracheal intubation has been the gold standard for maintaining an active airway and providing ventilation during cardiopulmonary resuscitation (CPR) since it provides the most reliable airway [1]. Diagram of an endotracheal tube inserted into the trachea is shown below.

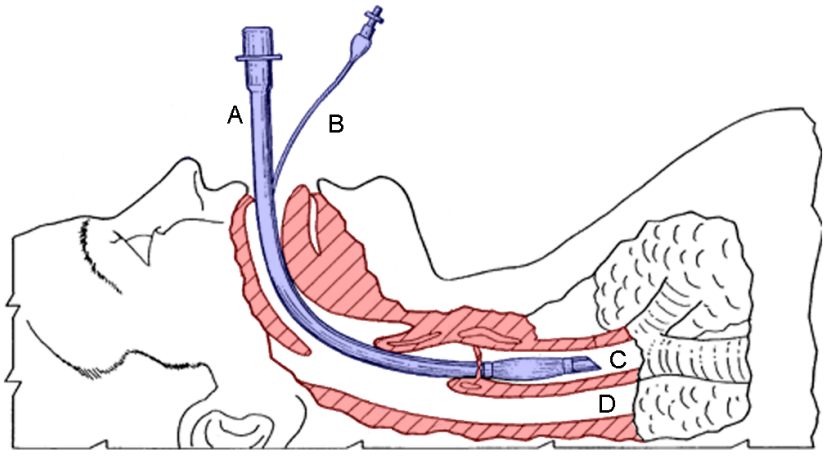

Figure 5. Endotracheal tube (A), cuff inflation tube (B), trachea (C), esophagus (D) [48]

Endotracheal intubation in the pre-hospital environment rarely occurs under favorable conditions and generally patients suffer from severe conditions like cardiopulmonary arrest, airway trauma, traumatic brain injury, shock etc. In most conditions intubation has reduced mortality rates. Intubation leads to controlled ventilation and has been proved to improve the outcome of traumatic brain injuries [1]. Intubation in the emergency department requires a higher degree of skill. Due to the lack of time to evaluate an airway correctly and understand the patient history, the risks are considerable in such situations. It is believed that the benefits outweigh the risks of intubation in the ED. The benefits include airway protection, controlled ventilation, and the provision of a secure airway. Whereas the risks might include esophageal intubation, pulmonary aspiration, and pneumothorax. These risks are more significant in emergency situations where intubation attempts are increased and are not seen in an operating room. Increased intubation attempts lead to potential tissue trauma, hypoxemia, ventilable airways to "cannot ventilate, cannot intubate (CICV)" situations. Difficult intubations are characterized by cases where the number of intubation attempts required exceeds three. Hemodynamic complications increase during the second attempt and exponentially so for every proceeding attempt [2].

Endotracheal intubations in the intensive care unit are done to treat severe respiratory failure and cardiorespiratory resuscitation. In anesthesia, intubations are performed when controlled ventilation, resuscitation, airway access, and duration are part of the surgery plan. The type of endotracheal tube is decided based on type of the surgery and varies across the board.

1.3 PROCESS OF ENDOTRACHEAL INTUBATION

Laryngoscopy is critical in maintaining and establishing an active airway for a patient undergoing endotracheal intubation. The preparation for laryngoscopy requires multiple factors to be taken into account to increase the probability of an easy access to the glottis. Obtaining good glottis visualization is one of the main determining factors for successful and easy intubations. Positioning of the head and neck is the first and in many situations

the most important maneuver to improve the outcome of intubation. In endotracheal intubation the optimal position is known as the "sniffing position". This position is accomplished by the elevation of the head and then its extension at the atlanto-occipital joint. The maneuver is done to align the three axes which define the airway—the axis of the mouth, pharynx, and the larynx [3]. The axis of the mouth is the line tangential to the tongue, the axis of the pharynx is the line joining the posterior surface of the epiglottis and the uvula, and the axis of the larynx is he line perpendicular to the vocal cords. To align these three axes, the head is raised by placing a pillow under it; this resembles a person "sniffing" and hence the expression "sniffing position" was coined [4]. The next step is the opening of the mouth to get access to the airway. There are two maneuvers used to open the mouth prior to laryngoscopy. One method is to apply pressure on the head along the axis of the body causing the mouth to open. The other method known as the scissor maneuver. The thumb of the right hand is used to press down on the lower right molars while the index finger of the same hand is used to press up against the upper right molars to keep the mouth open.

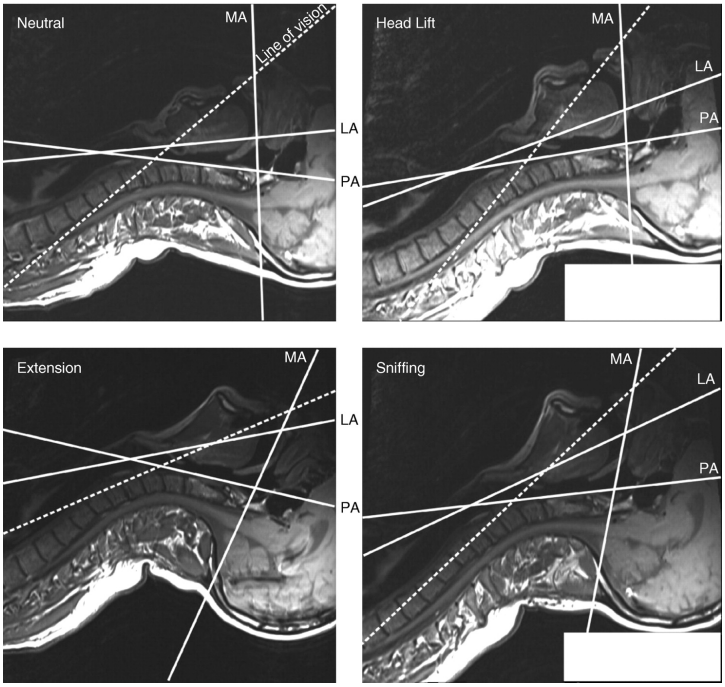

Figure 6. Head positions [5]

The next step of intubation is laryngoscopy; this is the process of providing adequate glottis visualization using a laryngoscope, aiding in the placement of the endotracheal tube into the trachea with minimum effort and time. The primary device used for direct laryngoscopy is the laryngoscope. The laryngoscope is designed to be used with the left hand; the right hand manipulates the endotracheal tube (ETT) during laryngoscopy. Laryngoscope consists of a handle and a blade. The blades have a flange on their left side and a channel on the right side. The light source is attached to the flange. This light source can either be a bulb or a light-emitting diode (LED). The two laryngoscopes differ in the shape of the blade, one being curved (Macintosh) and the other one straight (Miller). They also differ in the technique used during direct laryngoscopy.

The Macintosh blade is used very frequently in the adult population. During insertion of the blade the curvature of the tongue is followed and the tip of the blade is inserted into the vallecula. In the vallecula resides the hyoepiglottic ligament which connects anterior surface of the epiglottis and the body of the hyoid bone. During laryngoscopy with the Macintosh laryngoscope, the tip of the blade is use to push on the hyoepiglottic ligament, which lifts the epiglottis up and allows for glottis exposure. During laryngoscopy with the Miller blade, the blade tip is inserted past the epiglottis and used to lift the epiglottis directly to produce a direct line of sight to the glottis.

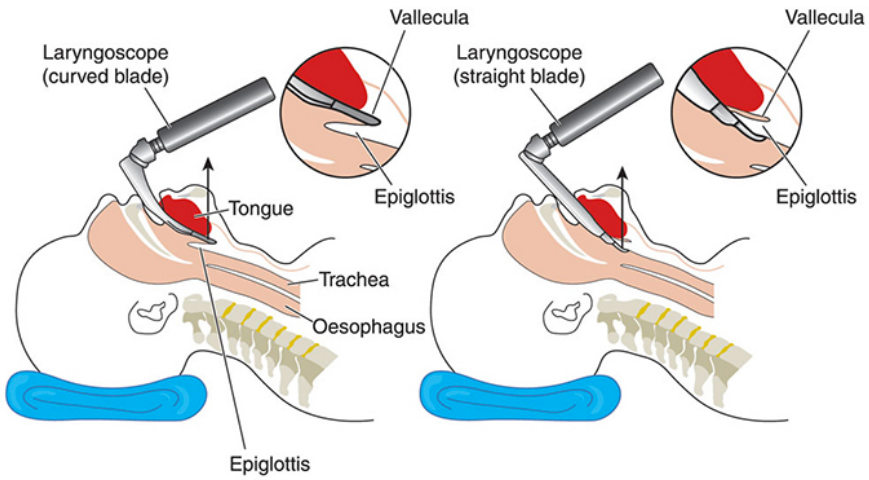

Figure 7. Laryngoscopy using a curved blade (left), straight blade (right) [49]

Once a clear view of the glottis is established the endotracheal tube with a stylet is inserted into the mouth, along the channel of the laryngoscope, and then into the trachea. As soon as tube is passed through the vocal cords, the bulb around the tube tip is inflated and the stylet is removed. A ventilator is attached to the open end of the endotracheal tube to control the patients' breathing for the rest of the procedure.

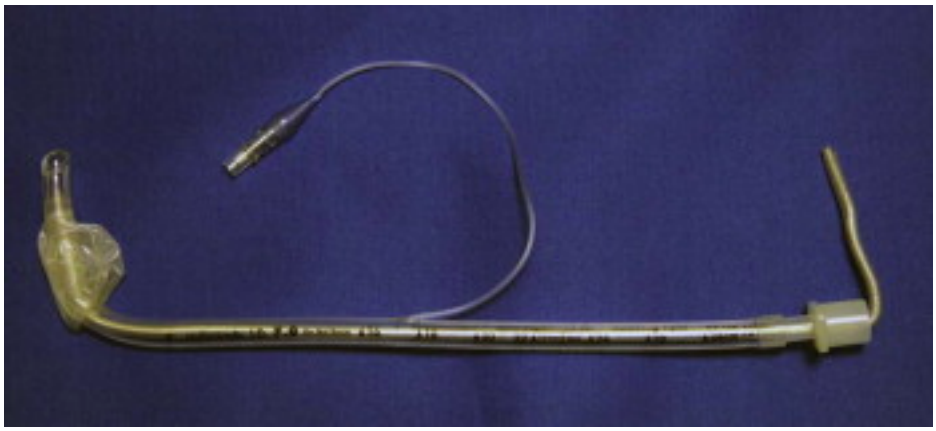

Figure 8. Endotracheal tube (ETT), with the stylet inserted [45]

1.4 OBJECTIVE OF THE THESIS

Airway management is critical in the pre-hospital and hospital setting and in some situations it can be the difference between life and death. It is the process of clearing and then establishing a stable airway. Maintenance of a stable airway is one of the most significant elements of patient care in either setting. Airway management has been designed to be a straightforward process but it has also been proven to be extremely challenging in many instances. This is due to the wide variety of clinical settings, patients, and circumstances under which such a critical procedure has to be performed. Each of these settings have documented complications ranging from soft tissue injuries to potential life threatening consequences [6]. Airway injuries have not only caused problems to patients but have also increased the financial burden on hospitals. These injuries have resulted in a 20% increase in hospital costs primarily due to extended patient recovery periods [6].

Direct laryngoscopy is an integral part of endotracheal intubation; the laryngoscope, the

primary device used in laryngoscopy, is used to create a clear view of the vocal cords for the insertion of the endotracheal tube. There are many complications associated with the laryngoscope which range from dental injury, arytenoid dislocation, soft tissue damage, vallecular damage, and sore throat. These complications primarily arise due to excessive forces being applied by the device in the airway. Although these complications have a low incidence percentage, their probability exponentially rises in “difficult airways”. Difficult airways are defined as airways which take either more than ten minutes to intubate or where the number of intubation attempts is greater than two. Based on these documented complications, a re-design of the laryngoscope is in order.

Therefore, the objectives of this thesis are,

- To design a laryngoscope to improve glottis visualization in average and difficult airways
- To design a laryngoscope to reduce intubation forces

An eight bar linkage was designed as a laryngoscope blade and handle system. Verification of the device effectiveness done by testing the newly designed blade on manikin simulators and compared with conventional laryngoscopes is presented. The design process and constraints chosen are documented as well.

2. ENDOTRACHEAL INTUBATION DEVICES

Airway management is done either by facemask ventilation, insertion of laryngeal mask airway, or endotracheal intubation by direct or indirect laryngoscopy, and is one of vital skills of an anesthesiologist. Endotracheal intubation by direct laryngoscopy is the topic of discussion in this thesis. The laryngoscope is defined as a device used for larynx visualization. After advances in anesthesia were made in the early 20th century, the laryngoscope, along with the skills to use it, became one of the primary devices used by anesthesiologists [7].

2.1 CONVENTIONAL LARYNGOSCOPES

As mentioned earlier, the laryngoscope is a device used to gain a view of the larynx; it consists of a blade with a light source and a handle. Laryngoscope blades are either curved blades (Macintosh) or straight blades with a slightly curved tip (Miller). Although these are the most frequently used laryngoscopes, there has been a proliferation of laryngoscopes ranging from partially flexible blades to video assisted laryngoscopes.

2.1.1 LARYNGOSCOPE BLADE FEATURES

The under-surface of a laryngoscope blade is called the spatula, and it is the portion of the device in contact with the tongue during intubation. The flange is the portion used to move the tongue out of the way to the left side of the mouth, out of the line of sight. The proximal flange is called the step and determines the thickness of the blade and potential contact of the blade with teeth during intubation. The blade tip (beak) is the portion which either goes under the epiglottis into the vallecula (in the case of a curved blade) or anterior to the epiglottis to lift the epiglottis directly. A generic representation of a laryngoscope is presented below.

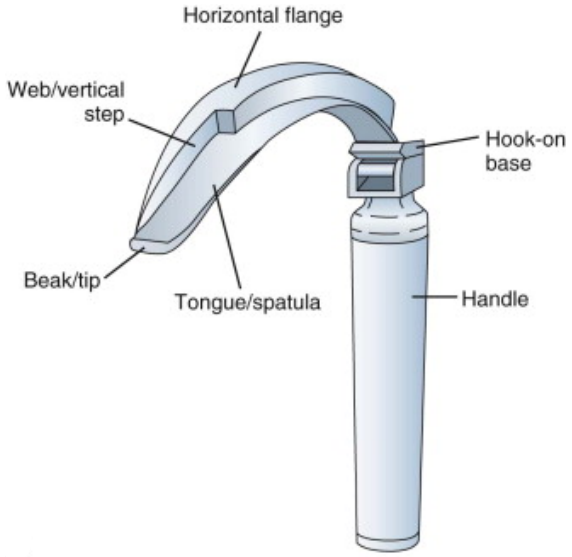

Figure 9. Standard Laryngoscope Design [45]

2.2 CURVED LARYNGOSCOPES

Curved blades are inserted into the right side of the mouth and advanced to the base of the tongue. The blade tip is inserted into the vallecula, anterior to the epiglottis and pushed down on the hyoepiglottic ligament. The blade is then elevated in a direction parallel to the axis of the laryngoscope handle to view the vocal cords.

2.2.1 MACINTOSH LARYNGOSCOPE

The Macintosh laryngoscope is most widely used curved blade. There are four main types of Macintosh blades—American, English, German, and Improved vision. The American Macintosh is also known as the Standard Macintosh and is characterized with a straight distal portion with a distal tip but without a flange and a large proximal flange.

The English and German laryngoscopes have similar geometries. They have shorter proximal flange heights in comparison with the American Macintosh blade, to reduce contact with the upper Maxillary incisors. The flange runs till the distal tip of the blade and the light-tip distance is less than that of the standard blade, to increase luminosity at the tip of the blade.

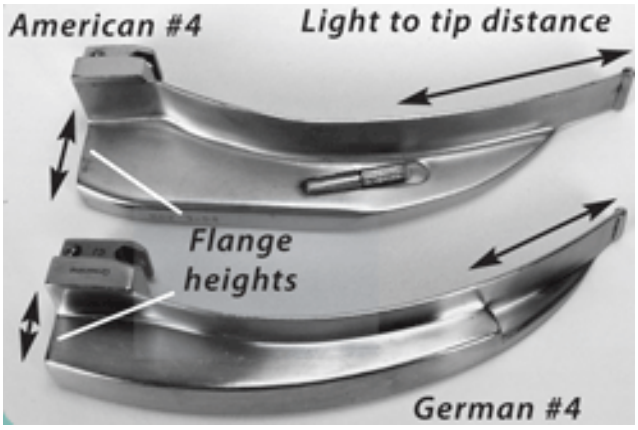

Figure 10. American 4 vs. German 4 Macintosh Blades [50]

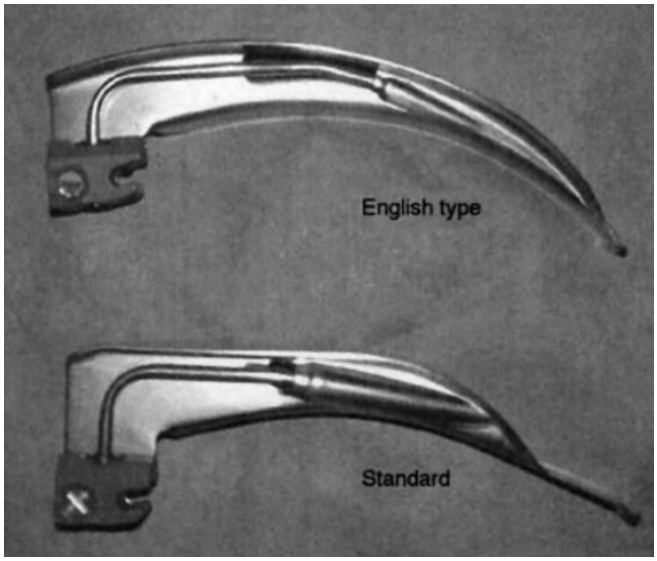

Figure 11. English vs. Standard Macintosh Laryngoscope [45]

The improved vision Macintosh laryngoscope blade spatula mid-portion has a concave cross-section. This flattens the mid blade in comparison to the standard Macintosh blade thereby increasing the view of the larynx.

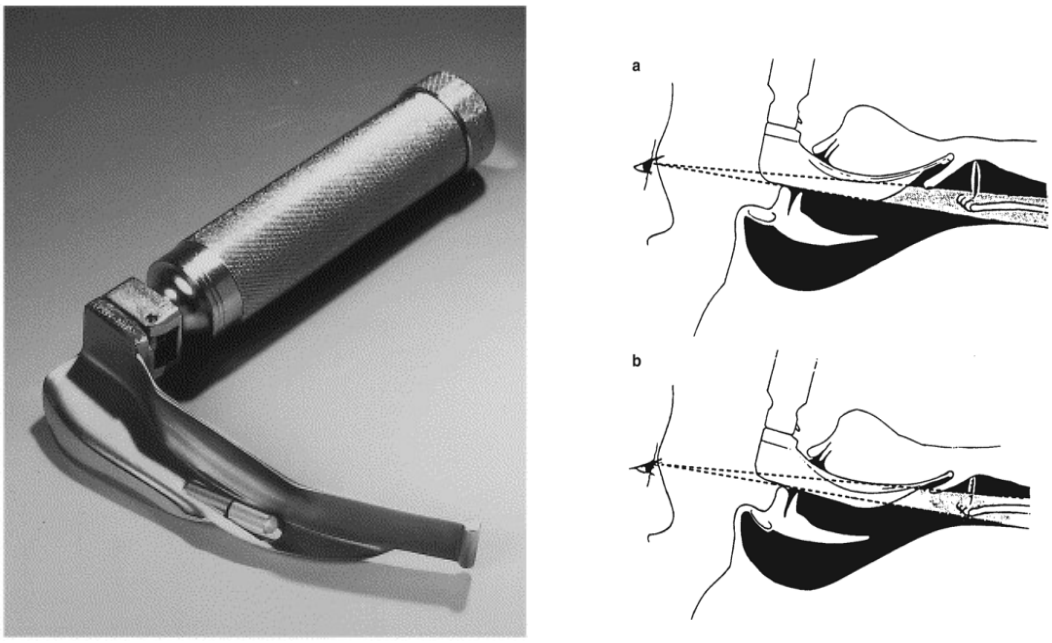

Figure 12. Improved Vision Laryngoscope (left); Improved Vision vs. Macintosh (right) [45]

2.3. STRAIGHT BLADES

Straight blades are passed underneath the epiglottis such that blade tip completely covers the epiglottis. The blade is then elevated at a 45^{o} angle to view the vocal cords. Straight blades are most effective in pediatric cases.

2.3.1 MILLER LARYNGOSCOPE

The most popularly used straight blade is the Miller laryngoscope. It has a straight blade spatula with a narrow flange to reduce dental trauma. The Miller blade has a curved tip to aid in lifting the epiglottis.

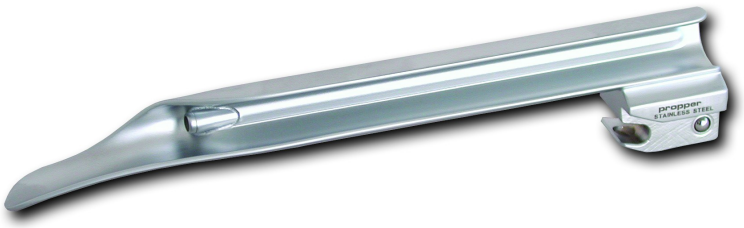

Figure 13. Miller Laryngoscope [51]

2.3.2 OTHER STRAIGHT BLADE LARYNGOSCOPES

Other commonly used straight blades are the Flagg, Wisconsin, Phillips, and Henderson. The Flagg blade has a distal tip curvature with a C-shaped cross-section tapering from the proximal to the distal end.

Figure 14. Flagg blade [45]

The Snow blade was designed to reduce the down-folding of the epiglottis and improve the passage of the ETT, a complication faced with the Miller blade. The vertical step at the heel and the flange were increased to create a C-shaped channel to improve the view and allow for easier tube passage [45].

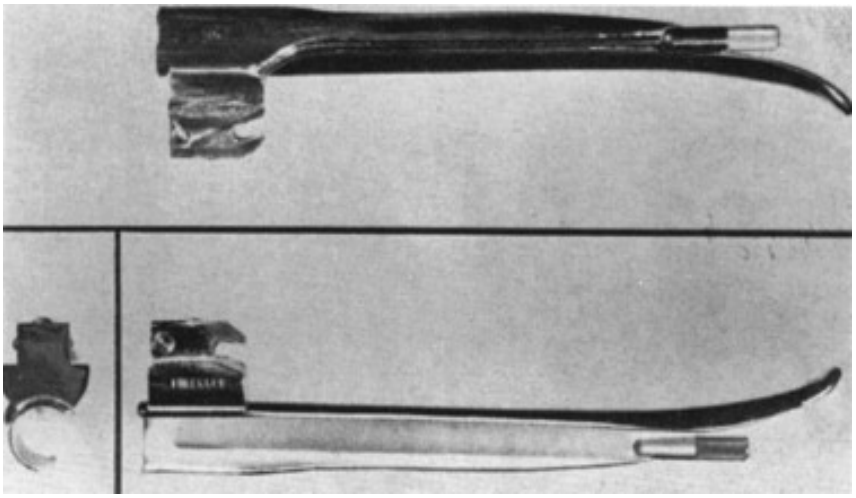

Figure 15. Snow blade [45]

The Phillips blade was developed in 1973 by Otto Phillips [8]. It has a curved distal tip like the Miller blade, a C shaped Wisconsin-like cross-section, and a small vertical flange making a good conduit for the ETT. It came in two sizes—1 for pediatrics and 2 for adults. The Phillips blade showed an 84% first attempt intubation success in a study performed by Otto Phillips [8]. Another popularly used straight blade laryngoscope is the Henderson laryngoscope. Unlike the Miller blade the Henderson is straight through its length, from proximal heel to the distal tip. The heel of the blade has a semi-circular step, which provides a wide channel for ETT delivery during intubation. The light source is placed 2.5cm from the blade tip to maximize light delivery and is shielded from the tongue since it's integrated into the lumen of the blade. The Henderson blades' efficacy was tested in 300 patients and it showed a 97% successful first intubation attempt [9].

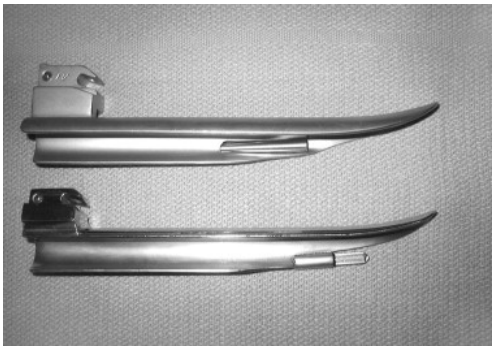

Figure 16. Phillips blade [45]

Figure 17. Henderson blade [45]

2.4 BELSCOPE

The Belscope laryngoscope is a multiple angulation blade; it consists of two equal straight segments 45^{o} to each other. The vertical step is less than that of the Macintosh blade and is available in three different configurations based on the lengths from the tip to the bend—6.7, 8, and 9.3cm. It is primarily designed to lift the epiglottis directly, therefore less compression of the tongue is required during intubation. This blade would be useful in situations where only limited atlanto-occipital extension is possible or in the case of a large tongue [9]. In cases where the larynx view may not be optimal, a prism is introduced

proximal to the bend to provide an indirect view of the glottis. The Belscope showed success in 3500 intubations without failure and in 12 cases provided a view of the glottis where the Macintosh laryngoscope failed [9]. Although the Belscope was successful in improving the laryngeal view in some failed cases it was proven that this blade required significant practice because it felt different from other conventionally used devices [9].

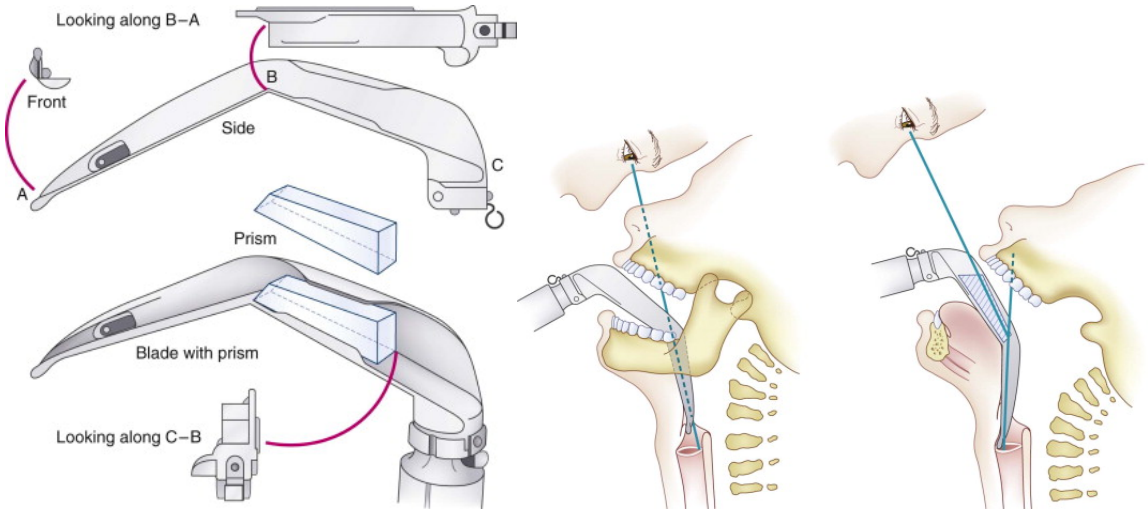

Figure 18. Belscope (left), Belscope during intubation (right) [45]

2.5 LEVERING TIP LARYNGOSCOPE

The levering tip laryngoscope, also known as the Corazzelli-London-McCoy (CLM) blade, has four distinct features distinguishing it from a conventional curved blade—hinged tip, lever at proximal end, spring loaded drum, and a connecting shaft [10]. The distal 1 inch of a standard blade was cut and joined to the rest of the blade through a pin at the under surface and the connecting shaft on the top surface. Other end of the connecting shaft is connected to the spring loaded drum which lies on the left side of the flange. The spring works in a clockwise manner when view from the left side of the blade. The lever is connected to the spring loaded drum at the proximal end of the blade through a pin in the flange. This blade can be attached to a standard laryngoscope handle. To engage the blade, the thumb is pressed down on the lever which causes the drum to rotate anticlockwise

thereby moving the shaft forwards. The forward motion of the shaft rotates the blade tip about the hinge at the distal end, elevating the distal segment. During laryngoscopy the elevating tip is expected to slide into the vallecula and apply pressure on the hyoepiglottic ligament to lift the epiglottis and expose the larynx.

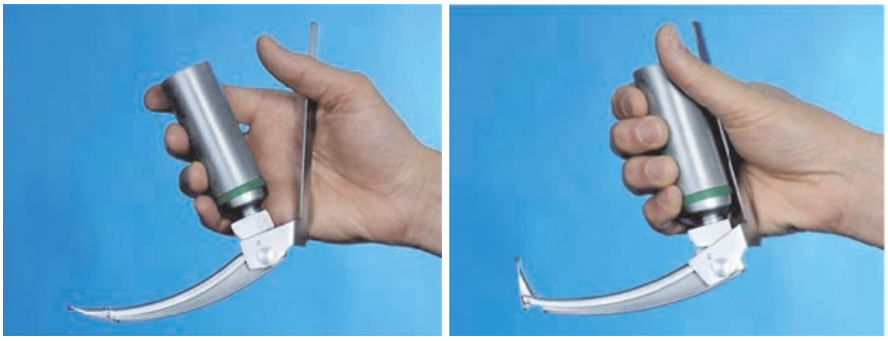

Figure 19. Levering tip laryngoscope [52]

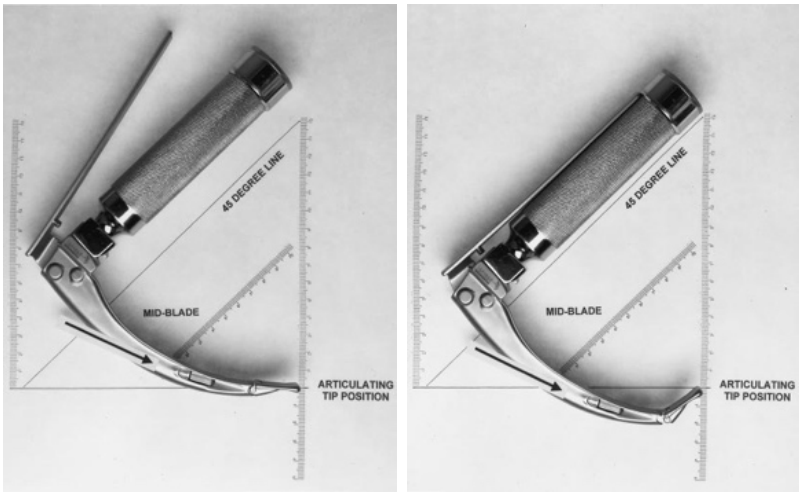

Figure 20. Degree of articulation of the McCoy laryngoscope (levering tip) [34]

2.6 FLEXIBLADE™

This laryngoscope has a flexible section and a rigid portion. It is flexible in the middle portion of the blade. The activation lever, unlike the CLM laryngoscope, is in the front of the handle. The flexible portion of the blade is made up of six smaller segments 3.5-10 cm from the blade tip. When the lever is engaged the blade goes from Miller blade like shape to a Macintosh blade. The maneuvering of this blade is similar to that of CLM laryngoscope. The blade is advanced into the vallecula and then engaged, thereby increasing the flexion to compress the tongue and apply pressure on the hyoepiglottic

ligament to lift the epiglottis and gain view of the vocal cords for ETT insertion. The Flexiblade™ has been tested in the clinical setting and showed improvement of CL grade 2 views to a grade 1 view [11]. It was also verified that in the neutral and engaged configurations the Flexiblade™ functioned similar to the Miller and Macintosh blades respectively [12].

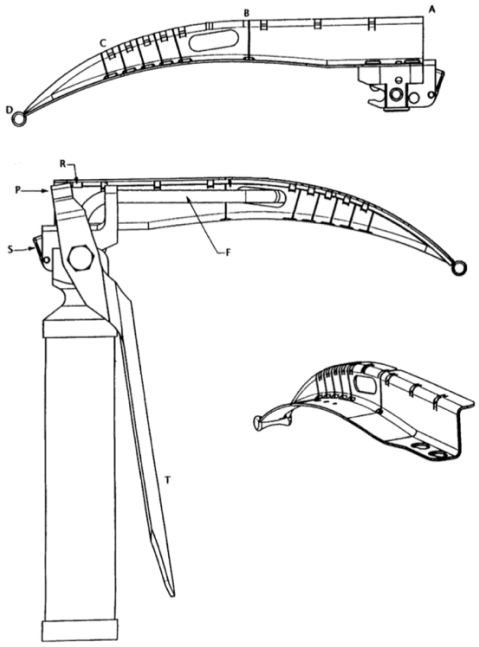

Figure 21. Flexiblade™,BC=Flexible intermediate section,R=rod,T=triggering lever,P=pusher[12]

2.7 MISCELLANEOUS BLADES

There have been other blades which are modifications of the Macintosh or Miller laryngoscopes. Their designs have been proposed to tackle very specific intubation issues, but most of them have not been extensively ratified through clinical tests. The Bizzarri blade has the same shape and curvature as that of a Macintosh blade but with no vertical step at the proximal end. This was done to reduce dental damage and aid in patients with limited mouth opening during intubation, otherwise it had the same functioning as the Macintosh blade.

The Polio blade was designed to reduce chest impingement during intubation and in patients with iron lung respirators. The blade was designed as a Macintosh but it fits on the handle at an angle of 170^{o}. This extreme angle has reduced the lifting force applied by the blade. Other modifications to avoid chest impingement have been made to the handle. There have been smaller handles made and ones which allow for different angulations of the blade with respect to the handle. The Patil handle is such a handle which allowed the blade to be positioned at 180^{o}, 135^{o}, 90^{o}, and 45^{o} to the handle [13].

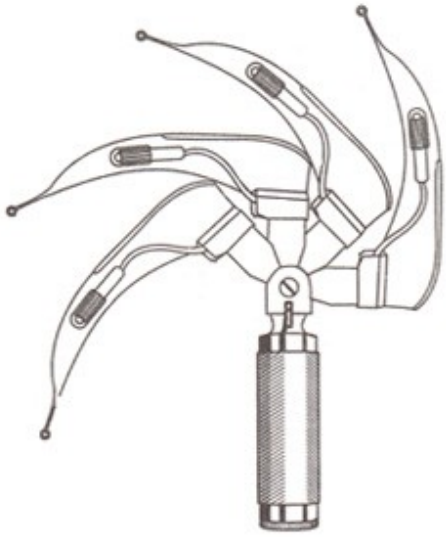

Figure 22. Patil handle with a Macintosh blade in multiple configurations [53]

2.8 PEDIATRIC BLADES

Intubation in pediatrics has led to a proliferation of blades of different shapes and sizes. Even in pediatrics based on the shape of the blade, it is either inserted anterior or posterior to the epiglottis for a direct or indirect lift of the epiglottis. The conventional Macintosh and Miller blades have smaller sizes which are used in infants and babies. The most commonly used blades in pediatrics are straight blades since they have been more effective than curved blades in moving the tongue out of the way to improve glottis viewing. They have also been more successful at directly lifting the epiglottis to view the vocal cords [14]. Popularly used blades are the Oxford, Seward, Srivastava, and the Robertshaw blade. The Oxford is a straight blade but is used like the Macintosh Laryngoscope. The blade width

tapers at the distal tip and has a U-shaped flange. The blade has a wide horizontal flange to prevent the upper lip from obstructing the view to the larynx. The Seward blade was initially made only for neonates but later additional sizes were made for children until five years of age. There is a slight distal angulation in the blade but a sharp taper with a prominent distal edge. The Robertshaw blade is a straight blade with a mild distal curvature and a step and flange with a slight C-shape. Another popular straight direct laryngoscope is the Diaz Pediatric Tubular Laryngoscope. It is a U-shaped handle and blade system. The blade is made up of two halves joined together by a removable screw. The channel of the blade consists of two light sources on each side of the channel; each light source is powered by a fiber-optic light. An advantage of the intraluminal lights is that it does not get blocked by secretions or edemas in the airway. The blade produces a sufficient view profile by compressing the surrounding tissue in the laryngopharynx. This is used in cases where fiber-optic laryngoscopy fails in pediatric cases [15].

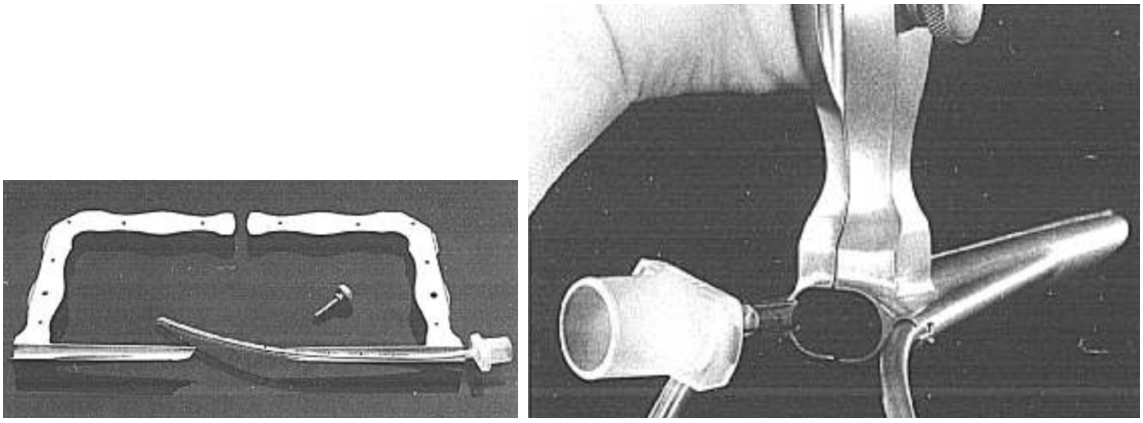

Figure 23. The Diaz pediatric laryngoscope [43]

2.9 LARYNGOSCOPE LIGHTING SOURCES

Light source is a very critical aspect in laryngoscope design. To view the larynx adequately an appropriate lighting field is necessary and it is not always proportional to the luminosity of the light [14]. It has been seen that blue/white light has also been effective since blue light enhances the view of capillary vessels within the mucosa [14]. Most laryngoscopes used incandescent bulbs which produce yellow light. LED’s have shown advantages over

incandescent bulbs wherein they produce light in a more appropriate part of the light spectrum and are more efficient. There have also been cases of burns caused by incandescent bulbs. A comparison was made between the irradiance of an incandescent bulb and an LED mounted in a Miller pediatric laryngoscope. The wavelength of the incandescent light is upwards of 600 nm which is near the infrared spectrum, whereas the LED radiated light is in the range of 400-550 nm which is blue/green range of the visible spectrum. This proves why most current laryngoscopes contain LED's instead of incandescent bulbs and why LED's are the future of all laryngoscope lighting.

2.10 LARYNGOSCOPE DISPOABILITY

There have been studies comparing the effectiveness of reusable and disposable laryngoscopes. Sterilization of laryngoscopes is critical in avoiding bacterial contamination during laryngoscopy, but this comes with an elevated associated cost in terms of monetary and manpower. In a few limited cases it has affected the performance of laryngoscope blades [14]. Temporary sheaths have been used to cover laryngoscope blades to avoid the sterilization process but those have negatively affected the lighting provided by the blade. This along with the discovery of the variant Creutzfeldt-Jakob disease has prompted a shift towards disposable blades [16]. Disposable blades are either plastic or metal. The metal disposable blades have been proven to be more effective than their plastic counterparts with higher user satisfaction rating, reduced forces on the airway, and reduced intubation times. Although disposable blades have become popular, due to the increased number of manufacturers, blade flexibility, light luminescence, and the angle of the light have varied significantly. This variability in manufacturing, which might seem insignificant, has been a problem in pediatric laryngoscopy. The disposable version of the Cardiff laryngoscope has obstructed the view of the vocal cords in a few cases where the bulb of the blade was in the line of view with the vocal cords.

2.11 VIDEO-LARYNGOSCOPES

Laryngoscopes in which a video camera replaces the line-of-sight visualization for intubation are known as video-laryngoscopes. Important indications for video-laryngoscopy have been identified to be difficult airways, cervical spine immobilization, education and teaching, and limited mouth opening. There are three main types of video-laryngoscopes—devices based on the Macintosh blade, highly curved blades, and with tube guiding channels. The A.P. Advance laryngoscope is a laryngoscope with a blade, handle with a battery, and a 3.5-inch LCD screen attached to the handle magnetically. Since the LCD screen is detachable, this device can also be used as a direct laryngoscope since the light source is powered by the battery in the handle. There are three blade sheaths available for this device—Macintosh 3, Macintosh 4, and a difficult airway blade (DAB). The DAB has a steeper distal curve; the distal third of the blade has a tube-guiding channel for indirect glottis view. Due to the guiding channel the DAB is used to directly lift the epiglottis like a straight blade direct laryngoscope [45].

The C-MAC laryngoscope has a blade curvature based on the original Macintosh laryngoscope design from 1943. Its step is less than that of the Macintosh and has a beveled proximal edge to reduce dental and oral injury during the intubation of patients with limited mouth openings. The blade tip has a light source and a camera. The handle is fixed to the blade and has a cable which is connected to a display onto which a live video feed of the intubation is relayed. The C-MAC is compatible with multiple Macintosh blade and Miller blade sizes. There is a D-blade for the C-MAC which is used in difficult intubations. This blade has a greater curvature and therefore aids in viewing the larynx; the D-blade has a low profile for patients with small mouth openings. The C-MAC pocket monitor (PM) is a laryngoscope with a 2.4-inch LCD screen with a battery and a laryngoscope handle onto which all standard C-MAC blades can fit. The light source built in the C-MAC is a high power and bright LED. The McGrath MAC video-laryngoscope is a device with a blade curvature mimicking that of the Macintosh blade, therefore it can be used both for indirect and direct laryngoscopy. The handle contains a battery which powers a 2.5-inch LCD screen attached to its base [45].

Video-laryngoscopes have also been developed with highly curved blades. The advantage of the increased curvature is that the alignment of the mouth, pharynx, and larynx is not necessary. Therefore, glottal visualization can be obtained through minimal or no head/neck/spinal manipulation. Due to the greater curvature, a malleable stylet is necessary with the ETT, and direct laryngoscopy is not possible. The most popular device in this category is the GlideScope®. This a one-part device attached by a cable to a 7-inch LCD external display to which the video is relayed. A miniature CMOS video camera along with a high powered LED is embedded midway along the blade. The GlideScope® Cobalt is the disposable version of this device and the GlideScope® Ranger is a portable version which is primarily used in the emergency department. There is higher blade curvature version of the McGrath MAC video-laryngoscope known as the McGrath Series 5. This contains a steel adjustable blade. The low step size of the blade accommodates patients with limited mouth opening and limited neck mobility. An LCD monitor is attached the base of the handle [45].

The third category of video-laryngoscopes are the devices with tube-guiding channels. The devices with higher blade curvatures have an integrated tube-guiding channel for the passage of an ETT without a stylet. This channel also protects the cuff of the ETT from damage. There are three commonly used devices in this category—King Vision laryngoscope, Pentax Airway Scope AWS-S100, and the Airtraq™. The King Vision is a disposable laryngoscope with a high curvature and an embedded CMOS video camera at the blade tip. The disposable blade comes with and without a guiding channel. It consists of a reusable-battery operated monitor. The Pentax Airway Scope is a portable battery operated video-laryngoscope. It consists of a transparent removable plastic blade with a port for a suction catheter. It consists of an LED light and a flexible wire for a charge-coupled device camera (CCD) instead of a CMOS video camera like other video-laryngoscopes. The Airtraq™ is a single use two channeled device; one for the ETT and the other for the image. The image is relayed through a viewfinder and series of lenses and prisms [45].

3. LITERATURE REVIEW

Airway management is one of the most important skills honed by an anesthesiologist. Complications associated with intubation are rare but are known to be life-threatening in many cases. The 'can't intubate can't ventilate' (CICV) situation occurs when the trachea cannot be intubated and the lungs cannot be ventilated; this is the most challenging situation for anesthesiologists. In CICV cases urgent and efficient care is necessary to avoid brain damage or cardiac arrest due to hypoxia. CICV cases are approximated to around 1 in 50000 cases but these situations account for about a quarter of the anesthesia related deaths [17]. Complications associated directly with laryngoscopy are only about 1% because most airways are easy. It is in the difficult airways where the complications are more significant. Due to the low frequency of difficult airways it can be concluded that most complications do occur in patients with easy airways. As mentioned earlier, intubation differs in different settings and therefore so does the incidence of failed cases. The range is from 1 in 2000 cases in an elective setting to 1-100 in the emergency department, intensive care unit, and the pre-hospital setting [17].

There have been studies comparing the effectiveness of different laryngoscopes in the hospital and prehospital setting. Papers have been published comparing the efficacy of different head positions, different intubation devices, and external laryngeal manipulations. This review documents studies that have aided in the understanding of intubation, laryngoscopy, and associated devices.

3.1 CORMACK LEHANE VIEWS

The primary goal of endotracheal intubation is to obtain a line of sight to the glottis; laryngoscopy is the procedure which provides the line of sight. Based on the degree of laryngeal exposure, four grades views have been established to define direct laryngoscopy. These views were established by R.S. Cormack and J. Lehane. Grade 1 is a standard easy intubation where the glottis is visible; grade 2 is a slightly difficult intubation where only the posterior of the glottis is visible; grade 3 is a difficult intubation where only the

epiglottis is visible but not the glottis; grade 4 is an impossible intubation where neither the glottis nor the epiglottis is visible [18]. Grade 3 and grade 4 are important indicators for difficult intubation but in most cases a grade 4 view has been synonymous with failed intubations. The four grades are depicted below.

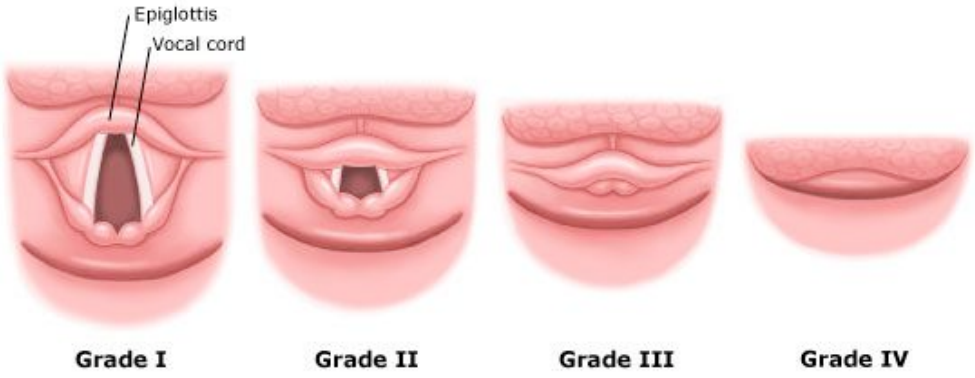

Figure. Cormack-Lehane Grade Views [55]

Although the Cormack-Lehane classification has become a gold standard for airway classification and research, there has been a discrepancy between the knowledge and use of this system. Yentis [19] proved that due to this rigid classification system, there is a population of patients who are not accurately intubated. Therefore, a new scale was proposed which split the grade 2 view into 2a and 2b. The grade 2a view was classified as partial view of the glottis and 2b was when either the arytenoids or just the posterior extremity of the vocal cords were visible. This modified CL system is in the figure below.

Original Cormack and Lehane system	1 Full view of the glottis	2 Partial view of the glottis or arytenoids		3 Only epiglottis visible	4 Neither glottis nor epiglottis visible
View at laryngoscopy	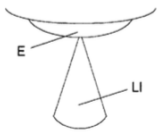				
Modified system	1 As for original Cormack and Lehane above	2a Partial view of the glottis	2b Arytenoids or posterior part of the vocal cords only just visible	3 As for original Cormack and Lehane above	4 As for original Cormack and Lehane above

Figure 24. Modified CL grade views [19]

Cook [17] further subdivided the CL classification system by dividing a grade 3 view into a grade 3a, and grade 3b. In this case grade 1 and 2a were classified as easy intubations, 2b and 3a as awkward, and 3b and 4 as difficult where an advanced technique needed to be used. Unlike previous classifications, the 'Cook classification' proved to be a better metric to prove the feasibility and effectiveness of difficult intubation [17].

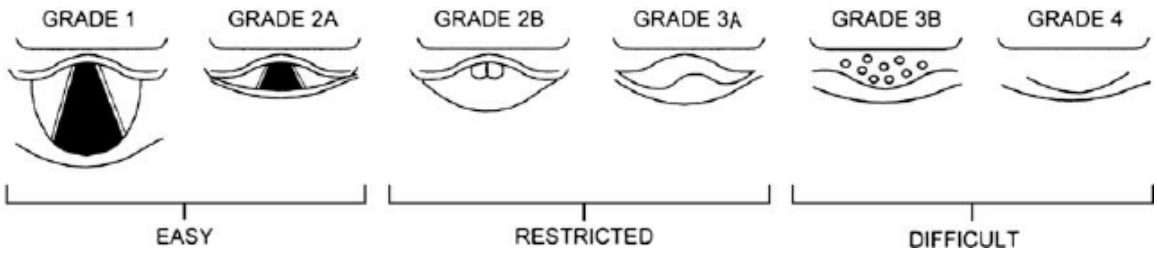

Figure 25. Modified CL Grade Views Developed by Cook [20]

3.2 LARYNGEAL EXPOSURE AND INTUBATION FORCES

Laryngeal exposure has been established as one of the most important metrics in intubation. Poor exposure has been directly associated with difficult intubations, and excessive blade forces have been associated with airway injury during intubation. The potency of different laryngoscopes has been tested by many authors based on the CL classification, its modifications, and forces experienced by the blades during intubations. The first comprehensive study documenting forces on a laryngoscope showed the mean and maximum forces applied during laryngoscopy [21]. The study was performed on the Laerdal Airway Management Trainer by experienced and novice operators. This study showed that the difference between the maximum forces applied by the novice and experienced operators was negligible, but the time of intubation by experienced operators was shorter than that by novice operators. The maximum forces recorded during intubation at the distal end were in the range of 45-50 N whereas average forces during the intubations were 24-29 N. Although this study set a standard for approximate intubation forces, it has been proven that practice on simulators can be counter-productive. Since airway simulators do not accurately represent the physiological airway, practicing on them may cause novice operators to use the laryngoscope incorrectly in an actual clinical situation, leading to patient morbidity and mortality [25].

3.3 DENTAL AND SOFT TISSUE DAMAGE

The intricate complications related to airway management and intubation have been classified based on the CL classification system and are an incidence of specific grade views. Dental damage during anesthetic airway management is a significant complication and has been estimated to be an incidence of nearly 12% [22]. Approximately half of the incidences of dental trauma are associated with laryngoscopy [23]. Dental damage is also the most common complication associated with laryngoscopy. During laryngoscopy if the laryngoscope blade is rested on the maxillary incisors the technique used is incorrect [24]. The incisors are then used as fulcrum about which the blade is rotated to lift the head and the anterior region of the larynx to obtain a better view of the glottis. This technique causes incisor damage due to direct blade contact and the grazing of teeth. Ideally there should be no force applied on the incisors since the laryngoscope, once inserted into the mouth, should be pulled in the direction perpendicular to the axis of the handle, to lift the head. Unfortunately, in some difficult intubations levering on the maxillary incisors is common [24]. There have been documented cases of teeth being avulsed during intubation. In those situations the tooth is removed immediately since aspiration of the tooth could cause complications which might require bronchoscopy for removal [25]. It has been established that video-laryngoscopes give a better view of the glottis and reduce traumas during intubation. A study performed by Lee [26] compared the forces recorded on the blade of the Macintosh laryngoscope and a video-laryngoscope. The blades were embedded with force resistive sensors to record the force and all contacts with the maxillary incisors. The maximum force recorded on the conventional Macintosh was approximately twice that of the value recorded on the video assisted laryngoscope. Range of forces on the mac was 0-87 N with a median of 15 N, and 0-45 N with a median of 2N on the video assisted laryngoscope. It was proven that the forces applied on the maxillary incisors was less due to the video laryngoscope than the conventional Macintosh laryngoscope, regardless of operator experience/expertise, patient variability, and standard metrics such as the CL grade views. There was no correlation between difficult intubation due to poor glottis view, forces on the maxillary incisors, and the intubation success with video-laryngoscopes.

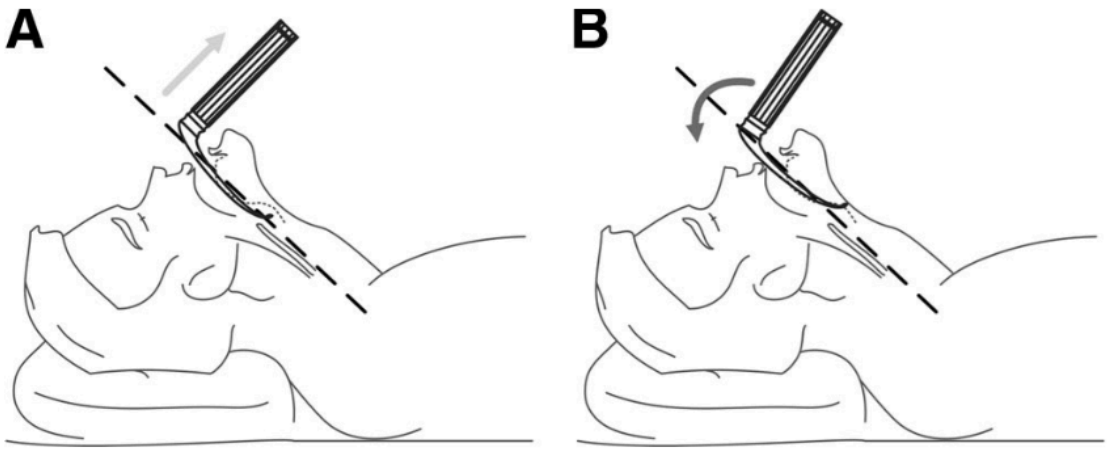

Figure 26. A demonstrates the correct use of a laryngoscope; B shows a case there the upper incisors are used as a fulcrum during intubation (incorrect technique) [26]

Soft tissue damage has not been a major concern during intubation but is a complication associated with the practice. Arytenoid dislocation is a rare complication mostly seen when multiple intubation attempts are made, during retrograde intubation, and caused by McCoy (levering tip laryngoscope). Other oral injuries associated with laryngoscopy are lip lacerations and edemas; these are usually a cause of inattentive laryngoscopy performed by an inexperienced practitioner [26].

3.4 MACINTOSH LARYNGOSCOPE VS. OTHER INTUBATION DEVICES

There have been further studies comparing the efficacy of the conventional Macintosh laryngoscopes to commonly used video-laryngoscopes. Forces were compared between the Macintosh 3 laryngoscope and the Glidescope® in the Laedral SimMan manikin [27]. To show the proficiency of each device in scenario this study simulated a patient with a normal airway, cervical immobilization, and tongue edema. Each laryngoscope was mounted with a pressure film transducer (LLLW Prescale Pressure Film, Fuji, full scale 0.6 MPa, accuracy 10%) on the lower surface of the blade. This film was used to record the force distribution along the blade surface during intubation. As expected, the force applied by the laryngoscopes on the difficult airways was higher than that on the normal airway. It was also concluded that the forces on the Macintosh laryngoscope were significantly higher

than those on the Glidescope®; the difference in the skill level of the operator did not show any statistical significance. In accordance with previous work [23], the Glidescope® showed a higher success rate in the difficult airway scenarios, and on average an improvement of the CL views from a 4 or 3 to a 2 or 1.

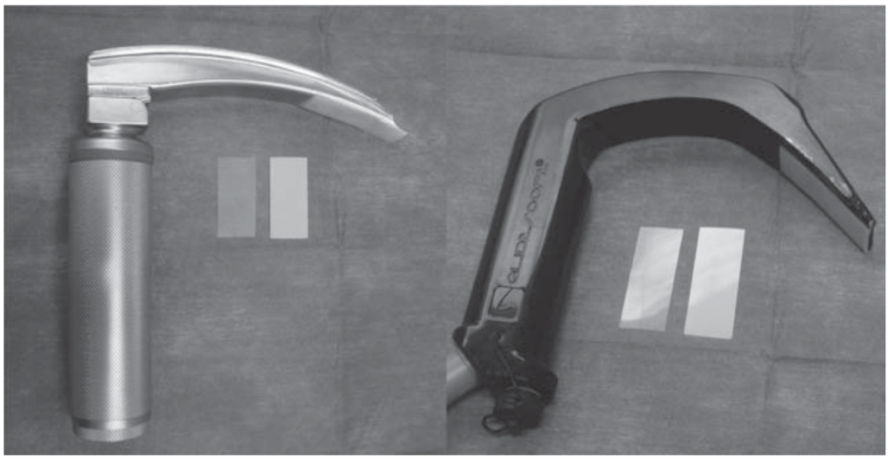

Figure 27. The laryngoscopes mounted with the pressure films [27]

The inability to secure the airway and successfully intubate the trachea is one of the leading causes of mortality and morbidity in the emergency and hospital settings. An intubation difficulty score (IDS) was developed to objectively quantify the complexity of intubation. This score was developed to evaluate factors related to difficult intubation and to provide a uniform approach to comparing studies on intubation [56]. Therefore, the Macintosh blade has been compared to other blades in the effort to potentially finding a versatile device that has higher probabilities of success in as many scenarios as possible. Patients with cervical spine injuries generally have immobilized necks; cervical spine immobilization makes for difficult larynx visualization during direct laryngoscopy [28]. Malik [28] compared the Macintosh laryngoscope with the Glidescope®, AWS, and Truview EVO2. The IDS scores showed that the Glidescope® and AWS laryngoscopes were more advantageous in comparison with the Macintosh and Truview EVO2 laryngoscopes in patients suffering from cervical immobilization.

Conventional laryngoscopy has been heavily compared to video-laryngoscopy under the premise that video-laryngoscopes are more effective in difficult airways. This hypothesis that video-laryngoscopy results in a better glottis view was verified by Mort [29]. This study proved the effectiveness of video-laryngoscopy in cases with limited glottis visualization and where endotracheal tube (ETT) exchange was needed. Causes of limited glottis viewing was obesity, trauma patients, cervical spine immobilization, and head/neck edema. Endotracheal tube exchange is a challenging procedure in high risk patients and may lead to life threatening complications. The endotracheal tube, edema, secretions, and restricted positioning capabilities limits visualization, especially during direct laryngoscopy. Since video-laryngoscopy has been beneficial in difficult airways [23], it was used and compared to laryngoscopes in difficult airways and high risk situations. The direct laryngoscopy was performed either with a Macintosh blade size 3 or 4, while the video-laryngoscopy was performed using the reusable GlideScope®-GVL or the one time use GlideScope® Cobalt. Approximately 85% of the study group showed a CL grade 3 or 4 with direct laryngoscopy whereas a grade 1 or 2 was achieved for about 89% with video-laryngoscopy. The reduced glottis viewing through direct laryngoscopy did not aid in ETT exchange, either. Direct laryngoscopy was riddled with complications such as esophageal intubation, hypoxemia, need to use rescue alternatives, and cardiac arrest. Whereas the improved glottic visualization reduced the placement of the ETT into the esophagus due the reduced forces applied by the operator on the ETT while reinsertion.

McElwain [30] compared the Macintosh laryngoscope with the C-MAC and Airtraq™ laryngoscopes in patients with cervical spine immobilization. In patients with cervical spine injury or suspected of injury, manual inline axial stabilization (MIAS) is performed to mitigate the risk of spinal cord injury during intubation. IDS scores were calculated for each intubation, and were significantly lower for the Airtraq™ in comparison to the CMAC and Macintosh laryngoscopes. This did not correlate with the preliminary data obtained through manikin testing; it was expected that the Airtraq™ and CMAC both would be more effective than the Macintosh laryngoscope and in some cases the CMAC would outperform

the Airtraq™ . The patient data showed no significant difference between the CMAC and the Macintosh laryngoscope. The Airtraq™ reduced the IDS score, improved the CL grade view, reduced the number of external manipulations, and was the only device to have a 100% intubation success in the study.

The Venner™ A.P. Advance™ video-laryngoscope (APA) was also compared with the Macintosh laryngoscope in a manikin. As mentioned earlier, the APA video-laryngoscope has two primary blades designs, the one resembling the Macintosh blade and the Difficult Airway Blade (AP DAB). The study by Marshall [31] compared the AP normal blade, AP DAB, and the Macintosh laryngoscope in simulated normal and difficult airways; intubation was performed by non-anesthesiologists. The AirSim™ manikin was used to simulate a normal and difficult airway as is shown in the figure below.

Figure 28. Normal airway (left), Difficult airway (right) [31]

The AP DAB showed a 100% success rate in the easy airway, as expected, but the Macintosh laryngoscope showed more successful first attempt intubations than the AP normal blade. Similarly, there were more failed intubations with the AP normal blade than with the Macintosh in the simulated difficult airway. This directly negates previous studies where video-laryngoscopes showed better success than the conventional Macintosh when used by novices. The technique expected to be used by the AP normal blade was similar to that of the Macintosh laryngoscope due to similarities in the design. It was then concluded

that the AP normal blade video-laryngoscope did require a learning curve and that there is not always a direct transferability of skill from one device to another. The high intubation times experienced with the AP normal blade in the simulated difficult airway suggested a higher patient morbidity through possible desaturation [67] with this device. It was also seen that the AP DAB was associated with longer intubation times than the Macintosh blade in the simulated difficult airway. The number of first attempt successes with the DAB were lower than that of the Macintosh. This led to greater two attempt intubations by the DAB. A study by Burdett [32] showed that the DAB was more effective than the AP normal blade and the Macintosh blade in the simulated difficult airway based on the time of intubation and view achieved; this study included experienced operators. The efficacy of the Macintosh was also tested against the McGrath® Series 5 video-laryngoscope. The APA DAB, APA Mac, McGrath® Series 5, and the Macintosh were compared in a simulated easy and difficult airway. As expected there was no significant difference in the time of intubation by each blades in the simulated easy airway; the Macintosh had the shortest intubation time. The APA DAB and the McGrath® blades only gave CL grade 2 views whereas the APA Macintosh and the Macintosh both had grade 3 views. In the difficult scenario the APA DAB and the McGrath® showed similar average intubation times 10.4 s and 10 s respectively. The Macintosh proved superior to the APA Macintosh based on the time of intubation; average intubation times were 14.0 s and 17.5 s respectively. The APA DAB and McGrath® showed similarity in the CL grade views obtained; all intubations only had grade 1 or grade 2 views. The Macintosh and APA Macintosh blade showed primarily grade 2 and grade 3 views. This study proved that video-laryngoscopes demonstrated greater efficiency in difficult intubations while no increase in efficiency in easy intubations.

Intubation has three main challenges, laryngeal and glottis viewing, insertion of the endotracheal tube into the larynx, advancing the tube past the vocal cords and into the trachea [33]. The degree of laryngeal visualization and control of the tongue affects the endotracheal tube insertion and passing into the trachea. This is based on the line of sight

created by the device in use. Direct laryngoscopy devices provide a direct line of sight with the glottis whereas indirect laryngoscopy devices provide the view of the glottis through imaging techniques like digital displays and prisms [33]. As seen even in previously cited studies, video-laryngoscopes make laryngeal exposure easier, and without the need of a direct line of sight to the larynx required. The cameras in video-laryngoscopes provide a wide angle view of the larynx along with the distal end of the blade. Although these devices provide a better laryngeal view, there are complications associated with endotracheal tube insertion which have led to pharynx and hypopharynx perforations.

3.5 REPEATED INTUBATION ATTEMPTS

Complications associated with intubation have been recognized in many studies and have been repeatable. The shortcomings of intubation devices have been documented extensively and have been clearly understood from the perspective of easy and difficult airways. One of the primary reasons behind failed intubations and airway damage during intubation is the repetition of intubation attempts. Dr. Thomas C. Mort investigated the incidence of airway and hemodynamic complications outside the OR and attempted to draw a correlation between the number of intubation attempts and airway complications [34]. Based on the extensive list compiled it was seen that a third of all anesthetic deaths were those resulted due to airway complications. Airway related complications which arose due to emergency airway treatment outside the OR often lead to patient morbidity and sometimes mortality. The complications were categorized as hypoxemia, severe hypoxemia, esophageal intubation, regurgitation, aspiration, bradycardia, and cardiac arrest. The incidence of severe conditions such as severe hypoxemia, cardiac arrest, and esophageal intubation in two or fewer intubation attempts were at approximately 2%, 5%, and 1% respectively. These numbers rose 28%, 51%, and 11% for greater than 2 intubation attempts. This study focused on the pre-hospital setting but a parallel can be drawn to the OR with respect to the complications listed. Another study, performed by Hasegawa [33], corroborated the aforementioned work done by Dr. Mort. The study focused on emergency departments in Japan. The most adverse complication experienced in the population

observed was esophageal intubation.

These two studies showed that there is a need to improve intubation in the emergency department and pre hospital settings. Both studies also concluded that the aim is to limit the intubations to three to reduce the risk of morbidity and mortality.

3.6 ANATOMY MAPPING

Frederic [4] demonstrated the change in angles of the mouth axis and laryngeal axis from the neutral, extension, and sniffing positions. The angle between the mouth and laryngeal axis was determined to be 42° ± 12° in the neutral position, 29° ± 9° in the extension position, and 29° ± 10° in the sniffing position. Schebesta [35] measured upper airway distances from the CT scans of 20 patients to calculate the volume of the pharyngeal airspace. All patients were evaluated supine in the neutral position. The primary goal was to compare these values to those of manikin simulators to assess their effectiveness. The diagram is below shows all the measurements taken of the upper airway.

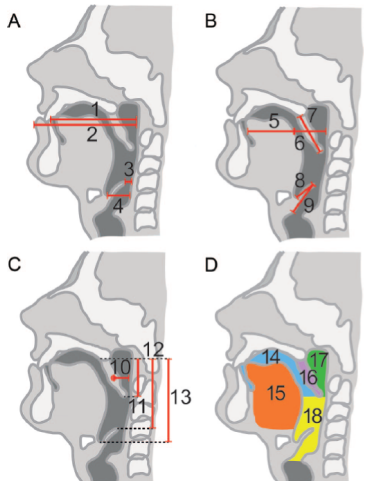

Figure 29. Airway dimensions [35]

The dimensions for the anterior (8) and posterior (9) length of the epiglottis, cross-section of the tongue, horizontal diameter of the tongue (5), pharyngeal volume, and the distance of the epiglottis from the hard palate (12) were of consequence for blade design. These

results documented in the study are presented in the table below.

Table 1. Airway dimensions [35]

Feature	Dimension	Standard Deviation	95 % CI
Anterior epiglottis (cm)	1.6	0.4	1.4 – 1.7
Posterior epiglottis (cm)	2.8	0.7	2.5 – 3.2
Tongue horizontal diameter (cm)	6.3	0.7	5.9 – 6.6
Cross section area of tongue (cm^2)	25.6	3.7	23.8 – 27.5
Hard palate to epiglottis (cm)	4.4	0.9	4.0 – 4.9
Pharyngeal airspace (cm^3)	13.5	7.7	9.9 – 17.1

4. PRELIMINARY TESTING

Although there have been studies discussing the forces on a laryngoscope, some initial testing was performed to better understand the force distribution on a Macintosh laryngoscope blade during intubation.

4.1 FORCE AND MANIKIN STUDY

A study was arranged to evaluate various airway simulators and their effect on endotracheal intubation training through objective measurement of intubation forces and subjective reporting of the force applied. The other objective was to assess the need to design a better simulator with airway structures that are anatomically correct and material properties that match the human larynx more closely. A fiber-optic one-time use Macintosh laryngoscope that is popularly used by the US Army was the choice of laryngoscope in this study. Each device was fitted with three Sparkfun 0.5" force-resistive sensors which were used to calculate forces and the torque experienced by the laryngoscope during intubation. A figure of the instrumented laryngoscope is seen below.

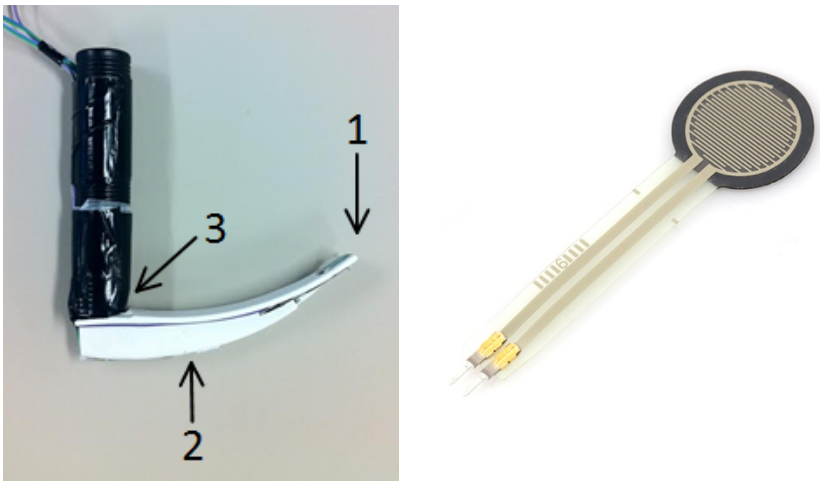

Figure 30. Instrumented Laryngoscope (left), Force resistive sensor (right) [57]

The forces were recorded using the Arduino Uno; the circuit was set-up on a bread board for each manikin. The force resistive sensors were interfaced with the Arduino Uno using a voltage-divider circuit.

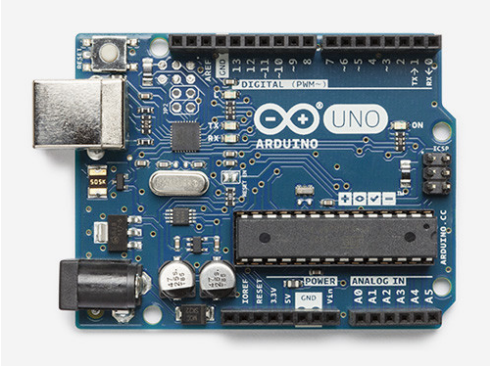

Figure 31. Arduino Uno [58]

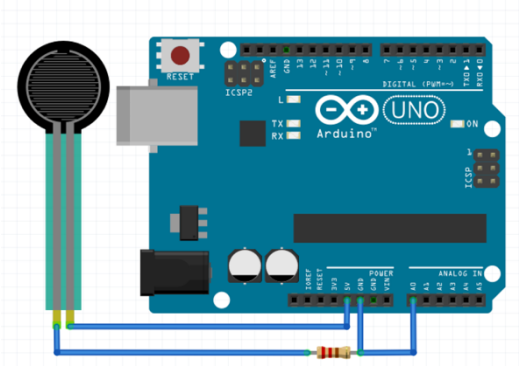

Figure 32. Voltage divider circuit set up for one sensor; schematic developed using Frtizing

One sensor was placed at the blade tip to record lifting forces and conversely the force applied in the vallecula, one was placed on top of the laryngoscope step to record any contact with the teeth, and one was placed between the handle and the blade to calculate the torque experienced by the device during intubation. Intubation was performed on four modalities—three manikins and a cadaver. The three manikins chosen were the TruCorp® AirSim®, Laerdal Airway Management Trainer, and the VMN Air Management Simulator Bill I as seen below.

Figure 33. TruCorp AirSim Standard (left), Laerdal Airway Management Trainer (middle), and VBM Air Management Simulator Bill I (right)

The three objective metrics measured in the experiment were the maximum force on the laryngoscope tip, maximum force on the trainer/cadaver's teeth, and the maximum torque on the laryngoscope blade. The testing was grouped in two categories—competency test represented intubations on the manikins before the cadaver was intubated, and the assessment test represented the intubations on the manikins and the cadaver after each model was intubated once. Paired t-test were performed between the competency and assessment test for the three measured metrics. It was concluded that the highest forces were applied on the Laerdal simulator for all measured variables. Only the torque and tip

forces were significantly different for the TruCorp® and VBM group. Welch's ANOVA revealed that all three measured force variables were significantly different between the various training groups within the competency test (Torque – $p = 0.003$, Teeth Force – $p = 0.001$, Tip Force – $p = 0.004$). Torque data, shown in the graph below demonstrates differences between competency and assessment tests and differences between groups.

Table 2. t-Test Results for Force and Torque on Macintosh Blade

	Paired Differences between the Assessment test and Competency test			**p(2-tailed)**
	Mean	Std. Deviation	Std. Error Mean	
TruCorp				
Torque (N-m)	-2.96	2.05	0.84	**.017**
Teeth Force (N)	1.61	4.23	1.73	.393
Tip Force (N)	0.06	20.30	8.29	.995
Laerdal				
Torque (N-m)	-5.52	2.58	1.29	**.012**
Teeth Force (N)	-1.99	0.91	0.46	**.022**
Tip Force (N)	-28.95	15.78	7.98	**.035**
VBM				
Torque (N-m)	0.02	2.84	1.16	.990
Teeth Force (N)	1.64	8.97	3.66	.763
Tip Force (N)	-29.56	25.76	10.52	**.038**
Cadaver				
Torque (N-m)	-0.58	0.73	0.30	.107
Teeth Force (N)	0.52	1.01	0.51	.376
Tip Force (N)	0.86	1.79	0.73	.295

The subjective part of the study was to rate the simulators based on difficulty; this could be verified with the force data obtained. Difficulty was based on two factors—perception of force applied on the manikin and ability to successfully intubate. Higher forces were directly correlated with greater difficulty. The subjective metrics were the Likert-based perceived intubation difficulty and Likert-based subjective rating of force applied. Again,

paired t-test and ANOVA were performed on subjective perception of difficulty and force applied. Significant differences in force used ($p = 0.018$) were found between competency and assessment tests for the Laerdal group. ANOVA revealed significantly different ratings in difficulty during assessment ($p= 0.027$). Participants voted simulators to be more difficult to intubate than the cadaver. These results are summarized below.

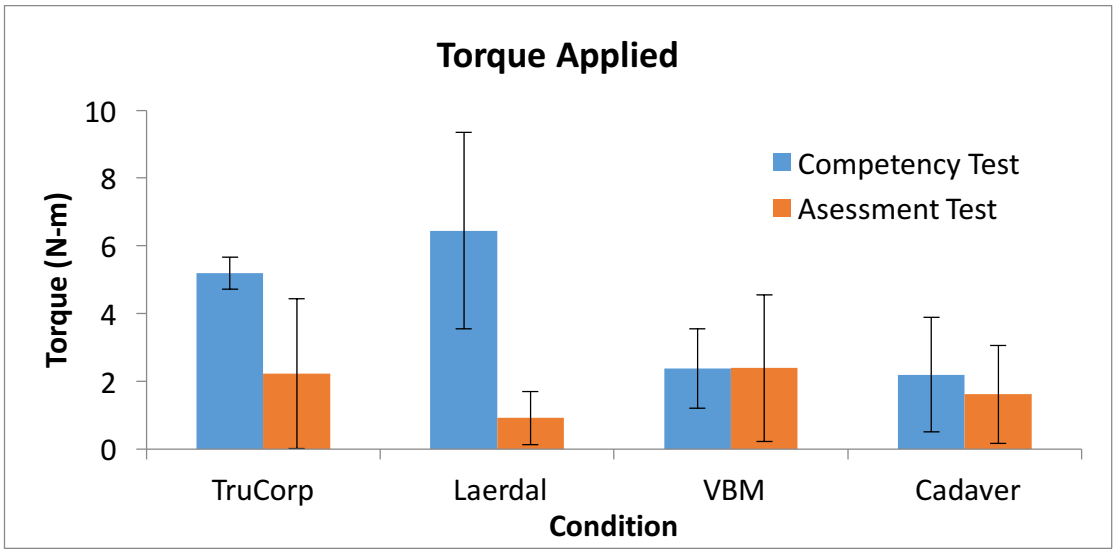

Figure 34. Toque applied on each Simulator

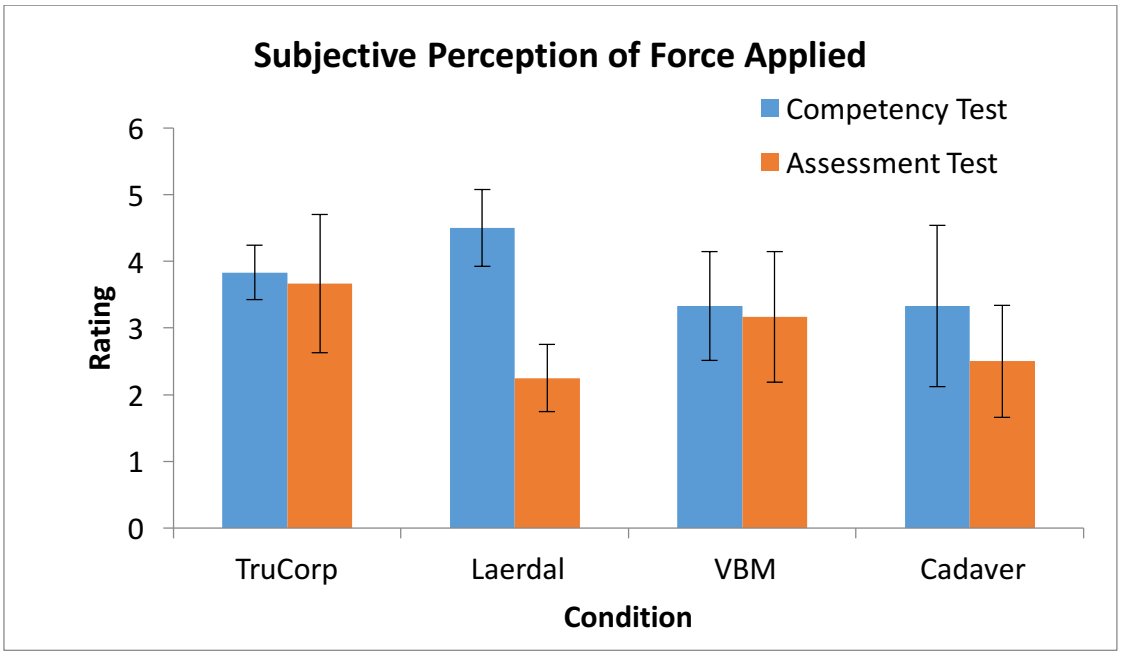

Figure 35. Subjective Force Applied

From the objective metrics, it was concluded that the participants who received training used significantly more torque, teeth, and tip forces while performing intubation on the simulator during the competency test than on a cadaver during the assessment test. Findings were consistent with subjective data that the Laerdal was more difficult to intubate. Welch's ANOVA demonstrated that all three measured variables were found to be significantly different for the competency test. Participants were asked to intubate different modalities supporting the hypothesis that simulator intubations do not equate to cadaveric intubations. Each modality required a different force profile to intubate. Therefore, a simulator that offers more realistic endotracheal intubations may be necessary for airway management training. Intubation forces for assessment test were not significantly different. Operators were able to adjust the amount of force used on different modalities.

The subjective intubation data showed that the cadaver group reported the assessment test to be easier and required less force than the competency test. Participants were allowed to practice on the same cadaver during training. Tissue disintegration may have played a role in intubation difficulty.

4.2 REENGINEERING OF THE LARYNGOSCOPE

The study discussed in the previous section supplemented with force analyses studies performed [21] [25] have shown the maximum force on a laryngoscope and forces at different locations. Although there was conclusive data obtained from the study discussed in the previous section there were aspects that could be improved. The sensors used were not robust enough to withstand multiple intubations. The sensors were secured onto the blade using non-conductive tape; due to the aggressive nature of intubation some of the sensor leads snapped-off and there were also cases of the sensors coming off the blade due to the loss of tape adhesive. To improve this shortcoming new type of sensor was considered.

A new type of sensor was provided by 7SIGMA, a local company which collaborated with the lab on multiple projects. Their Conformable Sensor Technology [59] represented a precise, inexpensive, and customizable substitute to standard resistive and capacitive sensors. Analogous to resistive sensors, a voltage divided circuit was used to operate the sensor. Unlike resistive sensors, conformable sensors are silicon-based, single-material units that can operate in ranges covering 8-orders of magnitude of force. Conformable sensors can be manufactured to satisfy spatial and loading constrains alike. To incorporate these sensors into the laryngoscope in a manner to avoid minor changes in the blade curvature, the sensors had to be embedded into the blade and kept flush with the surrounding material.

4.2.1 DESIGN REV. 1

The laryngoscope was therefore reengineered and designed based on the dimensions of the disposable Macintosh 3 blade used by the army. The blade was traced onto a graph paper and the curvatures and dimensions were calculated using a compass and caliper. These dimensions were then used to design the blade in SolidWorks, a 3D solid modelling package. The laryngoscope blade and handle were both rapid-prototyped using a Stratsys Fortus 250mc machine. The first revision 3D model is shown below.

Figure 36. First revision of the 3D printed laryngoscope

When tested in a manikin, this design failed at the hinge point of the blade with the handle. To mitigate this, the blade and handle assembly was made into a one-part device where the handle was directly fixed onto the handle.

4.2.2 DESIGN REV. 2

Previous literature [21] [25] [27] shed light on some potentially critical locations of stress on the laryngoscope. During intubation the blade tip experiences the maximum load during intubation, the top surface of the blade is an area of contact with the upper maxillary incisors, the under surface of the blade compresses the tongue, and the area of maximum bending stress and torque is the interface between the handle and the blade. This design was incorporated with cut-outs for sensor placement; 7SIGMA sensors were used. Rectangular slabs of sensor material were embedded in the slots made at the blade tip, mid-way along under-surface of the blade, and the top surface of the blade. To calculate the bending in the material the fourth sensor was stretched between two dove tail slots made in the device. One slot was placed in the handle and the other was in the under surface of the blade close to the junction of the blade and handle. The diagram below depicts the 3D printed version of the design with the slot labelled for their respective sensors.

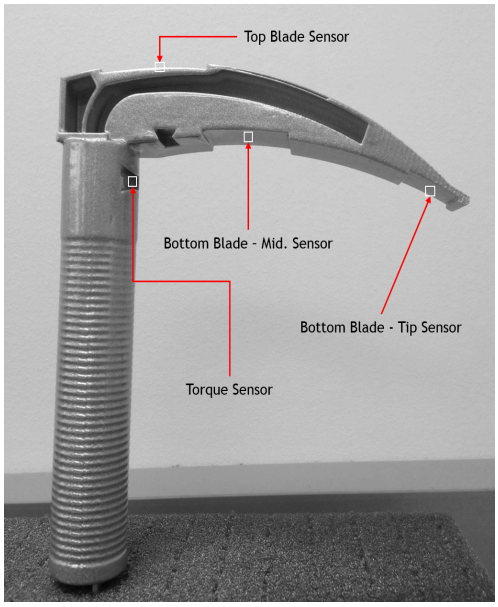

Figure 37. Design rev. 2 with slots for compliant sensors

Since these sensors could be modeled as force resistive sensors, a voltage divider circuit was built on a shield for each sensor and interfaced to an Arduino Mega microcontroller.

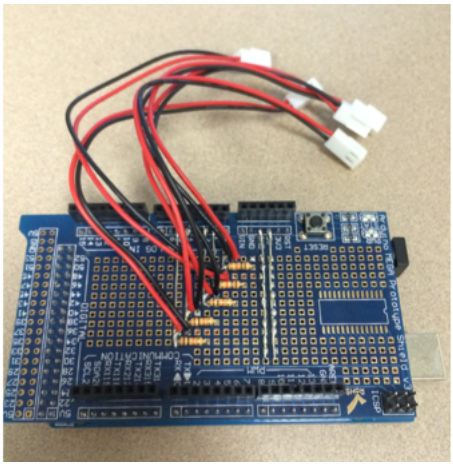

Figure 38. Arduino Mega with a shield. Voltage divider circuits for five sensors soldered onto the shield

The laryngoscope with the embedded sensors was used to intubate the CREST manikin, Cam. The anatomy of this manikin was proven to be more true to actual human anatomy than other popularly used off-the-shelf manikins. The airway of this manikin was instrumented with similar 7SIGMA compliable force resistive sensors. The sensors were placed in the teeth, epiglottis, trachea, esophagus, vocal cords, and the tongue. Intubations were qualitatively evaluated initially to understand the functioning of the sensors in use. Since the 7SIGMA sensors were not calibrated, only a relative force with respect to time was obtained but no accurate force values. This information was adequate to assess an intubation from the perspective of contact especially if the ETT was placed in the esophagus instead of the trachea. Although quantitative information was not obtained through this experiment, no qualitative information was obtained through the sensors embedded in the laryngoscope, too. Based on the construction of these sensors it was concluded that they gave an only adequate force range in axial tension or compression. Therefore, significant deformation of the sensor would be required for an amplified force range. The sensor was mounted on a hard surface (laryngoscope blade), and the force applied on the sensor was normal to its surface. This did not allow for adequate sensor deformation, and an adequate force range was not obtained.

4.2.3 PRESSURE FILM—A QUALITATIVE FORCE DISTRIBUTION EXPERIMENT

From the previous sections it was hence concluded that the SparkFun Electronics [57] force-resistive sensors and the 7SIMGA compliable force-resistive sensors were not applicable to this project. More was needed than to record forces at a guessed location along the laryngoscope, a pressure distribution along each face of the blade would be more relevant.

A pressure film was chosen to replace the sensors; it was mounted on the top and bottom surface of the laryngoscope blade. The Pressurex micro® pressure film [60] was the choice of pressure film to map the pressure distribution around a Macintosh laryngoscope blade The figure below shows the position of the films on the blade.

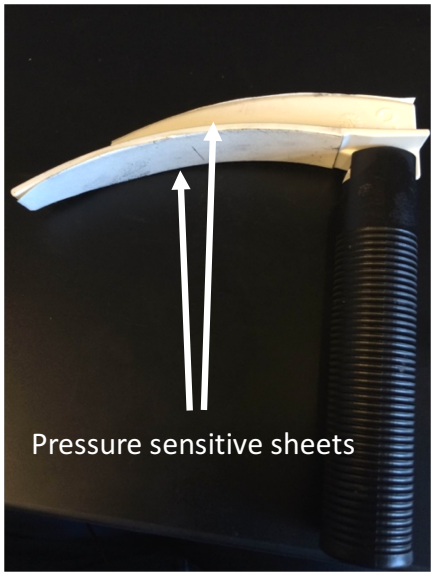

Figure 39. Macintosh laryngoscope blade mounted with Pressurex-micro pressure films

The Pressurex micro® was acquired from Sensor Products Inc. [60]. This film has two layers, the lower pressure sensitive layer for the impression and the upper carbon paper for imprinting. The pressure sensitive layer of the film was mounted on the laryngoscope using a spray-on adhesive and the carbon paper was placed on the lower layer and wrapped around using adhesive paper. Two laryngoscopes were mounted with the pressure-film; one was used to intubate the CREST manikin and the other was used to intubate the Laerdal

manikin. One successful intubation was performed on each manikin with a laryngoscope mounted with the pressure-film. The carbon layer was then removed from the blade and the underlying pressure sensitive layer was photographed. A total of four images were captured from this qualitative experiment—the top and bottom films of both the laryngoscopes.

Image processing algorithms were used to map each film and to obtain an accurate recording of forces on them. First a grayscale filter was applied on the images. Then, to avoid the effect of varying lighting, each image was initially blurred using a Gaussian filter and then a contour plot of the image was produced. The Gaussian filter equation is presented below.

$$g(x,y) = \frac{\exp\left(-\frac{x^2+y^2}{2\sigma^2}\right)}{2\pi\sigma^2}$$

Where: $\sigma = 1.5$

The standard deviation of the Gaussian function was represented by σ. A value of 1.5 adequately blurred and darkened the image such that the brightness of the film was perceived as constant throughout its length.

Top film dimensions: Width = 0.5”, length = 4.2”

Bottom film dimensions: Width = 0.9”, length = 4.2”

Contour plots created had x and y axis scales in terms of pixels. Those were manually remapped to an inch’s scale using the formula below:

$$Position = \frac{pixel\ value}{max.pixel\ value} * width(or\ length) of\ film$$

Example calculation:

$$Position = \frac{1000}{3102} * 4.2"$$

$$\boldsymbol{Position = 1.35"}$$

Results and discussion from Laerdal manikin simulator

The image below shows a top view of the laryngoscope blade with the pressure film mounted on it. The coordinate system with a chosen origin is also labelled on it.

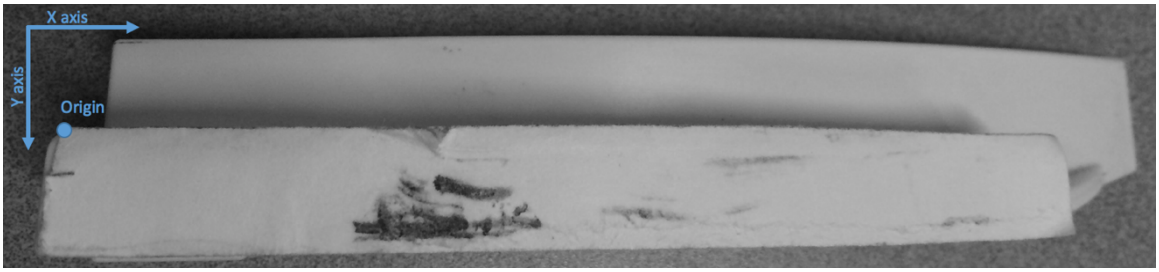

Figure 40. Top view of blade with pressure film

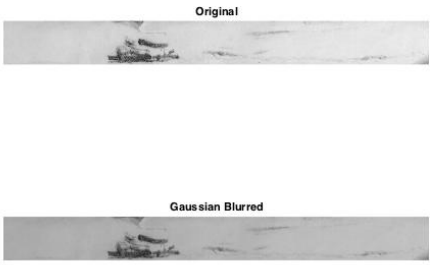

Figure 41. Original image and Gaussian blurred of the top film

The figure above depicts a black and white version of the original picture of the pressure film along with its Gaussian blurred form. The dark marks on the blade are the pressure points experienced by the blade. A contour plot of the modified image is shown below. This plot depicts an accurate distribution of forces on the film, along with dimensions.

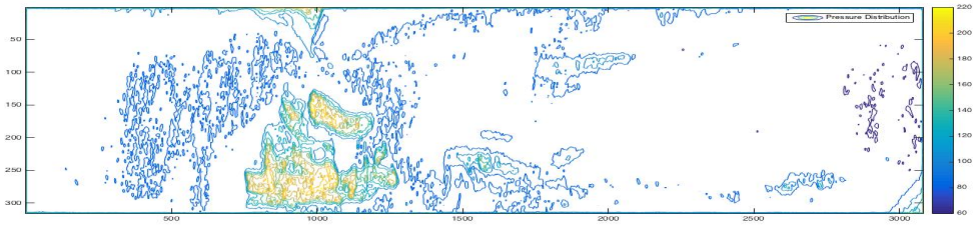

Figure 42. Contour plot of top surface film

The legend is a scale of the intensity of the pressure; this scale ranges from 0-255 and is a relative intensity. It can be concluded that the only area of high pressure is the region at 1.35” along the x-axis, and this is due to contact with the teeth. There are other regions of contact but with a fractional value of this pressure. These other regions are not representative of any critical forces on the laryngoscope or contact with anatomy during intubation. The only expected region of contact, the upper maxillary incisors, was verified by this test.

The same algorithm was applied to the lower surface of the blade. The image below is of the blade with the mounted pressure film and coordinate system used.

Figure 43. Bottom view of blade with pressure film

The original and Gaussian blurred versions of the film are shown below. Since the bottom film is not a perfect rectangle, the cut-out region was made completely white and then the Gaussian filter was applied. This ensured that no background area was considered in the contour plot.

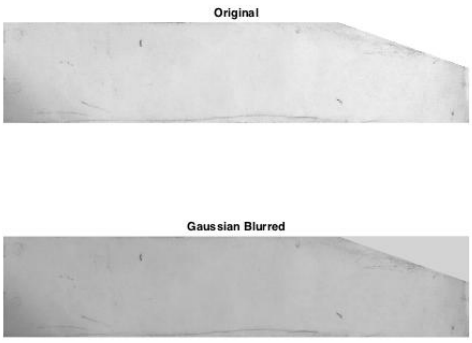

Figure 44. Original image and Gaussian blurred of the bottom film

The contour plot of the bottom pressure film is depicted below. It can be seen that there is no significant pressure region seen. This was attributed to the fact that the pressure paper did not record any readings from the contact with the epiglottis. Since the intubation was successful it can be concluded that there was adequate contact with the posterior surface of the epiglottis and the vallecula. It has been seen earlier that there are lifting forces on the tongue during intubation, but no significant forces were recorded on the pressure film. Therefore, it can be concluded that this pressure was only effective in recording high pressures but not forces. The area of contact with the teeth is very low, whereas with the tongue and vallecula is much larger. Hence there were significant values seen due to the contact with the teeth and not the epiglottis, tongue, or vallecula.

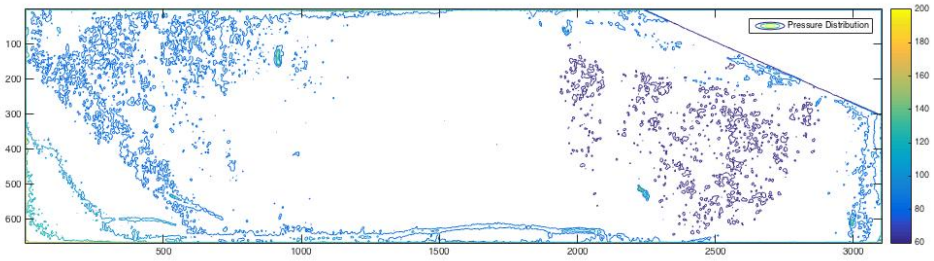

Figure 45. Contour plot of top surface film

Results and discussion from CREST manikin simulator

The same algorithm was applied to the films tested on the CREST manikin. The pressure film mounted on the top with a labelled coordinate system and origin, along with the original and Gaussian blurred version of the pressure film, and the contour plot is presented below.

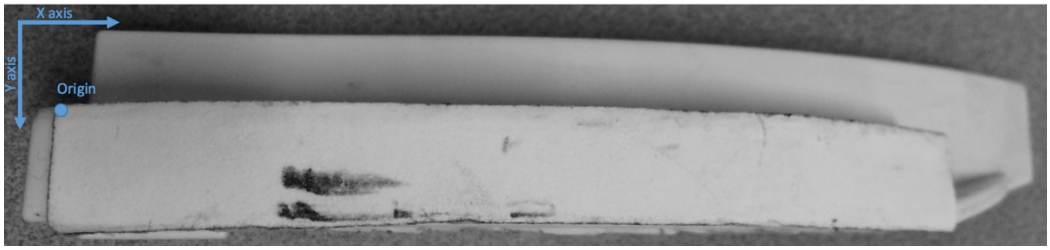

Figure 46. Top view of blade with pressure film (CREST manikin)

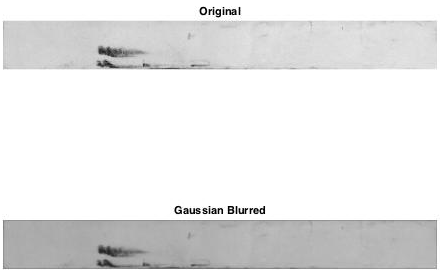

Figure 47. Original and Gaussian blurred version of the top film (CREST manikin)

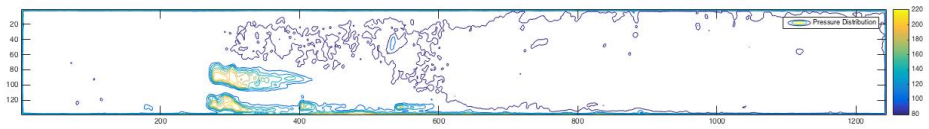

Figure 48. Contour plot of top film (CREST manikin)

The contour plot shows one region along the film where a significant impression was observed. Just as was seen on the top film that was tested on the Laerdal manikin simulator, this impression was due to contact with the upper maxillary incisors. Comparing the top films of both manikins it can be seen that there was less area of contact made, and the magnitude of the impression was lower with the CREST manikin. This is attributed to the fact that the CREST manikin had a larger/less stiff mouth opening in comparison to the Laerdal manikin simulator. The Laerdal manikin simulator has been known to have to rigid mouth opening, simulating an inaccurate intubation situation.

The results obtained for the bottom film are presented below.

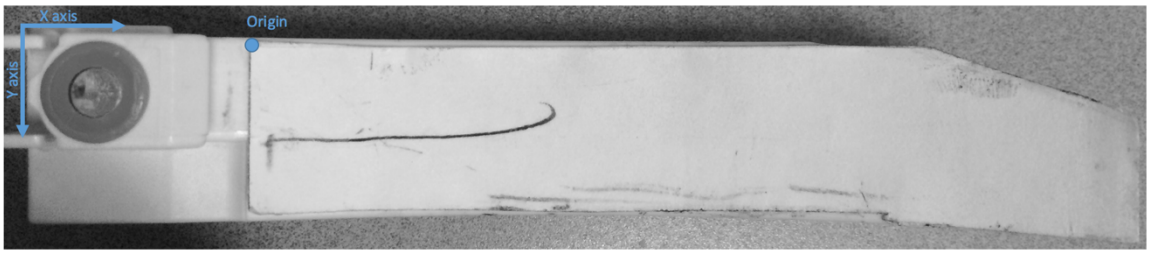

Figure 49. Bottom view of blade with pressure film (CREST manikin)

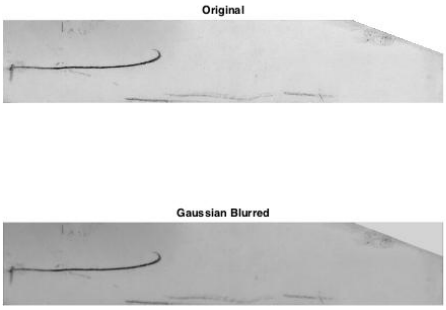

Figure 50. Original and Gaussian blurred version of bottom film (CREST manikin)

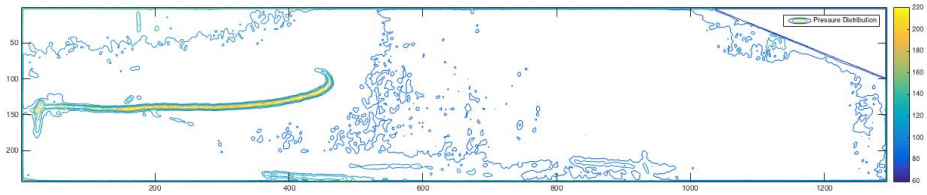

Figure 51. Contour plot of bottom film (CREST manikin)

The above film representation and contour plot it can been seen that there were no significant pressure peaks on the lower surface of the blade. There is one region close to the proximal end of the film with a marking, but that was made due to accidental contact of the handle with the lower surface of the blade. When the handle was installed onto the blade, a small area came in contact with the film and hence the impression is visible. This has no relevance with the procedure of intubation and laryngoscopy. The rest of the film shows no significant contact pressure with the tongue or the epiglottis. This was observed with the Laerdal manikin simulator, too, and the same conclusion was drawn. There wasn't adequate pressure applied on the epiglottis or in the vallecula to produce an impression on the film. There was no significant pressure applied on the tongue, too.

Through this experiment it was seen that the pressure film used was not adequate for this application. The only significant finding was the contact with the upper maxillary incisors in both the manikins, using a standard Macintosh 3 laryngoscope blade. Therefore, a film with a lower pressure and force threshold would produce a better pressure distribution understanding along the lower blade surface.

4.3 CONCLUSION

The above performed experiments coupled with previous force studies on laryngoscopes provide a good platform to design and test a new laryngoscope blade. Critical areas on the laryngoscope and in the upper airway have been identified. The Laryngoscope step came in contact with the upper maxillary incisors, the blade tip in the vallecular behind the epiglottis, and a large portion of the spatula with the tongue. Testing a laryngoscope blade is as critical as the design. Preliminary force testing verified forces on the laryngoscope and airway. The manikin and cadaver effectiveness study proved that the TruCorp® AirSim®, Laerdal, and the CREST manikin would be the apt tools to verify a laryngoscope design.

5. THEORY AND DEVICE DESIGN

The last few decades have shown a proliferation in intubation devices, both for direct and indirect laryngoscopy. Although there have been laryngoscopes that have proven to be more effective than the standard Macintosh laryngoscopes they have not become popular in the hospital and pre-hospital settings. Previously mentioned studies have shown the efficacy of the Glidescope®, Airtraq™, and CMAC over the Macintosh laryngoscope in difficult intubations [30] [31] [32]. Since these three are video-laryngoscopes they are not readily available in all operating rooms and in the prehospital setting. This is due to the high expense associated with video-laryngoscopes and the learning curve associated with them. Operators still prefer the Macintosh laryngoscopes in most settings.

5.1 DESIGN THEORIES

There have been no standards or algorithms set up or prescribed for laryngoscope design. Approximations based on previous manikin and clinical tests and studies and have been the driving factors behind new designs. These subjective tests do not ensure reproducibility or success in the long term. Some of these practical methods tried are x-ray laryngoscopy, clinical trials, and use of cadavers [36]. In the attempt to standardize intubation studies the standard sniffing position for intubation was used. Unfortunately, due to the limitations associated with standardizing clinical studies a critical theoretical analysis method was necessary. Marks [36] were one of the first people to developed and documented a method to evaluate blade design to aid in future device design and evaluation. This theory was developed after studying x-ray laryngoscopies in the standard intubation position of a 35^{o} neck extension and a 15^{o} face place extension. This is considered as the standard intubation position when the blade tip engages the hyoid bone and the top surface of the blade is in contact with the upper incisors. Two important labels were made—J was the mid-point between the mandibular condyles and S was the mid-point of the mandibular symphysis-menti [66].

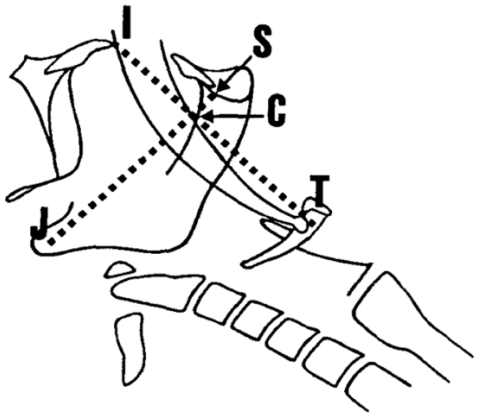

Figure 52. Sagittal view of the upper airway during laryngoscopy [36]

Blades were graphically evaluated by placing their tips at the origin of a graphing paper such that their proximal steps were parallel to the y axis. The tips of the blades were labelled T. A line was then drawn from the point of contact of the blade with the incisors (I) to the tip. This length was representative of the depth of insertion of the blade during intubation. The first angle measured was the eye-line displacement, EIT. The line IE originated from I and was drawn tangential to the upper surface of the lower surface of the blade. Another point, M (fig. 53), was chosen as a point on the lower surface of the blade. M was at the level of the mandible and along the line JS. The angle MIT was representative of the sub-mandibular space. The angle MIT could be either positive or negative based on the position, either posterior or anterior to IT. Angle MIT was taken as positive if the blade lay in front of IT, meaning that the blade would occupy the available submandibular space. If the blade would lie behind IT, MIT was taken as negative. This meant that there is space in the mandible for the tongue and soft tissue to be compressed into. Therefore, the ideal blade would possess the minimum eye-line deviation (EIT) and maximum negative mandible space, or the minimum sum of both angles. This study compared the Soper 3, Miller 3, and Macintosh 1, 2, 3, and 4 blades. Although the Soper blade possessed the lowest EIT, it wasn't suitable or difficult intubations due to the high value of MIT. The most suitable values were obtained with the Macintosh 3 and 4 blades; they had higher eye-line displacement values but the combination values were lower than the other evaluated blades. This study showed a reproducible method for blade analysis.

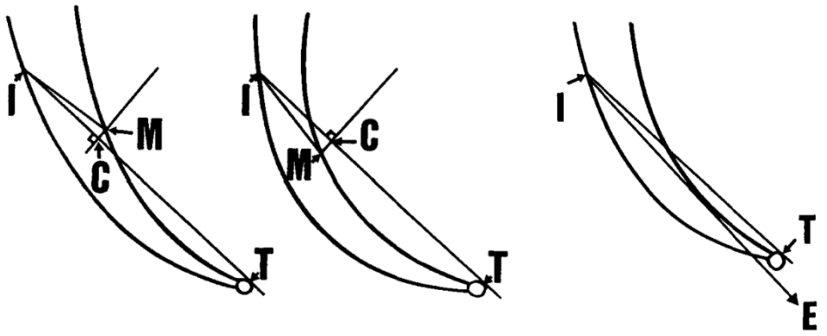

Figure 53. Hyoid bone movement angle MIT (left), eye-line displacement angle EIT (right) [36]

This theory was applied on contemporary rigid and flexible blades by Yardeni [37]. The Standard Macintosh, Classical Macintosh, Miller, English Macintosh, McCoy, and the Flexiblade™ were compared based on their eye-line displacement (EIT) and mandibular encroachment (MIT) with respect to blade insertion depths. The Flexiblade™ in the straight position and Miller blade had the minimum eye-line displacement but reduced the submandibular space for the tongue. This would result in excessive upward forces and head extension during intubation, therefore, a problem in patients with cervical spine injuries and difficult airways. Since only the tip of the McCoy laryngoscope is flexible, there was no difference in the line of view in the neutral and fully engaged state. The final conclusion of the study was that the English Macintosh 4 blade was the most effective at all insertion depths; it would be the choice of instrument for routine intubations. Other conclusions made were that a longer blade length would be more effective, even if the entirety would not be inserted, and the Flexiblade™ would be a good solution for routine and difficult intubations. Due to its continuous flexible nature, the Flexiblade™ functioned as multiple blades based on the degree of flexure. It was also observed that the distal curved portion of a longer blade would be more effective than the entire length of a shorter blade.

Each feature of a laryngoscope has a function which decides the mechanics and maneuvering of the blade during intubation. External factors such as glottis viewing, mouth opening, dentition, size of tongue, and size and morphology of the epiglottis are what have

to be smoothly tackled by an anesthesiologist, using a laryngoscope, for a smooth intubation. The flange height, curvature of the blade, the presence of movable segments, and width of the blade, all decide the functioning of the blade; these are the modifiable features of a laryngoscope. Levitan [33] compared the range of view of eight laryngoscopes. It was concluded that the video-laryngoscopes did provide a better range of laryngeal view than the direct laryngoscopes. The drawbacks of the video-laryngoscopes were with the insertion of the endotracheal tube to establish the airway due to absence of an established line of sight to the larynx. Tube insertion during direct laryngoscopy has been more effective because of the line of sight established to the larynx; this mitigates the risk upper airway soft tissue damage from the tube tip.

5.2 CURRENT DESIGN THEORY—MULTILOOP SYNTHESIS

This review has proved that laryngeal exposure is the primary concern in direct laryngoscopy. Excessive forces applied on the airway in difficult intubations due to the lack of laryngeal exposure have also been proved to be detrimental to soft tissue. Therefore, it can be hypothesized that a blade which can provide an extra little lift, without increasing intubation forces, to push the tongue out of the way and lift the epiglottis might improve the laryngeal view. Levering tip laryngoscopes primarily focused on the epiglottis but were not conclusively proven to be more effective than the Macintosh blade laryngoscope. There have been several studies attesting to the efficacy of the levering tip laryngoscope in difficult intubations although in some situations this laryngoscope has worsened the view [38] [39]. The activation of the tip forces the blade to move downwards towards the larynx, thereby obstructing the view of the larynx in some situations [38]. It has been proven that this device has improved CL views from a 3 to a 2 or 1, but hasn't shown much improvement in CL grade 4 situations. The CLM (Corrazelli-London-McCoy) blade, also known as the McCoy laryngoscope, has been most effective in cases of CL grade 3 views in patients with cervical spine immobilization [40]. Macintosh laryngoscopes were more effective than levering tip blades in easy intubations. Adding flexibility to a larger portion of the blade would aid in tongue compression and easier access to the epiglottis for lift,

thereby improving glottis viewing. There have been flexible designs, but there has not been conclusive evidence that those devices would out-perform the Macintosh laryngoscope [41] [42].

5.2.1 DESIGN SYNTHESIS

Previous laryngoscopes have had one hinged segment which added a degree of freedom to the device. These blades were modified and incorporated by mechanisms to activate the hinged tip and control its rotation. To increase this flexibility, another movable segment can be added in conjunction to a flexible blade tip. Therefore, a mechanism could be employed to add and control the flexibility of a laryngoscope.

Problem Definition

To design a flexible laryngoscope blade with two movable segments using mechanism synthesis where one movable blade segment is distal to the other; the blade design will resemble a Macintosh blade design. The first task to define is the degree of freedom of the mechanism (DOF), which is the number of independent input parameters which can define the position of every link of a mechanism with respect to a reference fixed point (ground) [61]. The mechanism would have one DOF since an input angle would be sufficient to completely describe the rest of the mechanism. The mechanism constraints and tasks are the next aspects to be defined. A Macintosh laryngoscope blade has a slender and compact design with a limited space for additional features. All links should be constrained by the area of the blade to avoid altering the mechanism of intubation.

Type Synthesis

Type synthesis is the first step in mechanism design after the problem definition has been defined [61]. It is used to determine the number of links and joints in a mechanism along with other potential elements such as springs, cams, gears etc. Since the motion of two moving links is specified, where one is more distal than the other, this mechanism task cannot be achieved with a basic four bar design. A six bar mechanism can possibly achieve

this task. These mechanisms consist of binary and ternary links. Binary links are rigid members with two joints and ternary links are rigid member with three staggered joints. There are two topologies of six bar mechanisms—Watt and Stephenson. These mechanisms are classified based on placement of ternary links [61]. Ternary links are directly connected in Watt chains and are separated by a binary link in Stephenson chains. These six bar mechanisms have multiple forms based on the way the links are arranged with respect to each other and ground. There are two types of Watt chains (Watt I and Watt II) and three forms of Stephenson chains (Stephenson I, Stephenson II, and Stephenson III). These supplemental forms of the two aforementioned topologies are known as mechanism inversions and are presented below:

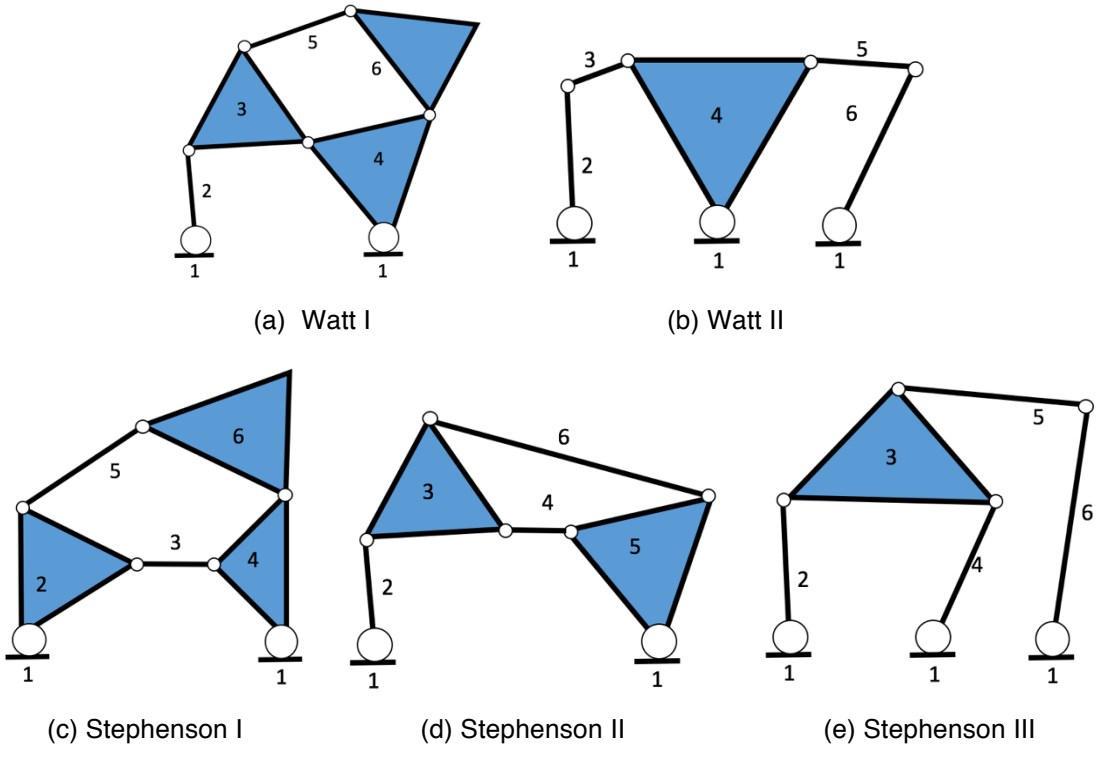

Figure 54. Schematics of the inversions of the Watt and Stephenson six-bar topologies

The next step is to determine which of the Watt and Stephenson topologies might work for the application. A blade with two movable segments and one fixed segment suggests that the fixed (ground) segment would be the most proximal segment. The first movable segment would be directly connected to the fixed part of the blade and the distal segment (blade tip) would be connected to the first movable segment. Therefore, the first movable blade segment would have at least three pin joints—one hinged to the ground, one to the blade tip, and a potential third for motion control of this segment. This segment would have to be connected to the distal laryngoscope element which can be represented as the output link. This output link will possess a complex motion; the shape of this output link will resemble the shape of a Macintosh blade tip. This rules out a Stephenson III topology because no ternary link is connected to the ground, and a Watt II mechanism because the output link has a circular arc motion. A mechanism is required which can produce a long reach and have a slender profile. The position of the fixed pivot of the input link I will be located at the proximal end of the vertical step. Another constraint is that no moving link can move out of the bounds of the Macintosh blade profile throughout the motion of the mechanism. A Stephenson I mechanism was chosen since the input link interfaces with other ternary link (movable segment) and the output link (distal tip), each, through a binary link, making it a ternary link. One hinge point of the input link is with ground and the other two are connected to each of the two movable blade segments through binary links. Therefore, the other ternary link of the mechanism is the first movable segment which is connected to the input link through a two force member. The output link is a binary link connected to input ternary through a two force member. There were two other chains which might have also fit the above design constraints—Stephenson II and Watt I. Those were neither synthesized or analyzed. This is the complete definition of the mechanism.

5.2.2 MECHANISM SYNTHESIS

Type synthesis concluded that a standard six-bar Stephenson I linkage would be suitable for this application. No higher order joints [62] or sliders were present in the mechanism. A three precision point motion generation with prescribed timing with ground pivot

specification was chosen for the synthesis [61]. This form of synthesis is applied when the ground (fixed) pivots and the trajectory of the output link are known. The ground (fixed) pivot locations are defined and an approximate blade tip trajectory is known. The initial configuration of the blade was treated as the first position of the mechanism. The synthesis method for a six-bar mechanism is known as a multi-loop synthesis; this synthesis form is developed using the dyad or standard form of loop equations [61]. Most mechanisms can be represented as a combination of dyads (vector pairs).

Multi-loop Synthesis

This synthesis method uses the standard form to write vector closed loop equations defining a mechanism. Each link is described as a complex number vector and has a rotation associated with it. This rotation defines the orientation change of a link when a mechanism is in a different precision position. A Stephenson I mechanism can be defined at each state by three closed vector loops. A schematic of the mechanism with the vector representation is shown below.

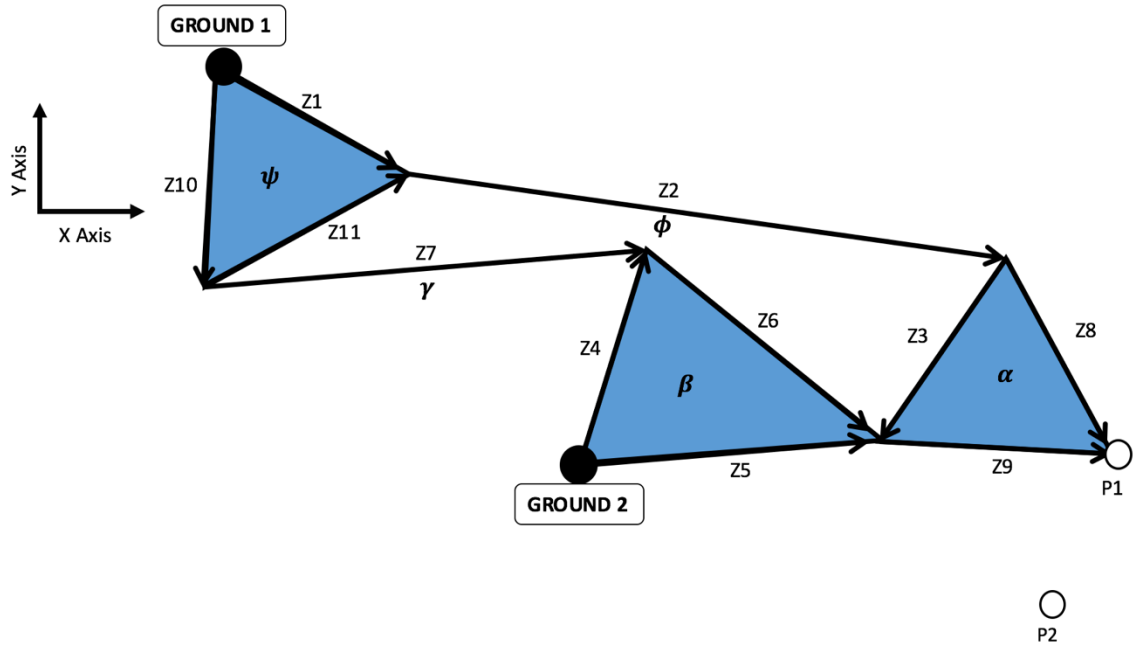

Figure 55. Schematic of the six bar mechanism with links. Angles labelled represent the rotations of the respective links

Choosing precision points

Precision point 1 was chosen on the basis of the length of the laryngoscope in the standard configuration and the shape of a Macintosh 3 laryngoscope. Precision point 2 was chosen at an approximate location such that the middle section of the blade would be deflected greater than the blade tip. Precision point 3 was chosen on the basis of the final desired position of the blade tip. The final position was chosen such that the final segment (under surface of the blade tip) would be parallel to the handle.

Standard Form and Multi-Loop Algorithm

The algorithm along with a sample calculation is presented below.

Known variables: **P1**, **P2**, **P3**, α_2, α_3, $\mathbf{A_o}$, $\mathbf{B_o}$, $\boldsymbol{\delta_2}$, $\boldsymbol{\delta_3}$, $i = \sqrt{-1}$**; (vectors represented in bold font)**

Where **P1**, **P2**, and **P3** were the three precision positions of the end of the blade, α_3 the final relative rotation of the coupler link, $\mathbf{A_o}$ and $\mathbf{B_o}$ the prescribed ground pivots, and $\boldsymbol{\delta_2}$ and $\boldsymbol{\delta_3}$the vectors joining **P1**-**P2** and **P1**-**P3** respectively. The mechanism was split up into three loops.

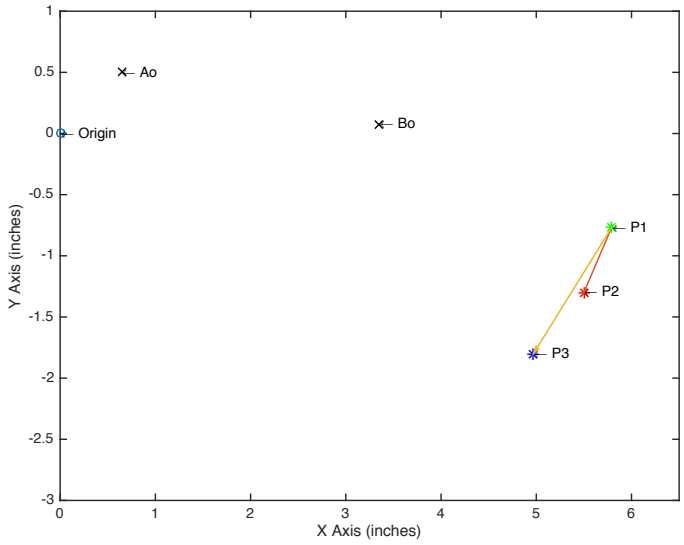

Figure 56. Ground pivots and precision points

$\boldsymbol{Ao} = 0.65 + 0.5i$

$\boldsymbol{Bo} = 3.35 + 0.075i$

$\boldsymbol{P1} = 5.79 - 0.77i$

$\boldsymbol{P2} = 5.5 - 1.3i$

$\boldsymbol{P3} = 4.97 - 1.8i$

Loop 1: Z1 – Z2 – Z8

The closed loop equations are presented below.

$$\boldsymbol{Z1}\left(e^{i\psi_2} - 1\right) + \boldsymbol{Z2}\left(e^{i\varphi_2} - 1\right) + \boldsymbol{Z8}\left(e^{i\alpha_2} - 1\right) = \boldsymbol{\delta_2}$$
$$\boldsymbol{Z1}\left(e^{i\psi_3} - 1\right) + \boldsymbol{Z2}\left(e^{i\varphi_3} - 1\right) + \boldsymbol{Z8}\left(e^{i\alpha_3} - 1\right) = \boldsymbol{\delta_3}$$

With four equations and ten unknowns, six free choices were available. Based on the geometry of a Macintosh laryngoscope **Z8**, α_2, and α_3 were the free choices; α_2, ψ_2 and ψ_3 were iterated through an acceptable range of angles. The rotation angle for the input link ψ_2 was iterated through values ranging from 5° to 50°, and ψ_3 was iterated from 5° to 90°. The rotation of the output link α_2 was iterated though -10° till -30°. It was a negative rotation since a clockwise motion of the output link is required. The rotation of the output link for the final position, α_3, was also a prescribed quantity and was chosen on the basis of the curvature of the blade and desired device movement. The final free choice of **Z8** was made on the basis of the shape of the distal end of the step. This way the closed loop equations could be rearranged as:

$$\boldsymbol{Z1}\left(e^{i\psi_2} - 1\right) + \boldsymbol{Z2}\left(e^{i\varphi_2} - 1\right) = \boldsymbol{\delta_2} - \boldsymbol{Z8}\left(e^{i\alpha_2} - 1\right) = \boldsymbol{\delta_2'}$$
$$\boldsymbol{Z1}\left(e^{i\psi_3} - 1\right) + \boldsymbol{Z2}\left(e^{i\varphi_3} - 1\right) = \boldsymbol{\delta_3} - \boldsymbol{Z8}\left(e^{i\alpha_3} - 1\right) = \boldsymbol{\delta_3'}$$

Where,

$\boldsymbol{Z8} = 0.8(cos(40°) - sin(40°))$

$\alpha_3 = 50^o$

For ground pivot specification vectors from the fixed pivots to the precision points were specified; those locations were at $\boldsymbol{\delta_2'}$ and $\boldsymbol{\delta_3'}$**.**

$$\boldsymbol{R1} = \boldsymbol{P1} - \boldsymbol{Z8} - \boldsymbol{A_o}$$

$$\boldsymbol{R2} = \boldsymbol{R1} + \boldsymbol{\delta_2'}$$

$$\boldsymbol{R3} = \boldsymbol{R1} + \boldsymbol{\delta_3'}$$

The augmented matrix of the above set of equations:

$$\begin{vmatrix} 1 & 1 & \boldsymbol{R1} \\ e^{i\psi_2} & e^{i\varphi_2} & \boldsymbol{R2} \\ e^{i\psi_3} & e^{i\varphi_3} & \boldsymbol{R3} \end{vmatrix} = 0$$

Expanding the above determinant:

$$\left(-\boldsymbol{R3}e^{i\psi_2} + \boldsymbol{R2}e^{i\psi_3}\right) + \left(\boldsymbol{R3} - \boldsymbol{R1}e^{i\psi_3}\right)e^{i\varphi_2} + \left(-\boldsymbol{R2} + \boldsymbol{R1}e^{i\psi_2}\right)e^{i\varphi_3} = 0$$

This can be written as:

$$\boldsymbol{d1} + \boldsymbol{d2}e^{i\varphi_2} + \boldsymbol{d3}e^{i\varphi_3} = 0$$

Where:

$\psi_2 = 10^o, \psi_3 = 23^o, \alpha_2 = 22^o$

Solving for φ_2 and φ_3:

$$\varphi_2 = cos^{-1}\left(\frac{D3^2 - D1^2 - D2^2}{2 * D1 * D2}\right) + \Delta 1 - \Delta 2$$

If:

$$cos^{-1}\left(\frac{D3^2 - D1^2 - D2^2}{2 * D1 * D2}\right) < 0$$

$$\varphi_2 = -cos^{-1}\left(\frac{D3^2 - D1^2 - D2^2}{2 * D1 * D2}\right) + \Delta 1 - \Delta 2 = \boldsymbol{-6.09^o}$$

$$\varphi_3 = angle\left(\frac{-D1e^{\Delta 1} - D2e^{\Delta 2}e^{\varphi_2}}{D3 * e^{i\Delta 3}}\right) = \boldsymbol{-13.8^o}$$

Where,

$$D1 = abs(\boldsymbol{d1})$$

$$D2 = abs(\boldsymbol{d2})$$

$$D3 = abs(\boldsymbol{d3})$$

$$\Delta 1 = angle(\boldsymbol{d1})$$
$$\Delta 2 = angle(\boldsymbol{d2})$$
$$\Delta 3 = angle(\boldsymbol{d3})$$

Using the standard form equation, **Z1** and **Z2** could be found using matrix inversion:

$$\begin{bmatrix} \boldsymbol{Z1} \\ \boldsymbol{Z2} \end{bmatrix} = \begin{bmatrix} e^{i\psi_2} - 1 & e^{i\varphi_2} - 1 \\ e^{i\psi_3} - 1 & e^{i\varphi_3} - 1 \end{bmatrix} \begin{bmatrix} \boldsymbol{\delta_2'} \\ \boldsymbol{\delta_3'} \end{bmatrix}$$
$$\begin{bmatrix} \boldsymbol{Z1} \\ \boldsymbol{Z2} \end{bmatrix} = \begin{bmatrix} \boldsymbol{0.487 - 0.206i} \\ \boldsymbol{4.04 - 0.549i} \end{bmatrix}$$

Since α_2, ψ_2, and ψ_3 were iterated through a series of values, there were distinct values of **Z1**, **Z2**, φ_2, and φ_3 obtained for each solution set.

Therefore from loop one, the known variables were **P1**, **P2**, **P3**, **Z1**, **Z2**, φ_2, φ_3, α_2, α_3, ψ_2, and ψ_3.

Loop 2: Z5 – Z9

$$\boldsymbol{Z5}\left(e^{i\beta_2} - 1\right) + \boldsymbol{Z9}\left(e^{i\alpha_2} - 1\right) = \boldsymbol{\delta_2}$$
$$\boldsymbol{Z5}\left(e^{i\beta_3} - 1\right) + \boldsymbol{Z9}\left(e^{i\alpha_3} - 1\right) = \boldsymbol{\delta_3}$$

Applying the same algorithm applied to loop 1:

$$\boldsymbol{R1} = \boldsymbol{P1} - \boldsymbol{B_o}$$
$$\boldsymbol{R2} = \boldsymbol{R1} + \boldsymbol{\delta_2}$$
$$\boldsymbol{R3} = \boldsymbol{R1} + \boldsymbol{\delta_3}$$

The augmented matrix of the above set of equations:

$$\begin{vmatrix} 1 & 1 & \boldsymbol{R1} \\ e^{i\alpha_2} & e^{i\beta_2} & \boldsymbol{R2} \\ e^{i\alpha_3} & e^{i\beta_3} & \boldsymbol{R3} \end{vmatrix} = 0$$

Expanding the above determinant:

$$\left(\boldsymbol{R3}e^{i\alpha_2} - \boldsymbol{R2}e^{i\alpha_3}\right) + \left(-\boldsymbol{R3} + \boldsymbol{R1}e^{i\alpha_3}\right)e^{i\beta_2} + \left(\boldsymbol{R2} - \boldsymbol{R1}e^{i\alpha_2}\right)e^{i\beta_3} = 0$$

This can be written as:

$$\boldsymbol{d1} + \boldsymbol{d2}e^{i\beta_2} + \boldsymbol{d3}e^{i\beta_3} = 0$$

Solving for β_2 and β_3:

$$\beta_2 = cos^{-1}\left(\frac{D3^2 - D1^2 - D2^2}{2 * D1 * D2}\right) + \Delta 1 - \Delta 2$$

If:

$$cos^{-1}\left(\frac{D3^2 - D1^2 - D2^2}{2 * D1 * D2}\right) < 0$$

$$\beta_2 = -cos^{-1}\left(\frac{\boldsymbol{D3^2} - D1^2 - D2^2}{2 * D1 * D2}\right) + \Delta 1 - \Delta 2 = \boldsymbol{-10.1^o}$$

$$\beta_3 = angle\left(\frac{-D1e^{\Delta 1} - D2e^{\Delta 2}e^{\beta_2}}{D3 * e^{i\Delta 3}}\right) = \boldsymbol{-22.3^o}$$

Where,

$$D1 = abs(\boldsymbol{d1})$$
$$D2 = abs(\boldsymbol{d2})$$
$$D3 = abs(\boldsymbol{d3})$$
$$\Delta 1 = angle(\boldsymbol{d1})$$
$$\Delta 2 = angle(\boldsymbol{d2})$$
$$\Delta 3 = angle(\boldsymbol{d3})$$

Using the standard form equation, **Z5** and **Z9** was found using matrix inversion:

$$\begin{bmatrix} \boldsymbol{Z5} \\ \boldsymbol{Z9} \end{bmatrix} = \begin{bmatrix} e^{i\beta_2} - 1 & e^{i\alpha_2} - 1 \\ e^{i\beta_3} - 1 & e^{i\alpha_3} - 1 \end{bmatrix} \begin{bmatrix} \boldsymbol{\delta_2} \\ \boldsymbol{\delta_3} \end{bmatrix}$$

$$\begin{bmatrix} \boldsymbol{Z5} \\ \boldsymbol{Z9} \end{bmatrix} = \begin{bmatrix} \boldsymbol{1.77 - 0.517i} \\ \boldsymbol{0.671 - 0.328i} \end{bmatrix}$$

Loop 3: Z10 – Z7 – Z4

$$\boldsymbol{Z10}\left(e^{i\psi_2} - 1\right) + \boldsymbol{Z7}\left(e^{i\gamma_2} - 1\right) + \boldsymbol{Z4}\left(e^{i\beta_2} - 1\right) = 0$$

$$\boldsymbol{Z10}\left(e^{i\psi_3} - 1\right) + \boldsymbol{Z7}\left(e^{i\gamma_3} - 1\right) + \boldsymbol{Z4}\left(e^{i\beta_3} - 1\right) = 0$$

The algorithm applied to loop 1 was applied to loop 3, too. **Z4** was the free choice, β_2 and β_3 were obtained from loop 2. The loop closure equation was then converted to the standard form:

$$\boldsymbol{Z10}\left(e^{i\psi_2} - 1\right) + \boldsymbol{Z7}\left(e^{i\gamma_2} - 1\right) = \boldsymbol{Z4}\left(1 - e^{i\beta_2}\right) = \boldsymbol{\delta_2''}$$

$$\boldsymbol{Z10}\left(e^{i\psi_3} - 1\right) + \boldsymbol{Z7}\left(e^{i\gamma_3} - 1\right) = \boldsymbol{Z4}\left(1 - e^{i\beta_3}\right) = \boldsymbol{\delta_3''}$$

Where,

Z4 = 0.25 + 0.2i

The vector equations for loop 3:

$$\boldsymbol{R1} = \boldsymbol{B_o} - \boldsymbol{A_o} + \boldsymbol{Z4}$$

$$\boldsymbol{R2} = \boldsymbol{R1} + \boldsymbol{\delta_2''}$$

$$\boldsymbol{R3} = \boldsymbol{R1} + \boldsymbol{\delta_3''}$$

The augmented matrix of the above set of equations:

$$\begin{vmatrix} 1 & 1 & \boldsymbol{R1} \\ e^{i\psi_2} & e^{i\gamma_2} & \boldsymbol{R2} \\ e^{i\psi_3} & e^{i\gamma_3} & \boldsymbol{R3} \end{vmatrix} = 0$$

Expanding the above determinant:

$$\left(\boldsymbol{R3}e^{i\psi_2} - \boldsymbol{R2}e^{i\psi_3}\right) + \left(-\boldsymbol{R3} + \boldsymbol{R1}e^{i\psi_3}\right)e^{i\gamma_2} + \left(\boldsymbol{R2} - \boldsymbol{R1}e^{i\psi_2}\right)e^{i\gamma_3} = 0$$

This can be written as:

$$\boldsymbol{d1} + \boldsymbol{d2}e^{i\gamma_2} + \boldsymbol{d3}e^{i\gamma_3} = 0$$

Solving for γ_2 and γ_3:

$$\gamma_2 = cos^{-1}\left(\frac{D3^2 - D1^2 - D2^2}{2 * D1 * D2}\right) + \Delta 1 - \Delta 2 = \boldsymbol{-1.72^o}$$

$$\gamma_3 = angle\left(\frac{-D1e^{\Delta 1} - D2e^{\Delta 2}e^{\beta_2}}{D3 * e^{i\Delta 3}}\right) = \boldsymbol{-4.15^o}$$

Where,

$$\boldsymbol{D1} = abs(D1)$$

$$\boldsymbol{D2} = abs(D2)$$

$$\boldsymbol{D3} = abs(D3)$$

$$\Delta 1 = angle(D1)$$

$$\Delta 2 = angle(D2)$$

$$\Delta 3 = angle(D3)$$

Using the standard form equation, **Z10** and **Z7** could be found using matrix inversion:

$$\begin{bmatrix}\boldsymbol{Z10}\\ \boldsymbol{Z7}\end{bmatrix} = \begin{bmatrix}e^{i\psi_2} - 1 & e^{i\gamma_2} - 1\\ e^{i\psi_3} - 1 & e^{i\gamma_3} - 1\end{bmatrix}\begin{bmatrix}\boldsymbol{\delta_2''}\\ \boldsymbol{\delta_3''}\end{bmatrix}$$

$$\begin{bmatrix}\boldsymbol{Z10}\\ \boldsymbol{Z7}\end{bmatrix} = \begin{bmatrix}\boldsymbol{-0.207 + 0.279i}\\ \boldsymbol{2.76 - 0.018i}\end{bmatrix}$$

Using vector difference equations it was concluded that,

$$\boldsymbol{Z3} = \boldsymbol{Z8} - \boldsymbol{Z9}$$

$$\boldsymbol{Z3} = -\ 0.058 - 1.86i$$

$$\boldsymbol{Z11} = \boldsymbol{Z1} - \boldsymbol{Z10}$$

$$\boldsymbol{Z11} = -\ 0.3 - 0.0004i$$

The only orientation of the laryngoscope known was the orientation of the coupler link at the final position. The above iterative process produced a list of solutions based on the constraints of the dimensions of the Macintosh laryngoscope and the orientations of the links such that they would not interfere with intubation in their final positions.

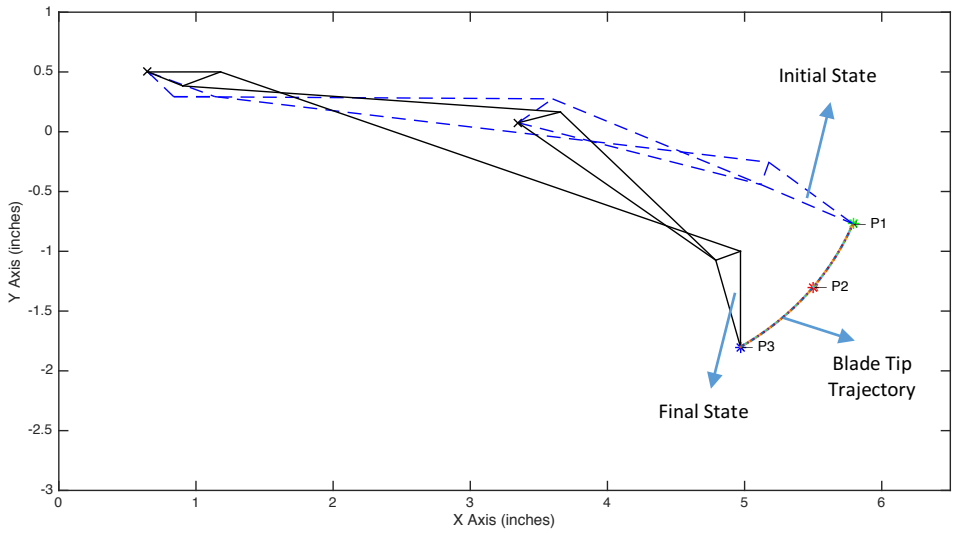

Figure 57. Six-bar chain wireframe at precision position 1 and precision position 3

5.2.3 TRIGGERING MECHANISM

The triggering mechanism of the device was a critical decision and it included an ergonomic factor. Previous devices have included a lever activation either in the front or in the rear of the handle. Both positions of levers pose complications during intubation. Based on the technique used by operators to grip the handle, a lever at the back can easily be engaged even when not wanted. The lever in the front could potentially obstruct the smooth functioning of the blade in patients with a large chest cavity and be engaged prematurely.

The method applied in the current device was the inclusion of slider along a channel in the laryngoscope handle, interfaced with the above six-bar mechanism. A four-bar crank slider mechanism was developed and appended to drive the six-bar mechanism. The slider link

was chosen as the input link and the crank was chosen to be part of the input ternary link of the six bar mechanism. The final binary link dimension was chosen such that the entirety of the motion of the six bar mechanism would be successful and it would not hinder the functionality of the device. The channel was designed such that the structural integrity of the handle was not compromised. The four bar chain and the appended version on the mechanism are presented below.

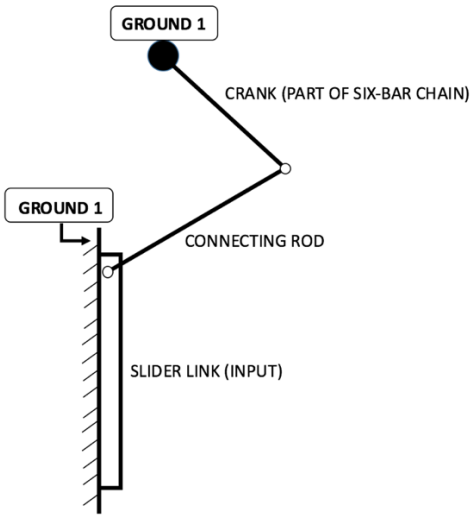

Figure 58. Schematic of a four-bar crank slider chain

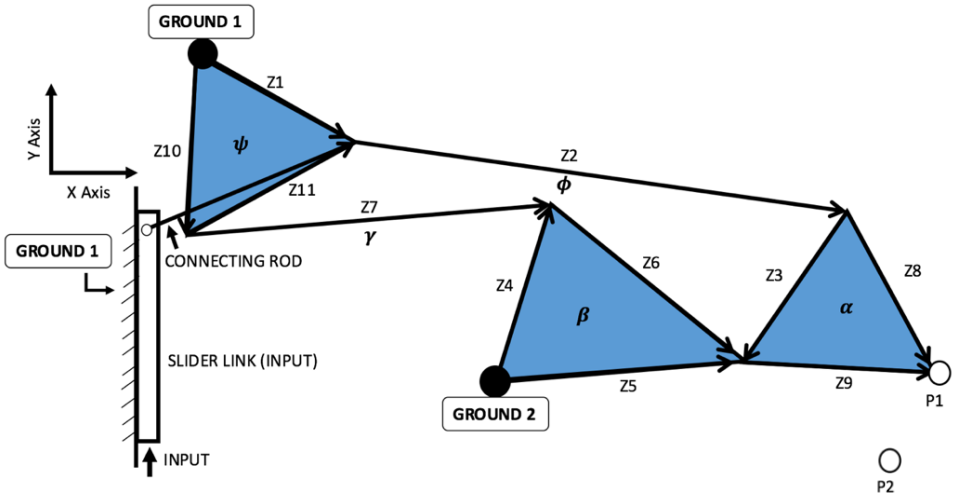

Figure 59. Schematic of the complete

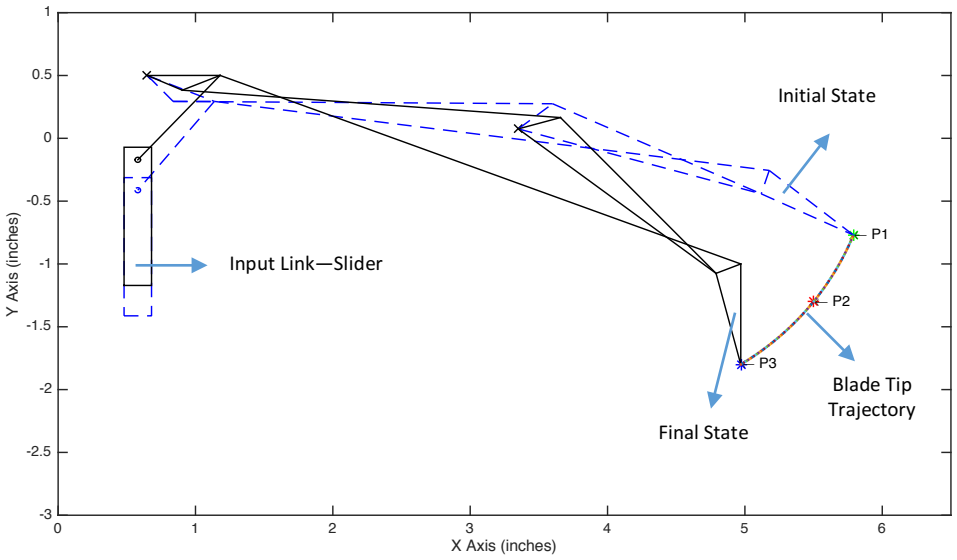

Figure 60. Wireframe of entire mechanism in the initial and final state; mechanism is to scale

5.2.4 MECHANISM ANALYSIS

The multi-loop synthesis described above resulted in a set of solutions based on the constraints set. All constraints set in the algorithm were link length ranges based on the available region of mechanism motion and laryngoscope shape. The two significant factors used to distinguish between mechanisms are transmission angle and mechanical advantage [62].

Transmission angle is the angle between the direction of the velocity of the output link and the relative velocity direction of the driving link of a mechanism [62]. Four-bar mechanisms therefore, consist of one transmission angle while six-bar mechanisms consist of two transmission angles [61][62]. Transmission angle is the measure of the quality of motion. Very large or small transmission angles result in large motion error, and high sensitivity to manufacturing [43]. A transmission angle with the least deviation from 90° is desired. The acceptable range of values are between 30^{o} and 140^{o}. The two transmission angles in a Stephenson I mechanism and the angle in crank-slider four-bar chain are depicted below.

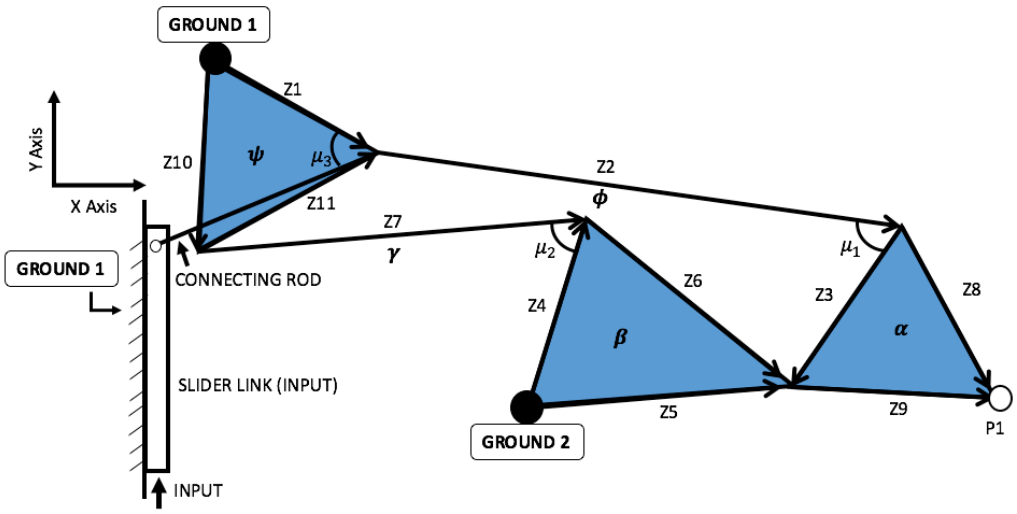

Figure 61. Transmission angles in a Stephenson I mechanism

This mechanism is made up of a four-bar and five-bar mechanism. The transmission angle for the four-bar is straight-forward. The transmission angles calculated below are shown for the initial state of the blade i.e. at precision-position 1.

$$\mu_1 = \cos^{-1}\frac{((\boldsymbol{d})^2 + abs(\boldsymbol{Z11})^2 - abs(\boldsymbol{Z2})^2 - abs(\boldsymbol{Z3})^2 - \boldsymbol{2} * abs(\boldsymbol{Z11}) * \boldsymbol{abs}(\boldsymbol{d}) * \cos(angle(\boldsymbol{p}))}{-2 * abs(\boldsymbol{Z2}) * abs(\boldsymbol{Z3})}$$

$$\boldsymbol{\mu_1 = 80.3^o}$$

Where:

$$\boldsymbol{d = Z5 - Z10 + ground2 - ground1}$$

$$p = angle(\boldsymbol{Z11}) - angle(\boldsymbol{d})$$

The transmission angle μ_2 was calculated the same way. **Z3** was considered the output link and the driven link, **Z2**.

$$\mu_2 = \cos^{-1}\frac{((\boldsymbol{g})^2 + abs(\boldsymbol{Z10})^2 - abs(\boldsymbol{Z4})^2 - abs(\boldsymbol{Z7})^2 - \boldsymbol{2} * abs(\boldsymbol{Z10}) * abs(\boldsymbol{g}) * \cos(angle(\boldsymbol{Z10}))}{-2 * abs(\boldsymbol{Z7}) * abs(\boldsymbol{Z4})}$$

$$\boldsymbol{\mu_2 = 46.8^o}$$

Where:

$$\boldsymbol{g = ground2 - ground1}$$

$$\mu_3 = angleZ1 + \theta_s$$

$$\boldsymbol{\mu_3 = 74.68^o}$$

$angleZ1$ and θ_s are depicted in the figure 62, below:

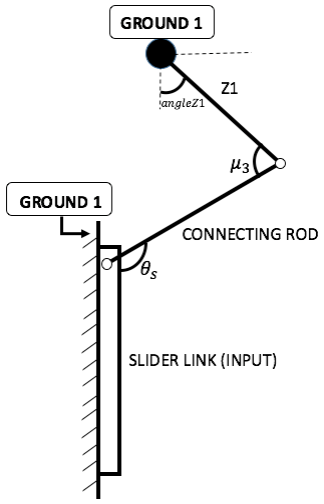

Figure 62. Transmission angle for a crank slider mechanism

Mechanical advantage

Mechanical advantage is a significant metric used in the design of mechanisms [61]. This is defined as the ratio of the output force and the input force applied to drive a mechanism. This is a more deterministic factor than the transmission angle since the effectiveness of the mechanism is quantitative rather than the qualitative nature of the transmission angle. The method applied to calculate the mechanical advantage was done by calculating the ratio of the distance travelled by the input link to that travelled by the blade tip. Two mechanical advantage values were calculated for this mechanism—one for the six-bar Stephenson I chain and the other for the six-bar chain with the input slider appended. A sample calculation is presented below with the mechanical advantage between the initial and final positions of the mechanism.

In a mechanism:

$$Power_{input} = Power_{output}$$

$$Force_{input} Velocity_{input} = Force_{output} Velocity_{output}$$

$$\frac{Force_{output}}{Force_{input}} = \frac{Velocty_{input}}{Velocity_{output}}$$

Based on the above definition of mechanical advantage,

$$\boldsymbol{Mechanical\ Advantage\ (MA)} = \frac{\boldsymbol{Velocty_{input}}}{\boldsymbol{Velocity_{output}}}$$

This was further simplified to:

$$\boldsymbol{MA} = \frac{\boldsymbol{Distance_{input}}}{\boldsymbol{Distance_{output}}}$$

Calculating for the entire range of motion,

$$MA = \frac{\Delta h}{|\boldsymbol{P3 - P1}|}$$

Where Δh is the distance the slider link travelled and $|\boldsymbol{P3 - P1}|$ is the distance between precision position 1 and precision position 3.

$$MA = \frac{\Delta h}{|\boldsymbol{P3 - P1}|}$$

$$MA = \frac{0.2418}{|(4.97 - i * 1.8) - (5.79 - i * 0.77)|}$$

$$\boldsymbol{MA = 0.18}$$

Mechanical advantage for the six-bar chain:

$$MA = \frac{|\boldsymbol{Z1_{initial} - Z1_{final}}|}{|\boldsymbol{P3 - P1}|}$$

Where $\boldsymbol{Z1_{initial}}$ and $\boldsymbol{Z1_{final}}$ are the vectors representing the link Z1 (figure 57) in the initial and final position and ϕ_3 is the angle of deviation of the input link in the final position from the initial position.

$$MA = \frac{|(0.49 - \mathrm{i} * 0.21) * (1 - \exp(\mathrm{i} * \phi_3)|}{|(4.97 - i * 1.8) - (5.79 - i * 0.77)|}$$

$$\boldsymbol{MA = 0.16}$$

5.3 DESIGN EVOLUTION

The first generation of prototypes were built to streamline the construction of the device and to test the range of motion of the movable segments.

5.3.1 DESIGN 1.0

The first design revision constraints were set based on the required motion of each link and design space set by the shape of the laryngoscope. The blade curvature and length were kept true to the disposable Macintosh 3 laryngoscope blade used by the army. The proximal step was reduced for patients with small mouth openings and to avoid dental contact. The 3D model of this construction is depicted below.

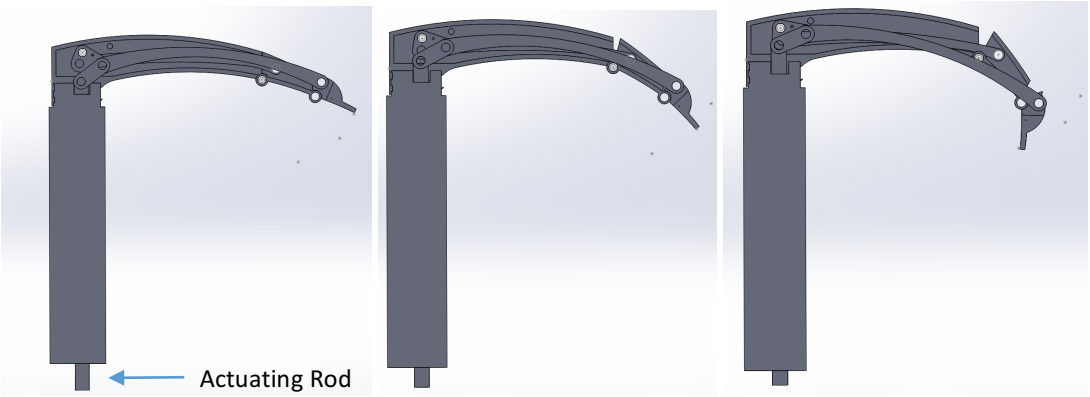

Figure 63. Design revision one of the flexible laryngoscope show in the standard state (left), at precision point 1 (center), and at precision point 3 (right)

The solid model was printed on a Stratasys Fortus 250mc machine [63]. All hole sizes were kept at a 0.1” diameter. The prototype was assembled with the handle but not the actuating rod. The link connecting the distal segment to the input link showed significant bending when tested, therefore, it was laser cut due to the lack of strength of the 3D printed version. It was concluded that the geometry of the link had to be modified to improve the strength. The figures below show two different views of the built model, and the device when completely engaged.

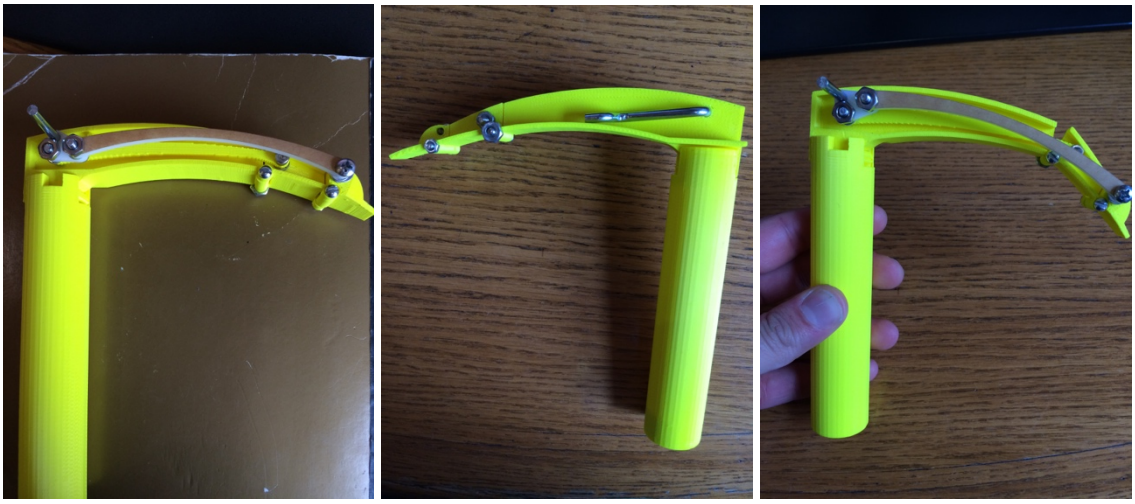

Figure 64. 3D printed model. Right view (left), left view (center), maximum input angle orientation (right)

It was observed that all the motion was not transferred to the output link and there was only complete motion transfer of the middle segment. This was attributed to backlash in the mechanism due to the use of pins, of inaccurate dimensions, in the pivots. Due to the unavailability of a bolt of the desired dimensions, a bent rod was used as the ground pivot for the input link.

This design also incorporated a two position handle setting. It was hypothesized that in situation where a greater angulation of the blade would be required, the blade could be rotated about the hinge point of the handle to provide the extra curvature. To achieve this the handle was designed with two channels—one parallel to the base (like what is seen in conventional direct laryngoscopes) and one at a 20° angle. The 3D mode of the handle is depicted below.

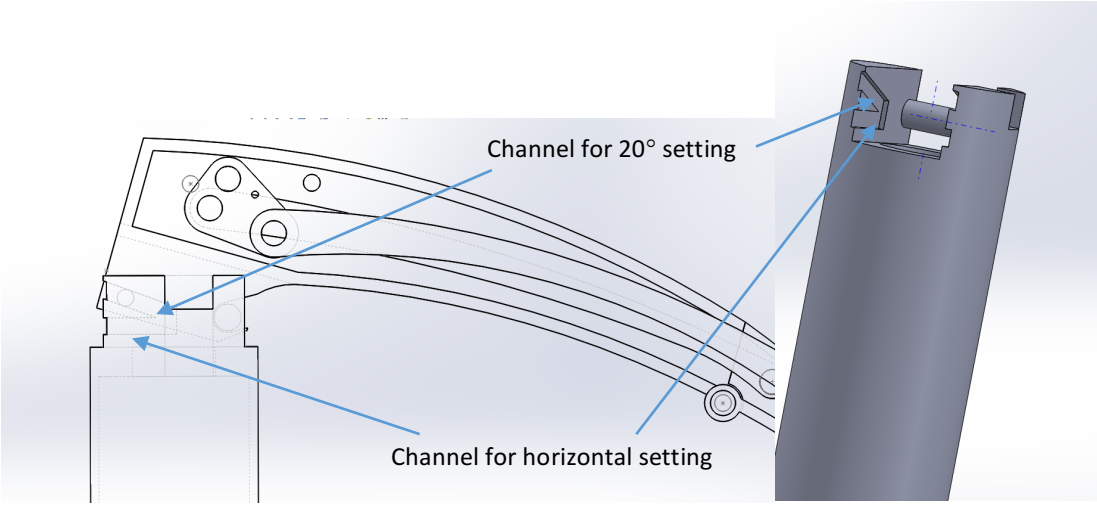

Figure 65. Two channel handle

The two setting handle was not determined as a viable solution for direct laryngoscopy. The extra 20° angulation provided would change the procedure from direct to indirect laryngoscopy, for which a camera at the distal end of the blade would be required. The angulation also resulted in increased dental contact with the proximal step. A requirement for this device is that it should be one-hand operated. Whereas, to move from one setting to another the blade would have to be removed from the airway, removed from the handle and then inserted into the other channel. This increases the number of intubation attempts, increases the time of intubation, and causes the inconvenience of using both hands to switch settings/channels.

5.3.2 DESIGN 2.0

The next design revision was made to address the issues with the previous design and set a standard for construction. The dimensions of the blade and curvature were slightly modified to more accurately mimic a conventional Macintosh 3 laryngoscope. A 3D modelled version of this design is presented below.

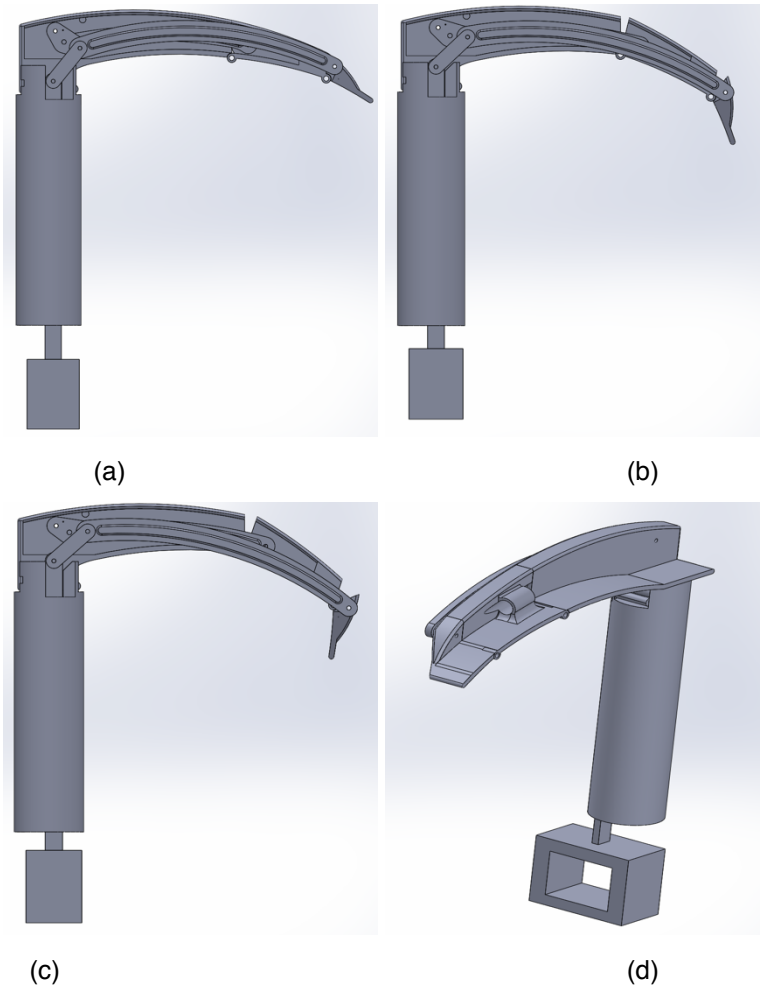

Figure 66. (a) Precision point 1, (b) Precision point 2, (c) Precision point 3, (d) Isometric view

The coordinate system used to plot the links is shown in the figure below.

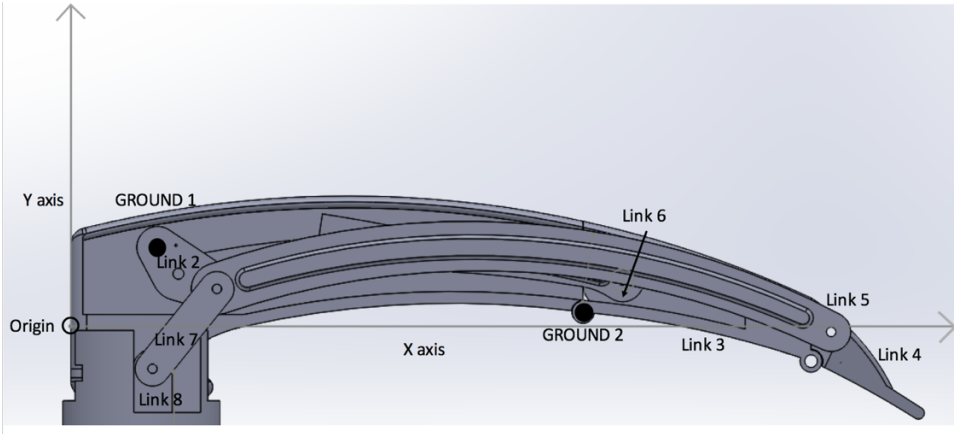

Figure 67. All numbered links and coordinate system used for mechanism synthesis. Refer to figure 59 for the schematic drawing

The free choices, ground pivots, and rotations associated with the links for each precision point is listed in the table below.

Table 3. Dimensions and rotations for design 1.1

Entity	Value	Entity	Value
Ground 1	0.55 + 0.5i	Z9 (inches)	0.791
Ground 2	3.25 + 0.09i	Z10 (inches)	0.213
Precision Point 1	5.39 – 0.6i	Z11 (inches)	0.262
Precision Point 2	5.214 – 1.03i	α_2 (degrees)	22
Precision Point 3	4.4 – 1.45i	α_3 (degrees)	70
Z1 (inches)	0.459	β_2 (degrees)	-7.99
Z2 (inches)	3.91	β_3 (degrees)	-18.8
Z3 (inches)	0.225	γ_2 (degrees)	-1.38
Z4 (inches)	0.32	γ_3 (degrees)	-3.63
Z5 (inches)	1.48	$\cdot l_2$ (degrees)	-4.96
Z6 (inches)	1.3	ϕ_3 (degrees)	-13.4
Z7 (inches)	2.82	ψ_2 (degrees)	9
Z8 (inches)	0.8	ψ_3 (degrees)	23

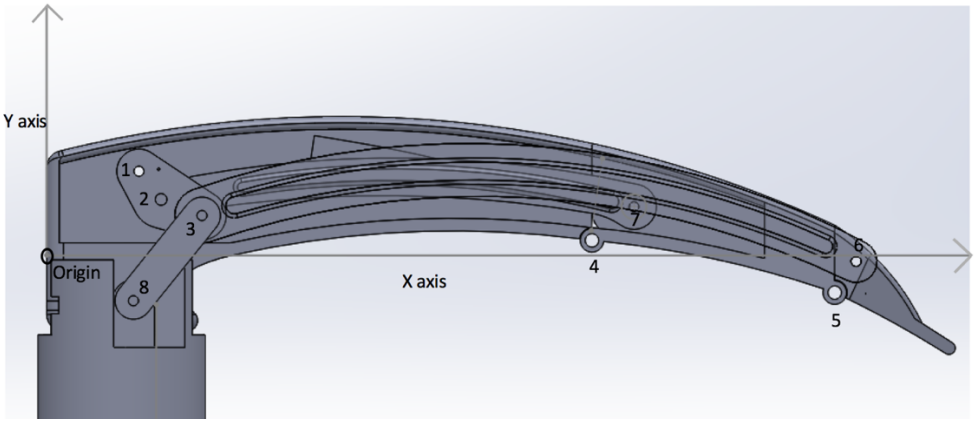

Figure 68. Laryngoscope blade with pivots numbered

Design Features

This design accurately resembles a Macintosh 3 laryngoscope blade with a handle where all the links fall within the form-factor of the Macintosh 3. The binary links connecting the input link to the movable segments of the blade were reinforced by adding a rib. The triggering slider link was designed with a slot for thumb insertion. Figure 66 (a), (b), and

(c) show the laryngoscope at all three prescribed precision points. Figure 66 (d) shows the isometric view where an additional extrusion with a channel is present. This channel was designed for an LED light source. The holes made for the fasteners and pins were designed based on standard off-the-self options. The table below lists the hole and the fastener size, length, and material used.

Table 4. Pins and fasteners used in device

Hole No.	Interface	Type	Diameter	Length	Material
1	Link 2—Ground1	Machine Screw	0.06”	1/2”	18-8 Stainless Steel
2	Link 2—Link 6	Dowel Pin	1/16 ”	3/16”	316 Stainless Steel
3	Link 8—Link 3—Link 6	Machine Screw	0.06”	11/32”	18-8 Stainless Steel
4	Link 3—Ground 2	Dowel Pin	1/16”	7/8”	316 Stainless Steel
5	Link 3—Link 4	Dowel Pin	1/16”	7/8”	316 Stainless Steel
6	Link 5—Link 4	Machine Screw	0.06”	1/2”	18-8 Stainless Steel
7	Link 6—Link 3	Machine Screw	0.06”	9/32”	18-8 Stainless Steel
8	Link 7—Link 8	Machine Screw	0.06”	9/32”	18-8 Stainless Steel

Figure 69. Machine screw (left), dowel pin (right) [64]

Mechanism Functioning

The mechanism operated smoothly with no impingement points. Due to the potential inaccuracies of a 3D printed model and the friction in the pin and fastener joints, all motion was not transferred to blade tip. In the final engaged state, the middle segment was maximally deflected but the blade tip did not move completely. The final 70^{o} angle deflection of the blade tip was not achieved because link 5 (figure 67) did not follow the trajectory set by mechanism synthesis. There was more vertical motion rather than horizontal motion of this link. This did not correlate with the working of the model designed in SolidWorks.

This mechanism was designed with one degree of freedom, therefore, if any link were to be locked, the entire mechanism would be in a locked state. The mechanism was completely engaged and locked in place by keeping the slider trigger steady in that state. When pushed back in the final state, the blade tip deflected to the extent that the mechanism was nearly back in its non-engaged state. This proved that although the construction of the device was robust, it would lose its functionality if any significant load were to be applied to the blade tip in a direction opposing the motion.

5.3.3 DESIGN 2.1

The previous design was a two-piece blade-handle design with low-cost, strong, and standard pins and fasteners that allowed free motion of the device, and had a perfect fit. The primary issue was the lack of transfer of motion along link 5 (figure 67) to the blade tip. This was due to the loss in rigidity of the mechanism in its full engaged state. Thus, two tabs were added, one above and one below link 5. These provided a channel for the link to guide it along the desired trajectory. Intubation forces have been observed to be very high and a link design without rigidity in the deployed state would not suffice. An important function of the tab on the top surface of the blade was to add mechanism rigidity. It was observed that a force applied in the fully flexed state on the blade tip would deflect the blade tip backwards only a small amount, due to material rigidity and possible construction inaccuracies. The tab on the top acted as a stop-surface providing the

appropriate rigidity for this application. The models below show the two tabs added to the main blade.

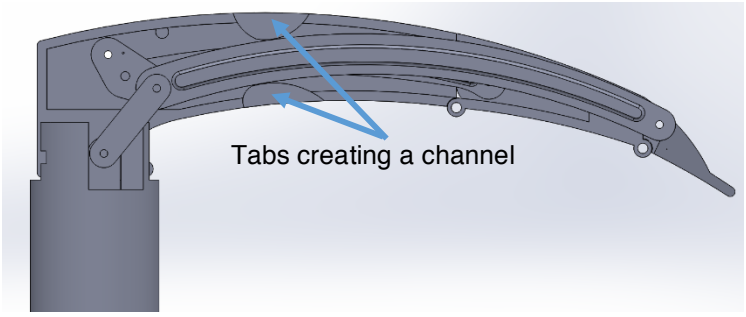

(a)

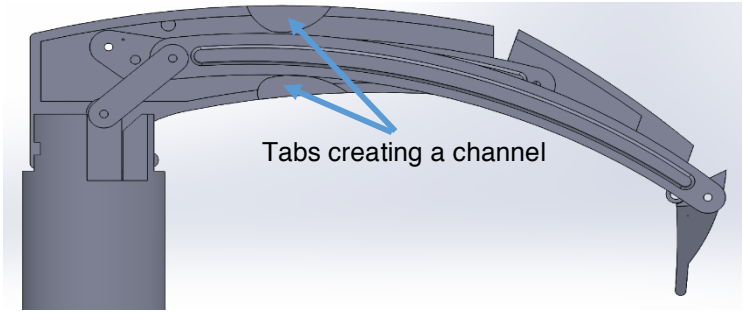

(b)

Figure 70. (a) Blade in initial state, (b) Blade in final state

Testing and Results

This version of the device was 3D printed and built and qualitatively tested on the AirSim manikin simulator and the Laerdal airway simulator. As established earlier, the Laerdal airway simulator is significantly stiffer than an average human airway while the AirSim manikin simulator has a more compliable airway and is similar to the human airway. Views obtained by the laryngoscope in the initial state and final engaged state were qualitatively assessed. A minimal CL view improvement was seen in the AirSim when the mechanism was fully engaged. The view was only improved by a half CL if a force along the axis of the handle was applied. The procedure was performed five times to test the structural integrity of the device; the intubation was successful each time. The device was then tested on the Laerdal airway, and five intubations were performed. There was no CL view

improvement seen in four of the intubations, but a minimal improvement was only seen if a significant lifting force along the axis of the handle was applied. This vertical force applied to gain the better view was greater than that seen in the AirSim; the physical model failed in the fifth intubation. The region of failure was the junction of the fixed blade segment (ground) and the first movable segment (middle blade segment). The diagrams below show the model before and after the intubations.

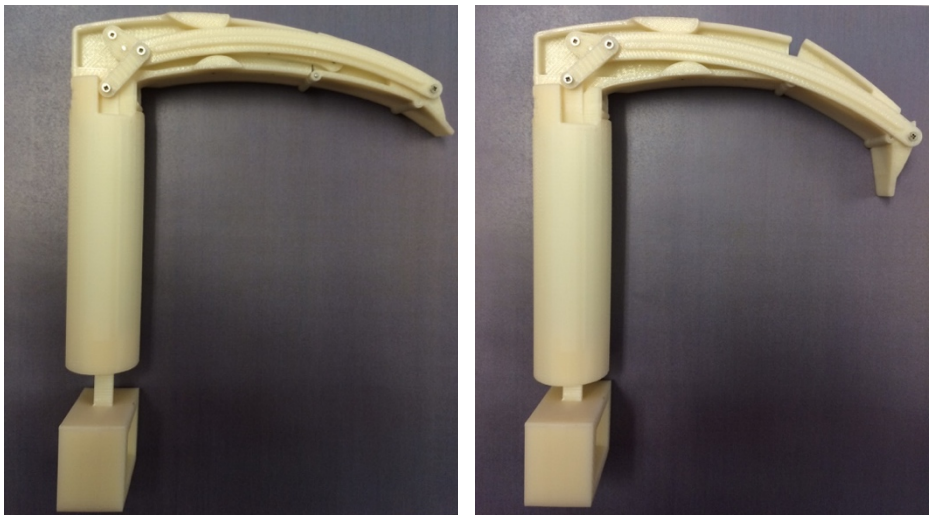

Figure 71. 3D printed model at precision position 1 and precision position 3

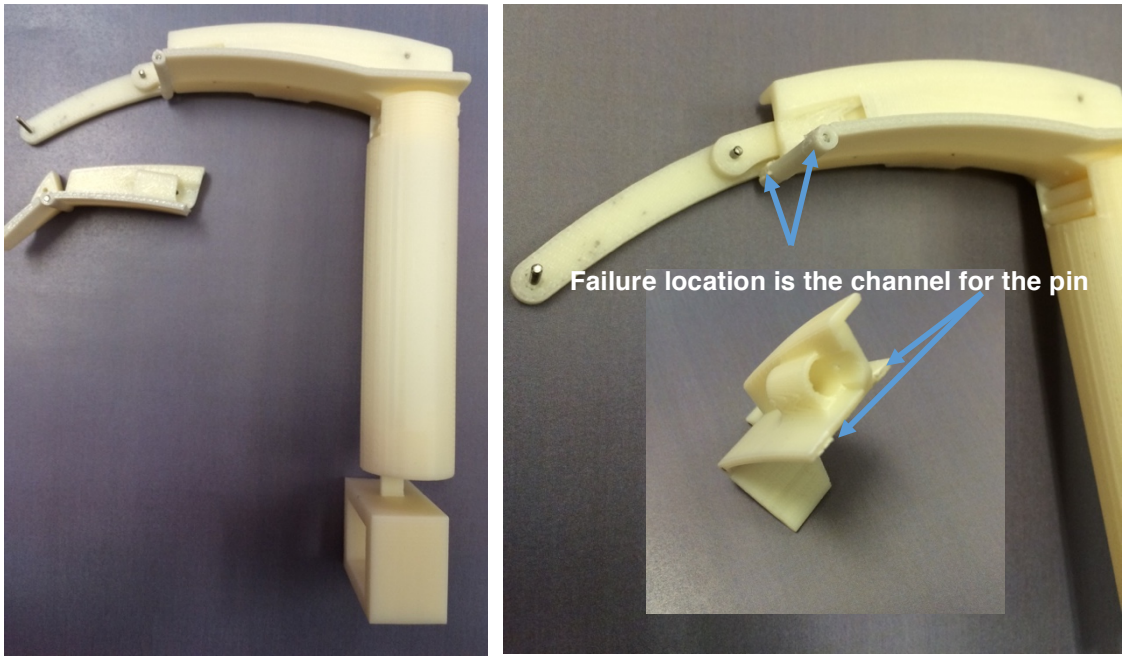

Figure 72. Broken laryngoscope (left), 3D printed model with failure locations highlighted (right)

Discussion and Conclusion

The above testing verified that the AirSim is a more suitable airway simulator than the Laerdal simulator. The critical stress location on the laryngoscope was also identified as the junction of the pin slot and the lower surface of the second blade segment as this was the area of failure. This was due to the high stress concentration in this region due to the sharp and abrupt change in curvatures. A fillet in the region would reduce the stress on this area. Qualitatively, it was assessed that the force required to successfully intubate the Laerdal simulator was greater than a standard intubation in the initial and the fully engaged state.

The conclusion was that elevated forces were required to improve the glottic view and the minimal decrement in the CL view. Therefore, it was hypothesized that a blade with a longer middle segment and a greater rotation would address these issues. A longer middle segment would compress a larger area of the tongue such that the blade tip would solely be used to engage the epiglottis. A longer middle segment would mean a longer and more versatile blade. Increased versatility was directly correlated with blade use in a larger population of patients. Multiple intubation attempts can also be caused due to an incorrect blade size used. Since longer blades can be used in patients with associated and smaller airways, a longer blade would serve a larger demographic of patients.

5.4 DESIGN 3.0

The previous designs transitioned from inaccurately functioning mechanisms to accurately functioning mechanisms with some effectiveness in intubation. The intubations performed showed that the design improved laryngeal view and possibly reduced intubation forces in standard intubations. Critical stress points and other design shortcoming were identified. The rotations of the movable blade segments in previous designs were chosen based on approximations; these rotations for the current design were calculated based on the empirical data collected from airway measurements from CT scans and previous studies on airway measurements [4] [35]. This data along with the results obtained from qualitative

testing provided a basis for blade design. Human anatomy defers from widely across the spectrum and there are even larger variances in people with disorders and injuries. No concrete data is available on people with irregular airways, therefore, there has not been a solution involving one device for all intubation cases. This collected data adds the quantitative aspect to blade features, which has not been seen to have been done for some other devices.

Blade features

The six bar chain appended with a crank slider input system was the basis for the design, as was seen in previous design iterations. The laryngoscope length was increased to a value between a Macintosh 3 and Macintosh 4 laryngoscope blade length. The blade length of the blade mid-section was increased to gain additional leverage on the tongue. The blade mid-section rotations were controlled by choosing precision locations for blade trajectory. The mechanism was designed such that the blade mid-section rotated more than the tip until the second precision location. After the second precision location, the mid-section rotation reached a maximum value followed by an extra rotation of the tip. This extra relative tip rotation was chosen to guide it down along the top surface of the tongue and into the vallecula to apply the necessary pressure on the hyoepiglottic ligament. The absolute rotation of the blade mid-section was less than that of the blade tip. It was hypothesized that the mid-section rotation required was the angle difference between the laryngeal and mouth axis. Based on the data presented in the literature review [4], this angle was lower in the sniffing position in comparison to the neutral position.

Blade dimensions

The table below presents the length of each link along with the associated rotations. The coordinate system is the same as that was seen in figure 68, the link nomenclature the same schematic in figure 59, and the and the fastener and pin data the same as that in table 3.

Table 5. Dimension for design 3.0

Entity	Value	Entity	Value
Ground 1	0.65 + 0.5i	Z9 (inches)	0.747
Ground 2	3.35 + 0.075i	Z10 (inches)	0.279
Precision Point 1	5.79 – 0.77i	Z11 (inches)	0.3
Precision Point 2	5.5 – 1.3i	α_2 (degrees)	22
Precision Point 3	4.97 – 1.8i	α_3 (degrees)	50
Z1 (inches)	0.529	β_2 (degrees)	-10.1
Z2 (inches)	4.08	β_3 (degrees)	-22.3
Z3 (inches)	0.195	γ_2 (degrees)	-1.72
Z4 (inches)	0.32	γ_3 (degrees)	-4.15
Z5 (inches)	1.84	$\cdot l_2$ (degrees)	-6.09
Z6 (inches)	1.68	ϕ_3 (degrees)	-13.8
Z7 (inches)	2.76	ψ_2 (degrees)	10
Z8 (inches)	0.8	ψ_3 (degrees)	23

Design Rationale

The figure below is taken from the paper by Schebesta [35] and two additional constructions were added to estimate the required length of the blade middle-section.

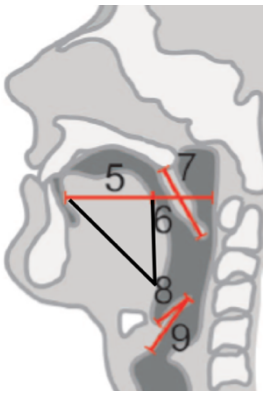

Figure 73. Approximate length of the blade middle segment [35]

The area of the tongue was approximated as a right angles triangle. The triangle base coincides with dimension 5, from figure 73, which was the tongue horizontal diameter—6.3 cm. The vertical black line constructed between the labels 6 and 8 was approximated as dimension 11 from figure 73. Using the Pythagoras theorem, the diagonal length was

calculated to be 6.8 cm. The length of the blade mid-section was link Z5 (figure 59) and measured at 4.67 cm. This was greater than the length of the middle segment in previous designs by approximately 1.25 cm and was thought to be a sufficient increase to gain addition leverage on the tongue.

β_3 is the relative rotation of the mid-section of the blade in the final blade position. This additional rotation of 22^o would improve the line of sight with the larynx. This flexion would provide enough compression of the tongue to reduce the angle between the mouth and laryngeal axes. This rotation coupled with the natural downward angulation of the blade could potentially improve the laryngeal view in the neutral position significantly enough to avoid the need of the sniffing position. This gain in line of sight would be beneficial in patients with cervical neck immobilization. The blade tip is link Z9 (figure 59) from the above table and was measured at 0.747 in, or 1.9 cm. This was designed to be longer than the anterior length of epiglottis to allow for complete tip insertion into the vallecula for adequate force application on the hyoepiglottic ligament. This would allow the anterior surface of the epiglottis to rest on the distal step and prevent it from getting caught between blade segments. This would also prevent an operator from deeper blade insertion and vallecula injury. The figure below is the 3D printed model of this design.

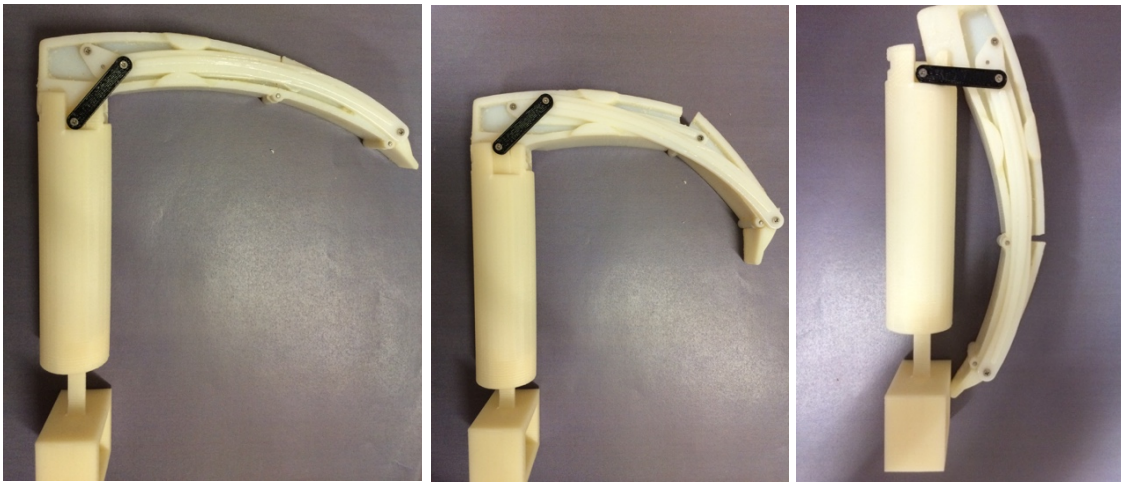

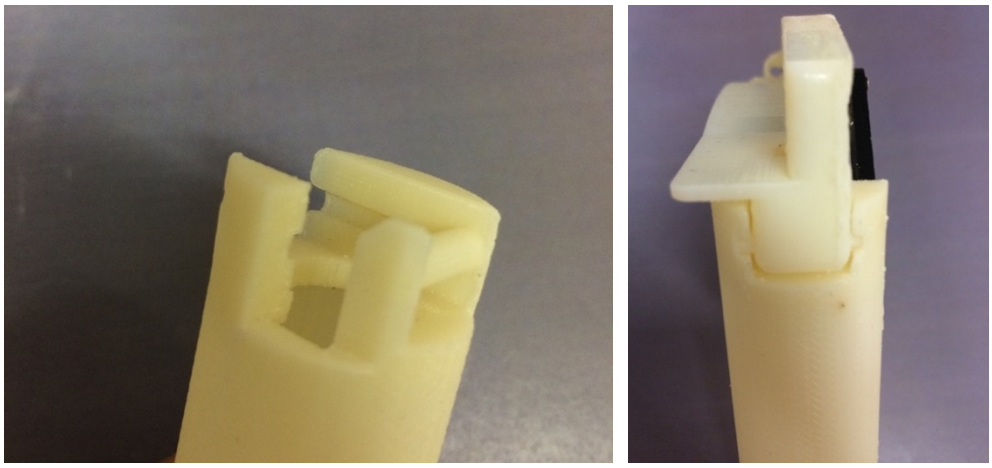

Figure 74. Blade in initial state (left), blade completely engaged (center), blade in collapsed state (right)

Mechanism analysis

The two analysis techniques were applied to this mechanism to understand the effective force transfer from the input to the output. The plot below shows the three transmission angles of the mechanisms through the motion of the mechanism.

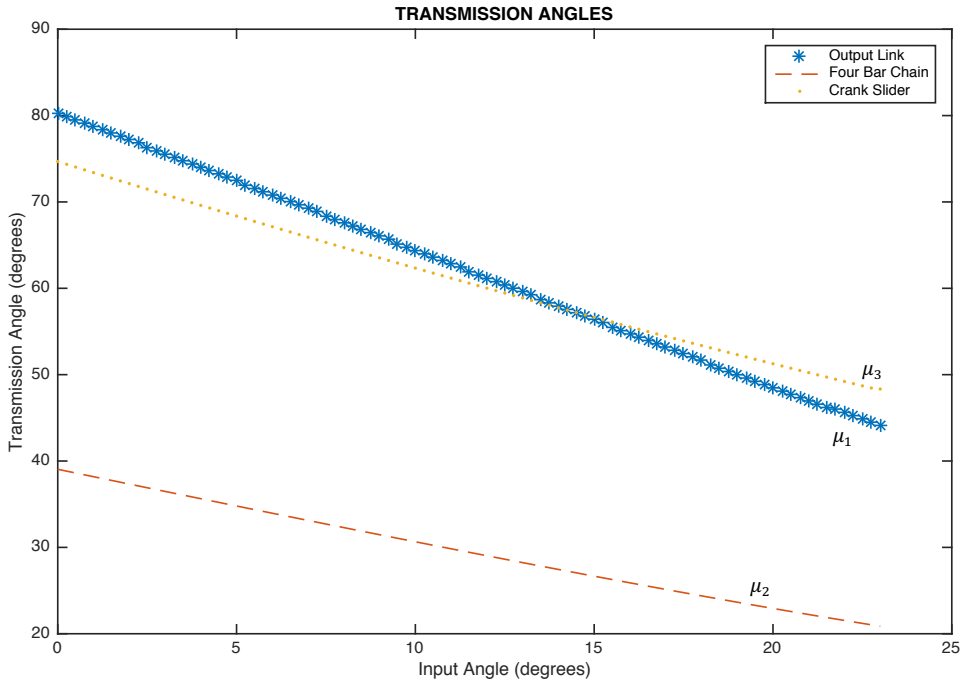

Figure 75. Transmission angles through the motion of the mechanism

The transmission angles of the mechanism in the above plot are in an acceptable range. The transmission angle of the four-bar chain dropped below 30^{o} but no locking or lack of motion transferability was seen. This metric showed that the mechanism operated smoothly throughout the range of input angles.

The mechanical advantage analysis was more representative of the force transferability to the blade tip from the input slider. The plot below shows the mechanical advantage of the six-bar chain and the entire mechanism. A low mechanical advantage is seen for the six-bar chain and was improved with the addition of the input slider chain, only for small input angles. Space constraints limited the size and range of motion of the input link of the six-bar chain. A small mechanical advantage is due to the long, slender, and compact form-factor of the mechanism. This is also due to the small range of motion of the input link in comparison to the blade tip. Therefore, the only method to increase the mechanical advantage of the mechanism would be through a modified triggering mechanism.

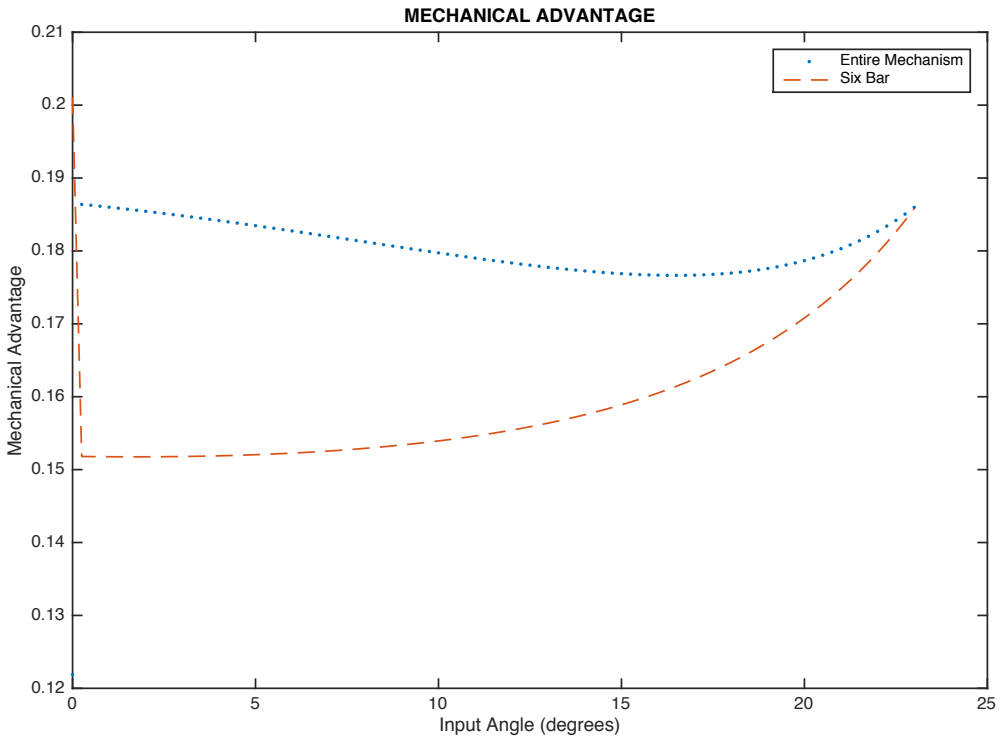

Figure 76. Mechanical advantage of the mechanism

Joint force analysis was the final metric used to assess the mechanism and the transfer of force through the links. This analysis is important for the manufacturability of a mechanism. The joint forces establish an estimate of the specifications of the pins and fasteners required for the mechanism. The joint force analysis also shows the distribution of forces at each joint through the range of motion of the mechanism. An input force of 150N was chosen and the force on the blade tip was calculated using the mechanical advantage calculated above. A static force and moment balance was done for each link to calculate the forces at each joint. The two figures below show the joint forces in the mechanism. The joint numbers are consistent with the convention used in figure 68.

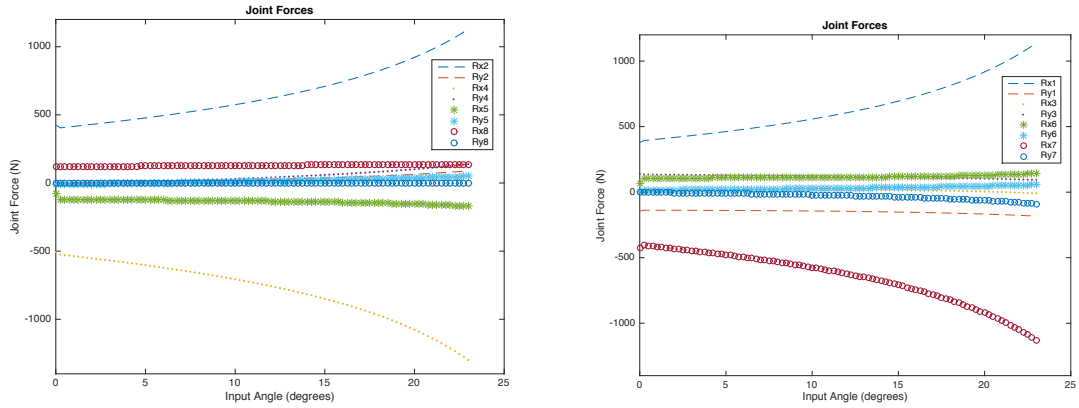

Figure 77. Joint forces for all 8 joints in the mechanism. Refer to figure 68 for joint location

The maximum force was seen at the hinge point of the input ternary link to ground. Similar forces were seen at joint 2 and joint 4. Joint 4 is the pivot connecting the main blade body to the first movable blade segment. High forces were expected there as that was a critical stress point in design 3.0, 3.1, and 3.2.

Preliminary Qualitative Testing

The same testing protocol was followed with this blade design. Two blades were 3D printed and assembled; one blade consisted of a smaller handle than the one shown above in figure 74. They were tested on the AirSim manikin head and the Laerdal airway simulator. No measurements were taken, but an understanding of the working of the design was gaged. Five intubations were performed on both airways by each blade. All five intubations by each blade were successful on the AirSim manikin head. An improvement of a half CL

grade view was observed in all intubations with the fully engaged device. Lifting forces were applied to increment the view by another half CL grade. Similar results were observed with the intubations performed on the Laerdal manikin simulator. Half CL grade views were improved in all three intubations with the first blade but the lifting forces applied were greater than those used in the AirSim manikin head. During the fourth intubation, due to the excessive lifting forces applied, one of the tabs which holds the blade in the handle failed. The intubation was unsuccessful, and a fifth intubation was not attempted. The same results were seen with the other laryngoscope; only two intubations were successful. During the third intubation attempt, the lifting forces produced a stress causing the hinge on the handle to fail. No further intubations were attempted. Figure 78 below shows an image of one tab missing on one blade and the image of smaller handle post intubation.

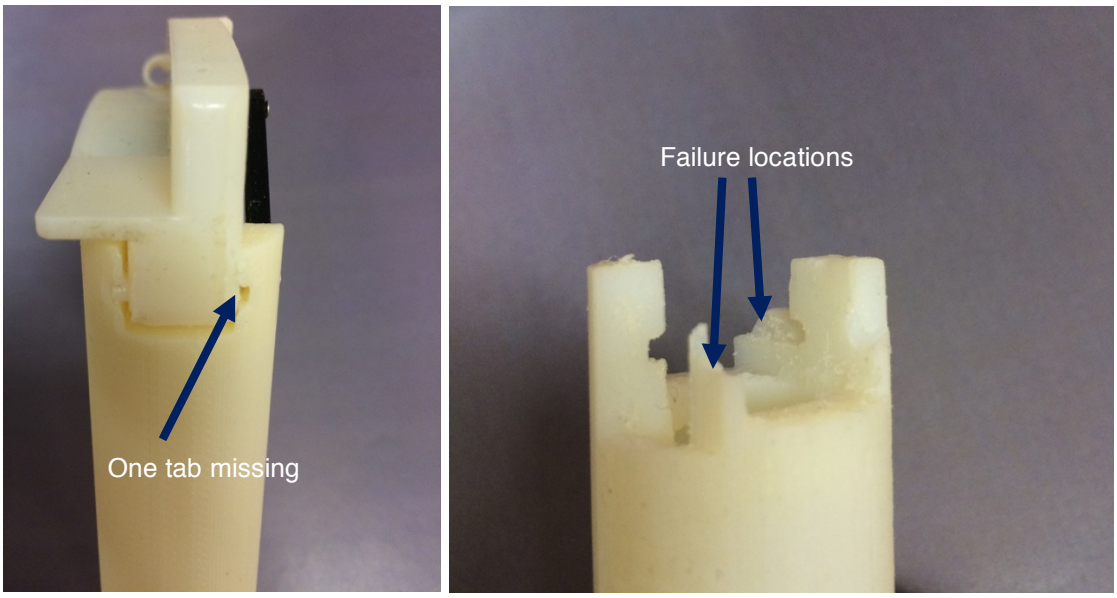

Figure 78. Failure locations highlighted in both tested devices

5.4.1 DESIGN 3.1

Since the intubations with design 3.0 were successful, the mechanics of the blade design were kept the same but the main blade segment and handle was then designed as one part. This reduced the number of parts in the device and potential moving components. This was

also done to strengthen the interface between the blade and the handle. The modified assembly is presented in the figure below.

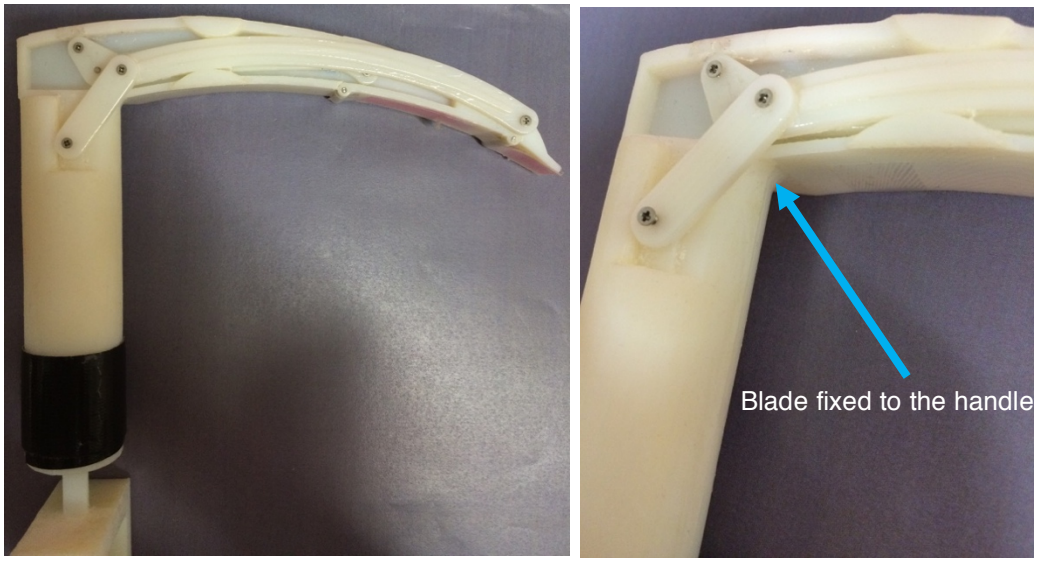

Figure 79. Design 3.1 with the fixed blade segment fixed to the handle

Three blades were printed, assembled, and tested. Five intubations were performed by each blade on the AirSim manikin. The blade shown below in figure 80 was mounted with a pressure film (LLLW Prescale Pressure Film, Fuji) at three locations. One strip was pasted on the blade step to record pressure data from incisor contact, one strip was on the first movable segment, and the third was on the blade tip.

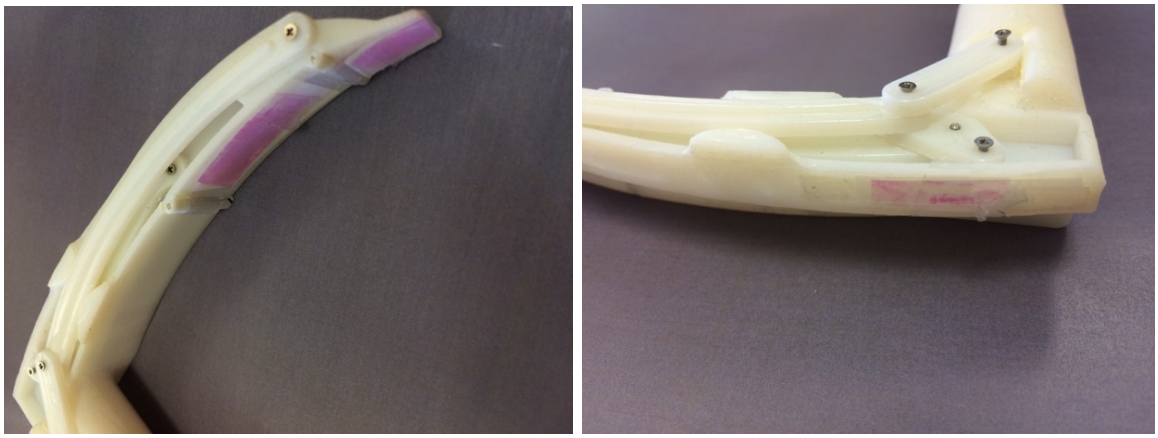

Figure 80. Pressure film on device

The pressure films were mounted to gage their performance in this application. Adequate coloration showed that this could be a viable solution for a quantitative pressure map around the blade. Coloration on the film applied on the blade step showed that there was minor contact with the upper maxillary incisors. Four consecutive successful intubations were performed but the blade failed in the fifth attempt. The region of failure was the same seen in design revision 3.0. The failure region was the pin joint interface between the largest blade segment and the blade mid-segment. The other two blades failed in their first intubation attempt at the same location. The failure region is highlighted in the figure below.

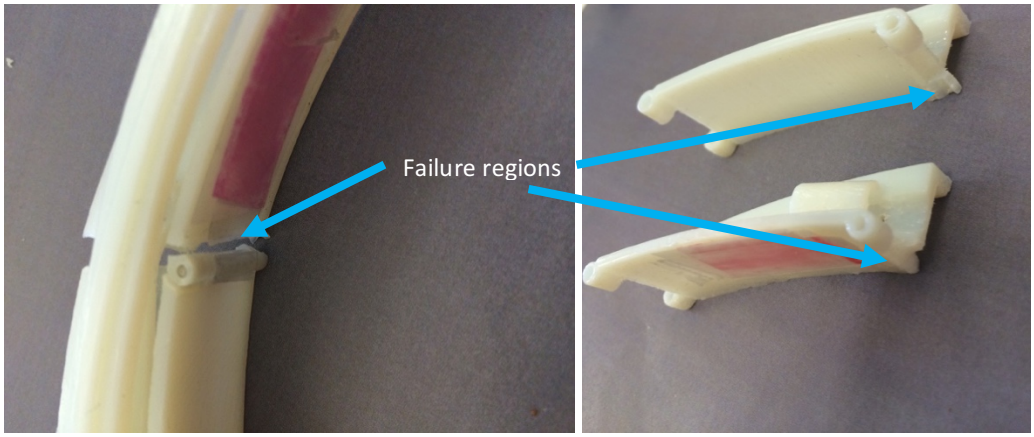

Figure 81. Failure region

Discussion and Conclusion

The region between the blade and the handle was sufficiently fortified to withstand the forces of intubation. The hinge between the main blade segment and the first movable segment failed in different laryngoscope. It was qualitatively observed that the failure was due to the high stress concentration at the failure location because of the abrupt change in curvature from the hinge to the under-surface of the blade. This area of high stress concentration was validated and a complete finite element analysis of the device was performed using ANSYS Workbench 16.1. This analysis showed all the regions of high stress and the deflection of the blade under loading. The loading on a laryngoscope blade as documented by Carassiti [17] showed average forces between 10-35 N on the pressure

films applied by them. That pressure film recorded forces at the distal tip. Since the current design has two segments wherein the middle segment will provide the maximum lifting force to lift the tongue, an average value of 25 N was set on this segment. A lower force was assumed for the blade tip and a value of 15 N was set for it. The stress was mapped based on these pressures. The stress distribution is shown below.

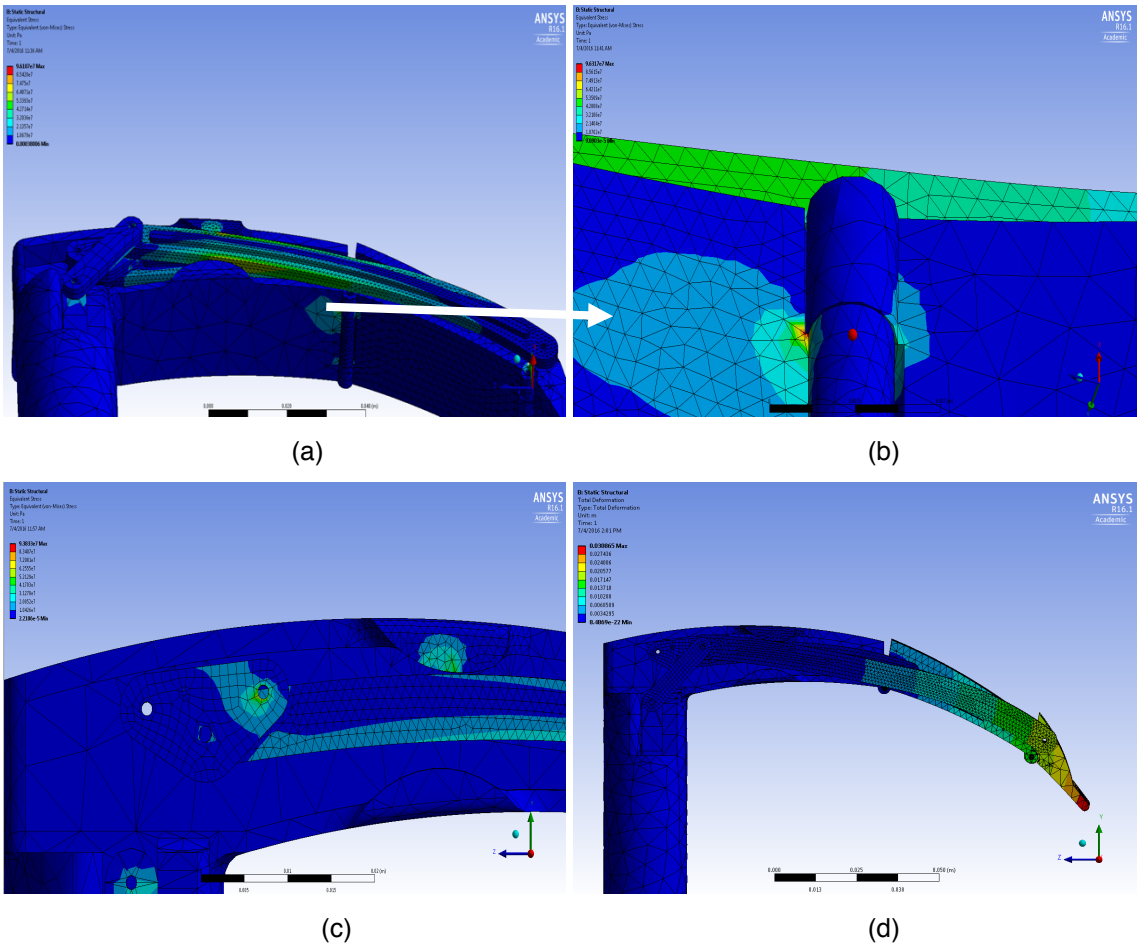

Figure 82. (a) Stress distribution, (b) Critical stress location at junction between main body and the middle blade segment, (c) Stress on higher order joint, (d) blade deformation

Figure 82 (b) shows the critical stress location at the pivots between the main blade body and the middle blade segment. The critical stress point is shown on the main blade body and a smaller stress value and region on the middle blade segment. This was not in line with the model tested as the pivots of the middle blade segment failed before the main blade body. This can be attributed to the fact that the pressure values chosen for the simulation were not accurate. The deflection of the blade tip due to elasticity of the

material, and was qualitatively accurate with the built model. High stresses were also seen on the link connecting the input link and the blade tip—this link experienced the maximum deflection and stress throughout but not significant enough to fail. Therefore, to reduce the stress at the location of failure (middle blade segment pivots), the stress concentration would need to be reduced by adding fillet at these locations. Design 3.1.1, below, incorporated the fillets to reduce the stress concentration and stresses at the pivots.

5.4.2 DESIGN 3.1.1

This design remained the same as design 3.1 but the middle blade segment was reinforced. A fillet was added at the junction of the pin joint and the blade surface to reduce the stress concentration. The reinforced middle segment in a prototype is presented below.

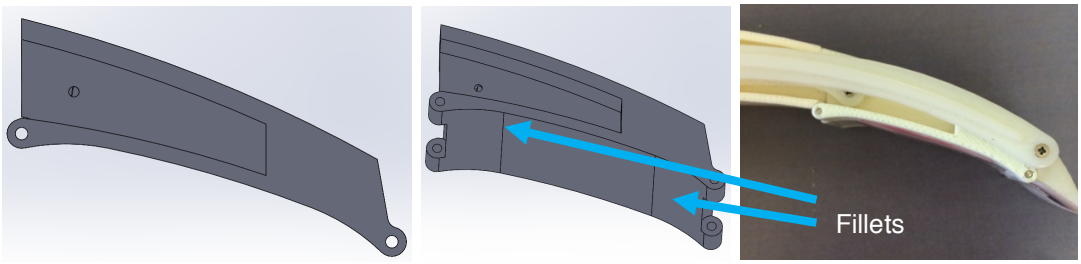

Figure 83. Reinforced middle blade segment

Two laryngscopes with the reinforced middle segment were printed and built and tested on the AirSim manikin. Both blades were instrumented with the Fujufilm pressure film at the middle movable segment and blade tip.

Figure 84. AirSim manikin used for testing

Two successful intubations were performed with one of the blades and three successul intubations with the other. There was a full CL grade view improvement with both blades. The unsuccessful intubations with both blades was either due to the inability of the blade to improve the CL grade view, or due to the failing of the blades. The channel for the pin for the first hinge between the main blade and the middle blade segment failed along its axis. The diagrams below depict the blades after intubation; the pressure film after an intubation are seen on both blades.

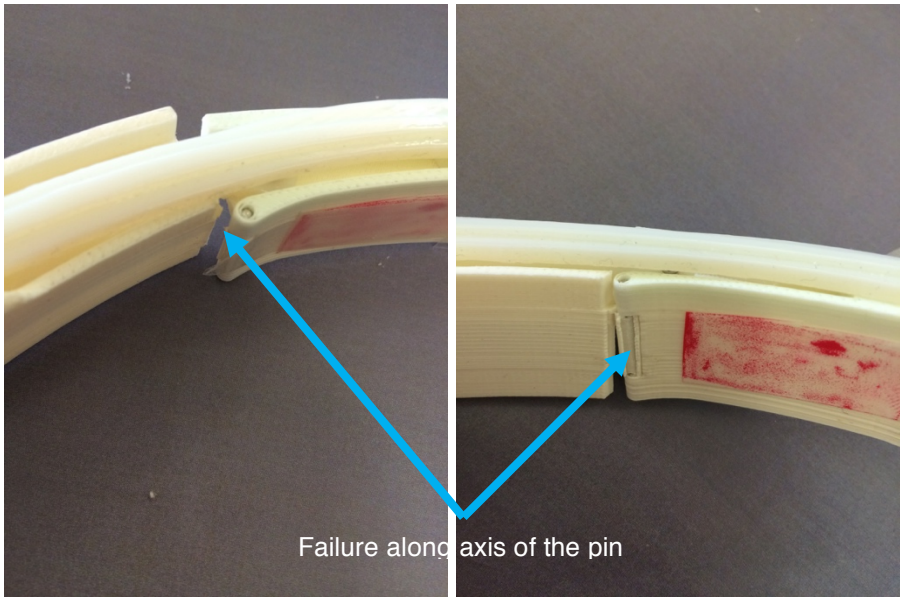

Figure 85. Blade 1 failure location

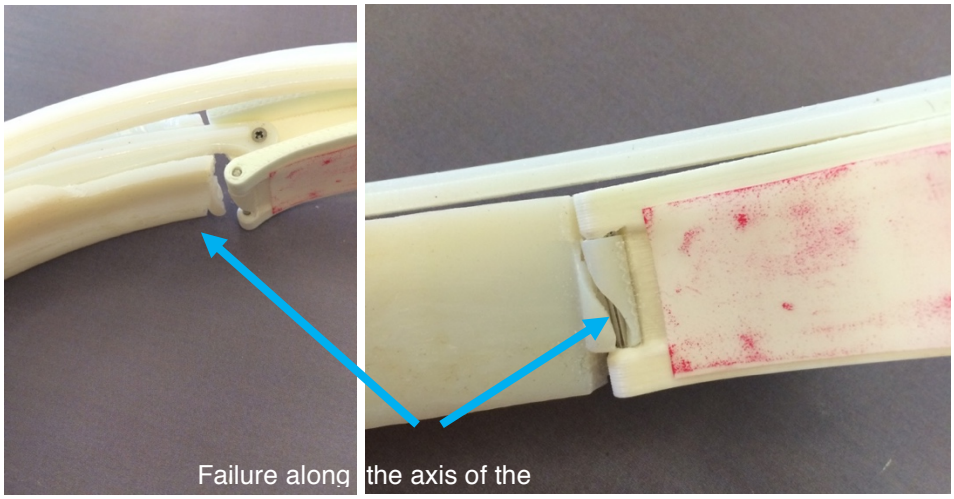

Figure 86. Blade 2 failure location

Discussion and Conclusion

Design 3.1.1 incorporated a reinforced middle blade segment that withstood the preliminary testing but the pivot in fixed blade segment was a critical stress location which experienced failure. ANSYS results are presented below.

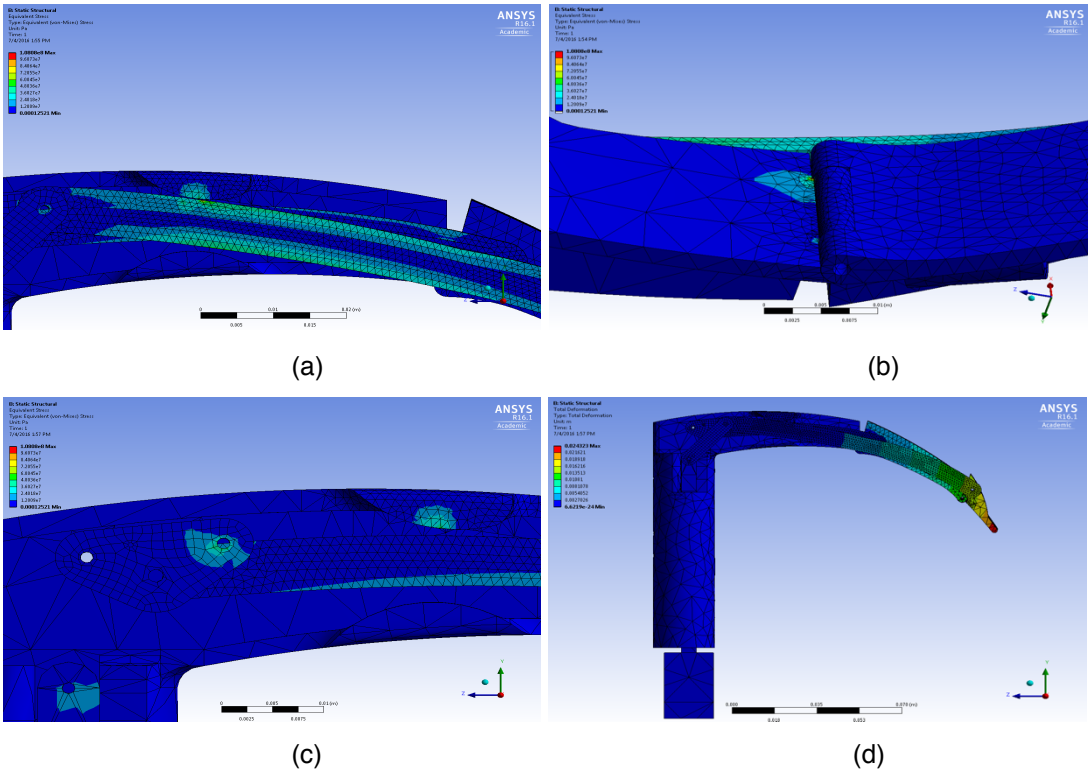

(a) (b)

(c) (d)

Figure 87. (a) Stress distribution, (b) critical stress location at pivot between main blade body and middle segment, (c) stress on higher order joint, (d) deformation

The stress analysis results obtained were similar to those for the previous design. The stress at the failure location of previous design was mitigated as is seen above in figure 87 (b). The tip deflection due to material elasticity was also reduced and the stress distribution around the device also showed a reduction. The location of failure in this design was the pivot of the main blade body and could be explained by the high stress seen at that location. The critical stress seen at the main blade body due the high stress concentration present and the high forces associated with lifting the mandible caused both prototypes to fail. The flexion of the binary link connecting the blade tip to the input ternary link is the primary reason behind the elevated stresses at the hinges and the input link. Hence, a material with a higher rigidity (reduced elasticity) would mitigate the stresses at other locations in the

mechanism and not cause the device to fail. The more rigid material coupled with the reduction in stress concentrations at the lower surface of the blade would provide for a more robust design that can withstand intubation.

5.5 DESIGN 4.0 [FINAL DESIGN]

Since the mechanism was determined, but all the previous designs failed in testing, adequate material additions to the blade design had to be made to reduce stress concentrations at critical locations and reduce the stress on pivots. The blade thickness was increased in such a way that under-surface of the blade was made smooth and no pivot ridges were exposed. Figure 88, below, depicts the final design.

This extra thickness added to the blade improved the blade rigidity and structural toughness. The ternary input link of the six-bar chain, link 5, and the connecting binary link between the slider link and the input ternary were laser cut Plexiglas parts (figure 59). The material of these parts was changed to add rigidity to the links. This allowed for overall greater mechanism rigidity. All other components of the blade were 3D printed using a Stratsys Fortus 250mc machine. As deduced from the ANSYS results for design 3.1.1, using a more rigid material for link 5 reduced the stress on other parts of the mechanism. A stress analysis with the same boundary conditions and external blade pressures was performed using ANSYS Workbench 16.1. The results are presented below in figure 89.

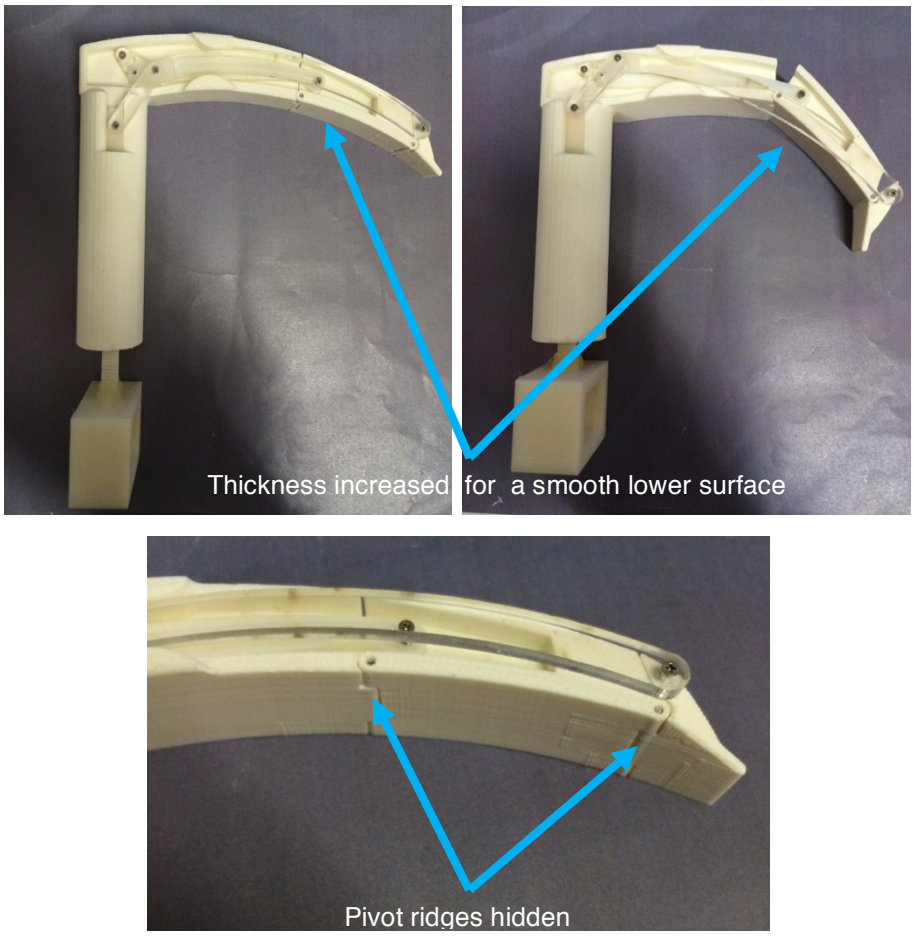

Figure 88. Final blade design with pivots hidden

The increased thickness of the entire blade along with the increase in the rigidity of the links mentioned earlier showed a reduction in stress at the pivots as seen below in figure 89 (b). The stresses transferred to the higher order joint in the input link also showed lower stress than what was observed in the previous two models because of the rigidity of link 5 (figure 59). The tip deflection was also the least in comparison to the previous two models. The table below lists the tip deflection of all three models.

Table 6. Tip deflections

Design	Tip Deflection (cm)
3.1	3.09
3.1.1	2.43
4	2.19

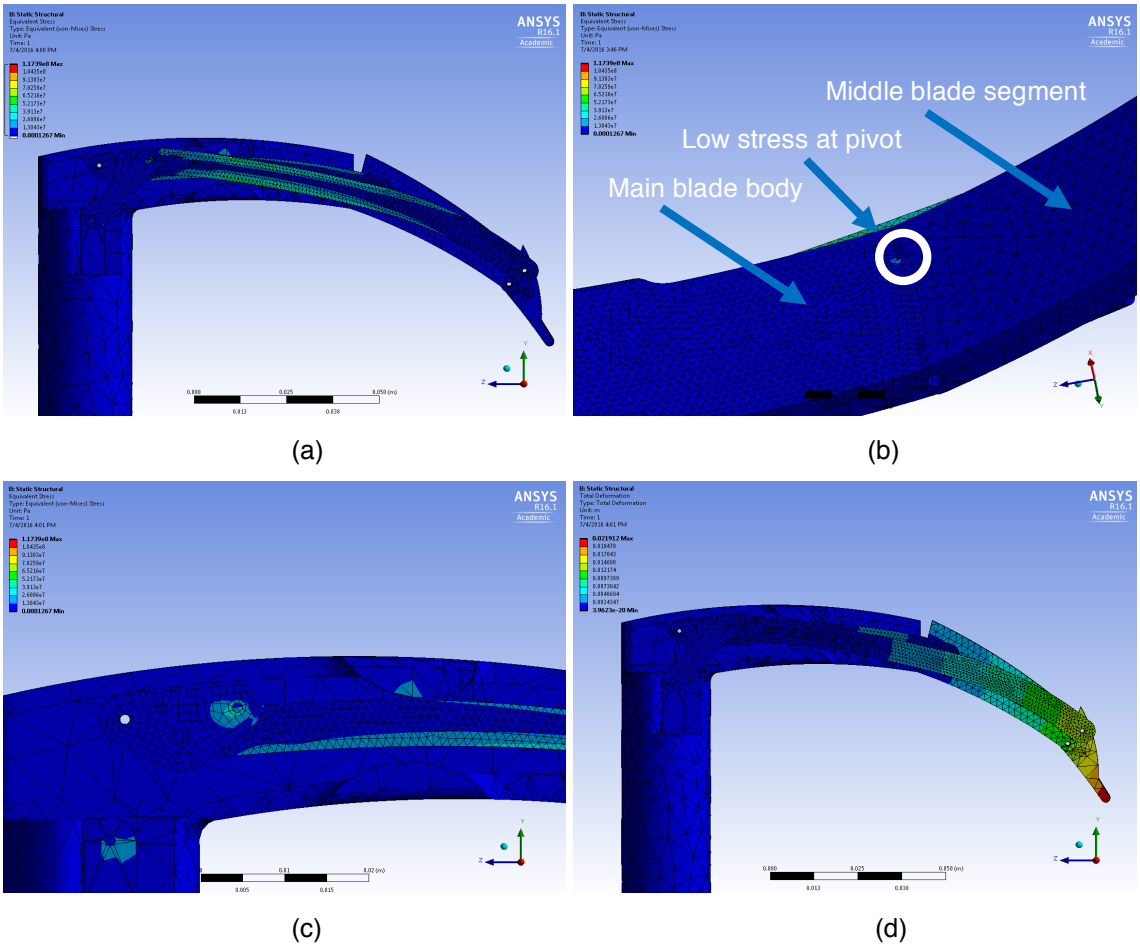

Figure 89. (a) Stress distribution, (b) reduced stress at pivot, (c) stress on input link, (d) total deflection

This device was tested on the TruCorp AirSim manikin simulator (figure 84). Ten intubations were performed and an improvement of either a half grade view or a full grade view was obtained for each of the ten intubations without failure.

6. DEVICE VALIDATION

Each step of the design evolution was qualitatively validated through manikin testing and quantitatively validated through finite element analysis. The objective behind the design changes was to build a blade that could withstand the high stresses experienced during manikin testing and improve the grade view during intubation without changing the intubation maneuvers of a Macintosh laryngoscope. A study was designed to objectively evaluate the final design through manikin testing performed by multiple experts (anesthesiologists). This study was set-up to verify the hypothesis of this thesis i.e. a flexible-blade laryngoscope will improve the grade view during intubation.

6.1 EXPERIMENTAL SET-UP

Six anesthesiologists, with a minimum experience of at least two years, were recruited for this study; the study was performed over a two-day period. All intubations were performed on the TruCorp AirSim manikin simulator. The set-up is depicted in the figure below.

Figure 90. Experimental set-up

Two sponge slabs were placed below the head of the manikin to keep it stable and in the same standard position for all intubations performed on it. The simulator was taped down onto the table to keep it steady during intubations. A standard Macintosh laryngoscope, the newly designed flexible-blade laryngoscope, and an ETT were provided to each expert for intubation. Each flexible blade was instrumented with an LED light source in the slot provided in the middle segment of the blade, and the LLLW Prescale Pressure film by Fujifilm (0.6 MPa, 10% accuracy) on the under-surface of the blade spanning the length of both the movable blade segments. The pressure range of this film is 28 – 85psi [65]. The same film was also applied on the lower surface of the Macintosh blade provided. These films were made up of two layers, one with microcapsules with an achromatic dye and the other where the capsules, once broken, would create the impression of the pressure. The layer with the impression was directly affixed onto each blade. This layer was 60 x 18mm (1080 mm^2) and was stuck to the lower surface of each blade using standard double sided tape. The layer with the microcapsules was affixed onto the lower layer gently using one-sided tape such that no premature pressure impressions were made. A cut-out was made at the edge of the film at the blade distal tip to avoid any area of the film being outside the under-surface of the blade and to identify the location of the distal end of each film.

6.2 PROCEDURE

Each expert was initially given both blades without the pressure films affixed, and allowed to intubate the manikin several times to gain familiarity with the manikin airway and especially understand the working and functioning of the flexible laryngoscope. Once the experts were comfortable with the blade and its usage, they performed a total of six intubations. The first intubation was with the Macintosh laryngoscope, to create a baseline, and then five successive intubations using the flexible laryngoscope. A new pressure film was used for each trial. Each anesthesiologist was instructed to insert the laryngoscope in the airway and into the vallecular, like what they do with a standard Macintosh laryngoscope, and lift to obtain a grade 1 view. They were then instructed to reduce the lifting force and adjust the laryngoscope in the airway such that they got a view between a

grade 3 and a grade 2. Once the view was established, the mechanism was engaged completely. The final view obtained after engaging the mechanism was noted and the ETT was inserted into the airway to complete the intubation. The data reported was the view obtained before the mechanism was engaged, the final view after the mechanism was engaged, the outcome of intubation, and the additional qualitative lifting force required by the expert to gain an adequate view for intubation after the mechanism was engaged. All intubations were video-recorded. After the six intubations, each expert was given a short survey to comment on the effectiveness of the device. The survey consisted of five questions, they are listed below.

1. Did you like the innovation—we are interested in the idea, not the physical design?

1	2	3	4	5
Strongly Disagree	**Disagree**	**Neutral**	**Agree**	**Strongly Agree**

2. Would you use this type of a blade, if the material was equivalent to the usual MAC blades?
   Y / N
3. Can the blade be used as regular MAC blade?
   Y / N
4. Did the deployment of the flexion mechanism change the view?
   Y / N
5. If yes, by how much?

Initial View	Final View

Table 7. Demographics of participating experts

Anesthesiologist	Gender	Experience (years)
1	F	4
2	F	4
3	F	2
4	F	12
5	F	20
6	M	32

6.3 RESULTS AND DISCUSSION

The primary objective of the study was to assess the change in view of the glottis provided by the flexible blade. A total of 30 intubations with the flexible laryngoscope were recorded, but only 27 pressure films were collected. The pressure film during three trials folded onto itself; this caused inaccurate pressure reading and the blade adhering to the tongue during insertion. Therefore, in those attempts the operators intubated without the films.

6.3.1 CORMACK-LEHANE GRADE VIEWS

The CL grade views recorded are presented below in the tables, and the following plot. The statistical analysis was done using the Mann-Whitney U test, in excel, because the data obtained was not necessarily normally distributed.

Table 8. Anesthesiologist 1

METRIC	INITIAL VIEW	FINAL VIEW	SUCCESS
MAC BLADE	1	1	YES
ATTEMPT 1	2	1	YES
ATTEMPT 2	2	1	YES
ATTEMPT 3	2	1	YES
ATTEMPT 4	2	1	YES
ATTEMPT 5	2	1	YES

Table 9. Anesthesiologist 2

METRIC	INITIAL VIEW	FINAL VIEW	SUCCESS
MAC BLADE	1	1	YES
ATTEMPT 1	2	1	YES
ATTEMPT 2	3	2	YES

ATTEMPT 3	2b	2a	YES
ATTEMPT 4	2	1	YES
ATTEMPT 5	2	1	YES

Table 10. Anesthesiologist 3

METRIC	INITIAL VIEW	FINAL VIEW	SUCCESS
MAC BLADE	1	1	YES
ATTEMPT 1	2	1.5	YES
ATTEMPT 2	3	2	YES
ATTEMPT 3	2	1.5	YES
ATTEMPT 4	2	1	YES
ATTEMPT 5	3	2	YES

Table 11. Anesthesiologist 4

METRIC	INITIAL VIEW	FINAL VIEW	SUCCESS
MAC BLADE	1	1	YES
ATTEMPT 1	3	3	NO
ATTEMPT 2	2b	2a	YES
ATTEMPT 3	2b	2a	YES
ATTEMPT 4	2b	2a	YES
ATTEMPT 5	2b	2a	YES

Table 12. Anesthesiologist 5

METRIC	INITIAL VIEW	FINAL VIEW	SUCCESS
MAC BLADE	1	1	YES
ATTEMPT 1	2	2	YES
ATTEMPT 2	2	3	NO

ATTEMPT 3	2	1.5	YES
ATTEMPT 4	2	1	YES
ATTEMPT 5	2	2	YES

Table 13. Anesthesiologist 6

METRIC	INITIAL VIEW	FINAL VIEW	SUCCESS
MAC BLADE	1	1	YES
ATTEMPT 1	2	1	YES
ATTEMPT 2	2	1.5	YES
ATTEMPT 3	2	1.5	YES
ATTEMPT 4	2	1	YES
ATTEMPT 5	2	2	YES

To assess the difference between the initial and final view, an average of the initial view and the final view was taken along with the respective standard deviations and standard error of mean. The plot below shows those results.

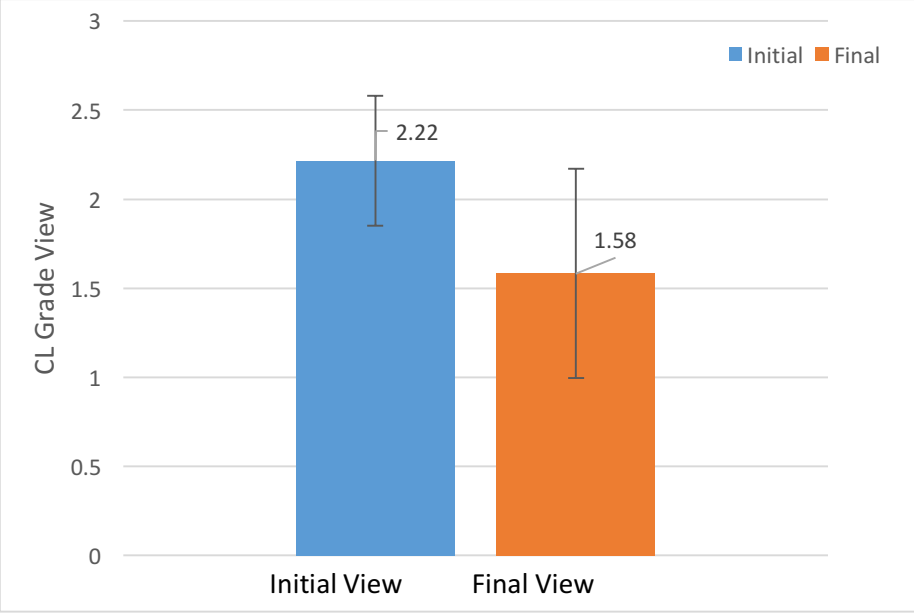

Figure 91. Initial and Final grade view

The CL grade view metric used was the modified version wherein the grade 2 is split into 2a and 2b [44]. To quantify these two intermediate grades, 2a was evaluated as a 2 and 2b as a 2.5. Hypothesis testing for this data set:

Null hypothesis H_o *=> Final grade view >= Initial grade View*

Alternate hypothesis H_a *=> Final grad view < Initial grade view*

A p-value with a 95% confidence ($p_{critical} < 0.05$) was considered significant. The Mann-Whitney U test produced a p_{study} (p-value)= 0.000038. The alternate hypothesis that the final grade view was less than the initial grade view was therefore verified because: $p_{study} << p_{critical}$.

Such a difference proves that the flexible design improved the grade view of intubation, significantly.

6.3.2 FORCE/PRESSURE (PRELIMINARY)

As mentioned earlier, the pressure distribution was recorded for 27 out of the 30 intubations performed with the flexible laryngoscope, but all six with the Macintosh laryngoscope were recorded. The three attempts for which the film was not used was due the film folding onto itself or adhering to the tongue or other anatomy structures during the intubation. This either caused an obstruction of the view of the larynx during intubation or did not allow the blade to smoothly glide over the surface of the tongue. During each intubation the only lifting force applied by the anesthesiologist was to obtain the initial view of a minimum of a grade 2. Then, once the mechanism was fully engaged and the final view was recorded, the anesthesiologists were asked about potential additional lifting forces applied by them to gain that final view. There was no additional force applied for either of the 30 intubations performed, as reported by them. The objective of the study was to only assess any additional lift required by the flexible laryngoscope, post engaging, to gain a view corresponding to an easy intubation. Therefore, the force required to obtain the initial view was not analyzed. The pressure film was used as a qualitative measure of the pressure distribution across the undersurface of the blade, specifically along the two movable segments of the blade.

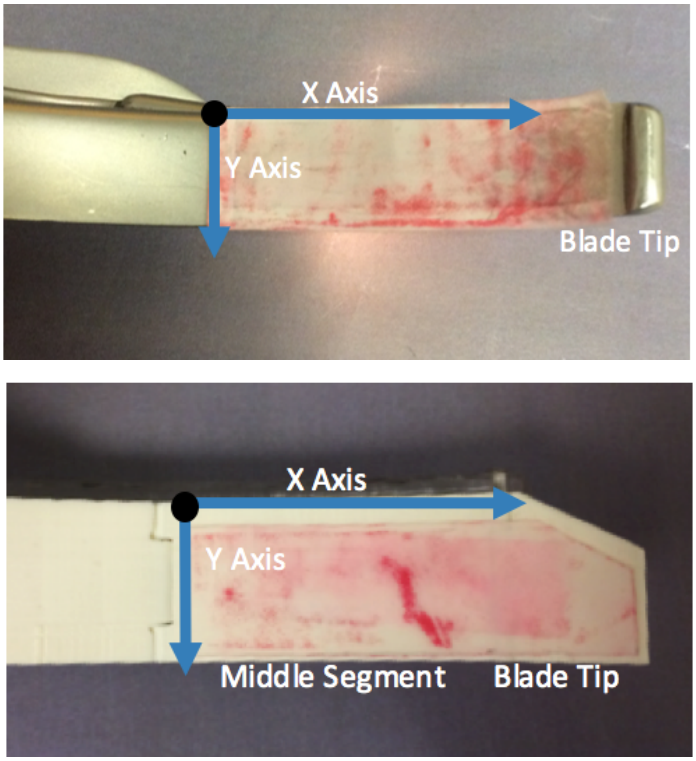

Figure 92. (Top) Coordinate system on the pressure film for the Macintosh laryngoscope; (bottom) coordinate system for pressure film for the flexible laryngoscope

Each pressure film recorded was scanned to maintain uniformity between the images and then converted to a gray scale image. To obtain an average distribution of the forces, each grayscale image was added together and then an average was taken. Each pixel of the final averaged image was an average of the corresponding pixel location of each of the 27 films. The same was done for the six Macintosh intubations. A heat map was produced for both blades to visualize the average pressure distribution across all recorded intubations. The pressure scale was standardized for both sets of data to obtain a clear understanding of the differences in the pressure distribution across each blade. The right edge of each heat map corresponds to the distal end of the respective blade and the left edge corresponds to the pivots between the main blade body and the middle blade segment. The color-bar represented on the right edge of each map corresponds to a relative pressure value varying from 0-255. A greater pixel intensity value translates to a greater pressure value.

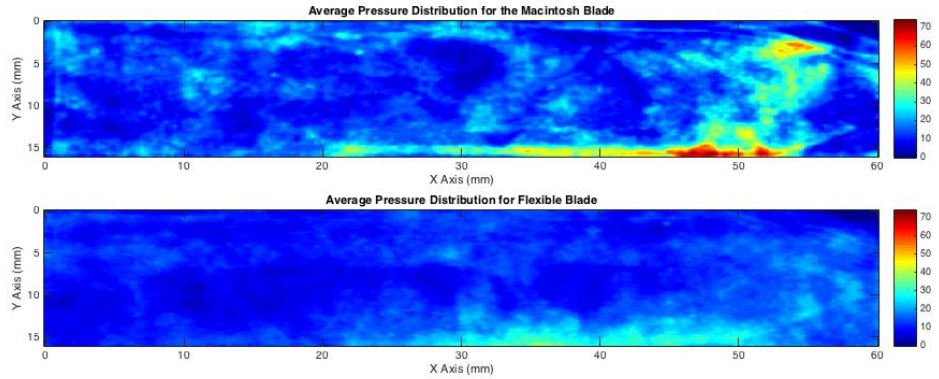

Figure 93. (Top) Average pressure distribution for all Macintosh blade intubations, (bottom) average pressure distribution for flexible blade intubations

A comparison made between the films shows that the pressures on the Macintosh were greater than those on the flexible blade. It is observed that the pressure was concentrated around the distal tip of the Macintosh laryngoscope; this is consistent with the literature [21] [27]. The higher pressures at the Macintosh blade tip are directly attributed to the high lifting forces during intubation with the Macintosh laryngoscope. Through figure 93 it can only be concluded that the pressures on the flexible blade were along bottom edge and equally distributed between both blade segments. The result does not show any remarkable or any critical pressure locations. The figure below shows the average pressure distribution along the flexible blade. The pressure scale was remapped to show only values between 0 and 37, out of a possible 255, as was seen in the previous figure.

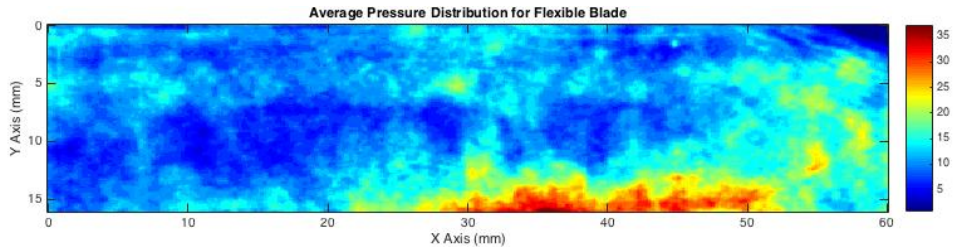

Figure 94. Pressure distribution on the flexible blade

The maximum relative pressure value was observed at the lower edge of the film, the edge which was in line with the edge of the blade. This corresponds to the junction between the blade middle segment and the distal tip. The high pressure in this region could be attributed to the film getting ‘pinched’. It can be concluded that the lifting force applied on the tongue and vallecula was provided by the distal 40 mm of the blade. The region from y=2.5 mm

till y=12.5 mm is the only conclusive region of force distribution along the blade. The markings also show a pressure applied by the blade mid-segment but not as significant as that applied by the blade tip. There was nothing remarkable seen on the proximal third of the pressure film. Therefore, it can be concluded that the maximum pressures applied by the blade were by the blade tip to engage the hyoepiglottic ligament and lift the epiglottis.

6.3.3 POST INTUBATION SURVEY

As mentioned earlier, each expert was requested to fill out a brief survey after all intubations performed by them were completed. This survey was designed for them to comment on the concept behind the device but not the material or aesthetics. This was done to understand the learning curve associated with the device, the likelihood of the device being used, and the change in the glottis view associated with their trails. They were also encouraged to critique the device. The table below tabulates the survey outcome.

Table 14. Survey outcome

Question	Outcome
Did you like the innovation—we are interested in the idea, not the physical design?	3/6 -> Strongly Agree; 3/6 -> Agree
Would you use this type of blade if the material was equivalent to the usual Macintosh blade?	6/6 -> Yes
Can the blade be used as a regular Macintosh blade?	6/6 -> Yes
Did the deployment of the flexion mechanism change the view?	6/6 -> Yes
If yes, by how much?	2.5 -> 1.5 (average)

All six experts commented to the lack of rigidity possessed by the 3D printed plastic and would prefer a material like stainless steel. Due to the low mechanical advantage and the elevated force required by the anesthesiologists to engage the mechanism to produce a

change in the view, they would prefer a more ergonomic solution to engage the mechanism rather than push-plunger. Since there was an improvement in the view because of the mechanism and that the device was able to improve add the additional lift, because of the flexible design, in comparison to a regular Macintosh blade they were content with idea behind the invention.

6.4 LIMITATIONS OF THE STUDY

Although the comprehensive nature of the study with respect to the metrics evaluated to assess the flexible laryngoscope, there were limitations which potentially reduced the accuracy of the results obtained. The sample size used in the study was small; to more accurately validate a device a greater sample size would be required. All anesthesiologists were recruited from one institution. Increasing the number of institutions would gather a larger demographic of anesthesiologists with a myriad of skill levels and techniques. Increasing both the number of intubations, participants, and institutions would be more representative of the general population of operators. Qualitative lifting forces documented were subjective and no method to quantify any potential additional lifting forces when the flexible-blade was engaged was included. The pressure film included in the study was not an accurate form of pressure measurement. Due to the sensitivity of the film there were possibilities of some imprints on the films before they were used in an intubation. Since the pressure film spanned the length of the two movable blade segments, there was a possibility of the film getting pinched at the pivot point between the middle blade segment and the blade tip. Those readings could not be distinguished from actual pressure impressions due to contact with airway anatomy. The primary limitation with respect to the device built was the material. The 3D printed plastic did not give the feel and rigidity of a conventional Macintosh laryngoscope. This was a major reason behind the failure of earlier design revisions of the device.

7. CONCLUSION AND FUTURE WORK

The laryngoscope has caused multiple complications in the airway as has been documented previously [8] [9] [10] [11]. That was the motivation behind developing a new device that could mitigate those complications. The primary objective was to develop a device that could improve the view during intubation by reducing the intubation forces, thereby avoiding airway damage. This device was therefore given a flexible design wherein the mechanism would lift and move airway structures out of the way during intubation. This was hypothesized to be the solution in cases where incremental lifting forces applied by a device would be insufficient to gain an adequate view for a successful intubation. The device created consisted of a six-bar mechanism and an appended crank slider engaging mechanism. The device was validated by testing it in a manikin by multiple experts. The hypothesis that the flexible design could improve the view of intubation was verified. The other hypothesis that a flexible blade was reduce the forces on the blade was qualitatively verified, too. Pressure distribution data was also collected during the device validation step. The pressures were compared between a Macintosh blade and the current design and the conclusion was that lesser forces were used by the flexible blade developed.

Future work in this project can be done to improve the functioning of the device and address the limitations mentioned earlier. Moving from a rapid prototyped device to a machined device could provide the rigidity and strength which lacked in the current version. This new design could be tested in manikins, by a larger sample size than used currently. The next steps would be to quantify the pressures obtained through the study performed for the device validation. The device design would also have to modified to include an engaging mechanism that would produce the necessary mechanical advantage to completely flex the middle blade segment and the blade tip during an intubation, while keeping it a one person, one-hand operated device. Moving towards commercialization, the complexity and the number of moving components in the device would have to be reduced.

BIBLIOGRAPHY

[1] C. D. Deakin *et al.*, "European resuscitation council guidelines for resuscitation 2010 section 4. Adult advanced life support," *Resuscitation*, vol. 81, no. 10, pp. 1305–1352, Oct. 2010.

[2] T. C. Mort, "Complications of emergency Tracheal Intubation: Immediate airway-related consequences: Part II," *Journal of Intensive Care Medicine*, vol. 22, no. 4, pp. 208–215, Jul. 2007.

[3] M. El-Orbany, H. Woehick, and M. R. Salem, "Head and neck position for direct Laryngoscopy," *Survey of Anesthesiology*, vol. 56, no. 3, pp. 117–118, Jun. 2012.

[4] F. Adnet, S. W. Borron, J. L. Dumas, F. Lapostolle, M. Cupa, and C. Lapandry, "Study of the 'sniffing position' by magnetic resonance imaging.," *Anesthesiology*, vol. 94, no. 1, pp. 83–86, 2001.

[5] K. B. Greenland, M. J. Edwards, N. J. Hutton, V. J. Challis, M. G. Irwin, and J. W. Sleigh, "Changes in airway configuration with different head and neck positions using magnetic resonance imaging of normal airways: A new concept with possible clinical applications," *British Journal of Anaesthesia*, vol. 105, no. 5, pp. 683–690, Sep. 2010.

[6] P. C. Pacheco-Lopez, L. C. Berkow, A. T. Hillel, and L. M. Akst, "Complications of airway management," *Respiratory Care*, vol. 59, no. 6, pp. 1006–1021, Jun. 2014.

[7] B. M. Pieters, G. B. Eindhoven, C. Acott, and A. A. J. Van Zundert, "Pioneers of laryngoscopy : indirect , direct and video laryngoscopy,", *Anaesthesia Intensive Care* pp. 4–12, 2015.

[8] O. C. Phillips and R. L. Duerksen, "Endotracheal Intubation," *Anesthesia & Analgesia*, vol. 52, no. 5, p. 691-697, Sep. 1973.

[9] C. Bellhouse, "An Angulated Laryngoscope for Routine and Difficult Tracheal Intubation", *Anesthesiology*, vol. 69, no. 1, pp. 126-128, 1988.

[10] E. P. Mccoy, "The levering laryngoscope,", *Anaesthesia* vol. 48, no. January, pp. 516–519, 1993.

[11] C. N. Perera, P. C. Wiener, M. Harmer, and R. S. Vaughan, "Evaluation of the use of the Flexiblade. Apparatus," *Anaesthesia*, vol. 55, no. 9, pp. 890–893, Sep. 2000.

[12] I. Yardeni, A. Abramowitz, V. Zelman and R. Katz, "A new laryngoscope with flexible adjustable rigid blade", *British Journal of Anaesthesia*, vol. 83, no. 3, pp. 537-539, 1999.

[13] V. Patil, L. Stehling and H. Zauder, "An Adjustable Laryngoscope Handle for Difficult Intubations", *Anesthesiology*, vol. 60, no. 6, p. 609, 1984.

[14] J. S. Doherty and S. R. Froom, "Review article Pediatric laryngoscopes and intubation aids old and new,", *Pediatric Anesthesia*, vol. 19, no. 1, pp. 30–37, 2009.

[15] J. Diaz, J. Guarisco and F. Lejeune, "A Modified Tubular Pharyngolaryngoscope for Difficult Pediatric Laryngoscopy", *Anesthesiology*, vol. 73, no. 2, pp. 357-358, 1990.

[16] N. Hirsch, A. Beckett, J. Collinge, F. Scaravilli, S. Tabrizi, and S. Berry, "Lymphocyte contamination of laryngoscope blades – a possible vector for transmission of variant Creutzfeldt-

Jakob disease,", *Anaesthesia*, vol. 60, no. 7, pp. 664–667, 2005.

[17] T. M. Cook, "Complications and failure of airway management,", *British Journal of Anaesthesia*, vol. 109, pp. 68–85, 2012.

[18] J. Lehane, "Difficult tracheal intubation in obstetrics,", *Anaesthesia,* vol. 39, 1984.

[19] S. M. Yentis and D. J. H. Lee, "Evaluation of an improved scoring system for the grading of direct laryngoscopy,", *Anaesthesia,* vol. 53, no. 11, pp. 1041–1044, 1998.

[20] M. F. Murphy, "Tracheal Intubation : Tricks of the Trade Tracheal I ntubation : Tricks of the Trade,", *Emergency Medicine Clinics of North America*, vol. 26, no. 4, pp. 1001-1014, 2008.

[21] M. Bishop, R. Harrington and A. Tencer, "Force Applied During Tracheal Intubation", *Anesthesia & Analgesia*, vol. 74, no. 3, pp. 411-414, 1992.

[22] N. Givol, Y. Gershtansky, T. Halamish-Shani, S. Taicher, A. Perel and E. Segal, "Perianesthetic dental injuries: analysis of incident reports", *Journal of Clinical Anesthesia*, vol. 16, no. 3, pp. 173-176, 2004.

[23] M. Kaplan, C. Hagberg, D. Ward, A. Brambrink, A. Chhibber, T. Heidegger, L. Lozada, A. Ovassapian, D. Parsons, J. Ramsay, W. Wilhelm, B. Zwissler, H. Gerig, C. Hofstetter, S. Karan, N. Kreisler, R. Pousman, A. Thierbach, M. Wrobel and G. Berci, "Comparison of direct and video-assisted views of the larynx during routine intubation", *Journal of Clinical Anesthesia*, vol. 18, no. 5, pp. 357-362, 2006.

[24] M. J. L. Bucx, C. J. Snijders, R. T. M. V. A. N. Geel, C. Robers, H. V. A. N. D. E. Giessen, W. Erdmann, and T. Stijnen, "Forces acting on the maxillary incisor teeth during laryngoscopy using the Macintosh laryngoscope,", *Anaesthesia*, vol. 49, no. 12, pp. 1064–1070, 1994.

[25] C. Hagberg, R. Georgi and C. Krier, "Complications of managing the airway", *Best Practice & Research Clinical Anaesthesiology*, vol. 19, no. 4, pp. 641-659, 2005.

[26] R. Lee, A. van Zundert, R. Maassen, R. Willems, L. Beeke, J. Schaaper, J. van Dobbelsteen and P. Wieringa, "Forces Applied to the Maxillary Incisors During Video-Assisted Intubation", *Anesthesia & Analgesia*, vol. 108, no. 1, pp. 187-191, 2009.

[27] M. Carassiti, R. Zanzonico, S. Cecchini, S. Silvestri, R. Cataldo and F. Agro, "Force and pressure distribution using Macintosh and GlideScope laryngoscopes in normal and difficult airways: a manikin study", *British Journal of Anaesthesia*, vol. 108, no. 1, pp. 146-151, 2011.

[28] M. Malik, C. Maharaj, B. Harte and J. Laffey, "Comparison of Macintosh, Truview EVO2®, Glidescope®, and Airwayscope® laryngoscope use in patients with cervical spine immobilization", *British Journal of Anaesthesia*, vol. 101, no. 5, pp. 723-730, 2008.

[29] T. Mort and B. Braffett, "Conventional Versus Video Laryngoscopy for Tracheal Tube Exchange", *Anesthesia & Analgesia*, vol. 121, no. 2, pp. 440-448, 2015.

[30] J. McElwain and J. Laffey, "Comparison of the C-MAC(R), Airtraq(R), and Macintosh laryngoscopes in patients undergoing tracheal intubation with cervical spine immobilization", *British Journal of Anaesthesia*, vol. 107, no. 2, pp. 258-264, 2011.

[31] E. Marshall, E. O'Loughlin and A. Swann, "First comparison of the Venner TM A.P. Advance TM versus the Macintosh laryngoscope for intubations by non-anaesthetists: A manikin study", *Emerg Med Australas*, vol. 26, no. 3, pp. 262-267, 2014.

[32] E. Burdett, D. Ross-Anderson, J. Makepeace, P. Bassett, S. Clarke and V. Mitchell, "Randomized controlled trial of the A.P. Advance, McGrath, and Macintosh laryngoscopes in normal and difficult intubation scenarios: a manikin study", *British Journal of Anaesthesia*, vol. 107, no. 6, pp. 983-988, 2011.

[33] K. Hasegawa, K. Shigemitsu, Y. Hagiwara, T. Chiba, H. Watase, C. Brown and D. Brown, "Association Between Repeated Intubation Attempts and Adverse Events in Emergency Departments: An Analysis of a Multicenter Prospective Observational Study", *Annals of Emergency Medicine*, vol. 60, no. 6, pp. 749-754.e2, 2012.

[34] Mort, Thomas C. "Emergency Tracheal Intubation: Complications Associated With Repeated Laryngoscopic Attempts". *Anesthesia & Analgesia*, 607-613, 2004.

[35] K. Schebesta, M. Hüpfl, B. Rössler, H. Ringl, M. Müller and O. Kimberger, "Degrees of Reality", *Anesthesiology*, vol. 116, no. 6, pp. 1204-1209, 2012.

[36] R. Marks, R. Hancock and P. Charters, "An analysis of laryngoscope blade shape and design: new criteria for laryngoscope evaluation", *Can J Anaesth*, vol. 40, no. 3, pp. 262-270, 1993.

[37] I. Z. Yardeni, A. Gefen, V. Smolyarenko, A. Zeidel, and B. Beilin, "Design evaluation of commonly used rigid and levering laryngoscope blades," *Acta Anaesthesiologica Scandinavica*, vol. 46, no. 8, pp. 1003–1009, Sep. 2002.

[38] R. M. Levitan and E. A. Ochroch, "Explaining the variable effect on laryngeal view obtained with the McCoy laryngoscope," *Anaesthesia*, vol. 54, no. 6, pp. 599–601, Jun. 1999.

[39] J. P. Tuckey, T. M. Cook, and C. A. Render, "An evaluation of the levering laryngoscope," *Anaesthesia*, vol. 51, no. 1, pp. 71–73, Jan. 1996.

[40] T. Uchida, Y. Hikawa, Y. Saito, and K. Yasuda, "The McCoy levering laryngoscope in patients with limited neck extension," *Canadian Journal of Anaesthesia*, vol. 44, no. 6, pp. 674–676, Jun. 1997.

[41] S. Uzun, İ. A. Erden, A. G. Pamuk, K. Yavuz, S. Çekirge, and Ü. Aypar, "Comparison of Flexiblade™ and Macintosh laryngoscopes: Cervical extension angles during orotracheal intubation," *Anaesthesia*, vol. 65, no. 7, pp. 692–696, May 2010.

[42] M. El-Orbany, "Laryngeal exposure using the Flexiblade™Laryngoscope," *Anesthesia & Analgesia*, vol. 103, no. 5, pp. 1330–1331, Nov. 2006.

[43] S. S. Balli and S. Chand, "Transmission angle in mechanisms (triangle in mech)," *Mechanism and Machine Theory*, vol. 37, no. 2, pp. 175–195, Feb. 2002.

[44] R. Krage, C. van Rijn, D. van Groeningen, S. A. Loer, L. A. Schwarte, and P. Schober, "Cormack-Lehane classification revisited," *British Journal of Anaesthesia*, vol. 105, no. 2, pp. 220–227, Jun. 2010.

[45] C. Hagberg and J. Benumof, *Benumof and Hagberg's airway management*. Philadelphia, PA: Elsevier/Saunders, 2013.

[46] "What is airway management? | Difficult Airway Society", *Das.uk.com*, 2016. [Online]. Available: https://www.das.uk.com/content/patient_info/what_is_airway_management.

[47] "vocal cords", *TheFreeDictionary.com*, 2016. [Online]. Available: http://medical-dictionary.thefreedictionary.com/vocal+cords.

[48] "Endotracheal tube having a beveled tip and orientation indicator", *Patft.uspto.gov*, 2016. [Online]. Available: http://patft.uspto.gov/netacgi/nph-Parser?patentnumber=6378523.

[49] R. Malones, "Patients with Endotracheal Tube – Nursing Roles, Management & Procedure", *Nursing Journal*, 2015. [Online]. Available: http://rnspeak.com/nursing-skills/endotracheal-intubation-nursing-roles-management-procedure/.

[50] "Airwaycam | Airway Cam - Airway Management Education and Training Products", *Airwaycam.com*, 2016. [Online]. Available: http://www.airwaycam.com/.

[51] "Miller Fiber Optic Laryngoscope Blade", *Proppermfg.com*, 2016. [Online]. Available: https://www.proppermfg.com/miller-fiber-optic-laryngoscope-blade-1192.html.

[52] R. Lieutenant Colonel Jeffrey V Rosenfeld, "Joint Health Command", *Defence.gov.au*, 2016. [Online].Available:http://www.defence.gov.au/health/infocentre/journals/ADFHJ_Dec08/ADFHealth_9_2_79.html.

[54] Patil-Syracuse Adjustable Laryngoscope Handle", *Bellmedical.com*, 2016. [Online]. Available: https://bellmedical.com/patil-syracuse-adjustable-laryngoscope-handle.

[55] *Cursoenarm.net*, 2016. [Online]. Available: http://cursoenarm.net/UPTODATE/contents/mobipreview.htm?23/30/24037.

[56] F. Adnet, S. Borron, S. Racine, J. Clemessy, J. Fournier, P. Plaisance and C. Lapandry, "The Intubation Difficulty Scale (IDS)", *Anesthesiology*, vol. 87, no. 6, pp. 1290-1297, 1997.

[57] Kit, T. 2, S. Manager, S. Breakout, W. Kit, P. 110mAh, S. Kit, S. White Tri-Color LED Strip - Addressable and S. Kit, "SparkFun Electronics", *Sparkfun.com*, 2016. [Online]. Available: http://www.sparkfun.com.

[58] "Arduino - Home", *Arduino.cc*, 2016. [Online]. Available: http://www.arduino.cc.

[59] [Online]. Available: http://www.7-sigma.com.

[60] [Online]. Available: http://www.sensorprod.com/pressurex_micro.php

[61] A. Erdman and G. Sandor, *Advanced mechanism design*. Englewood Cliffs, NJ: Prentice-Hall, 1984.

[62] A. Erdman, G. Sandor and S. Kota, *Mechanism design*. Upper Saddle River, N.J.: Prentice-Hall, 2001.

[63] "3D Printing Solutions | Stratasys", *Stratasys.com*, 2016. [Online]. Available: http://www.stratasys.com. [Accessed: 07- Jul- 2016].

[64] "McMaster-Carr", *Mcmaster.com*, 2016. [Online]. Available: http://www.mcmaster.com/.

[65] "Home", *Fujifilm Global*, 2016. [Online]. Available: http://www.fujifilm.com/.

[66] "joint - Symphyses | skeleton", *Encyclopedia Britannica*, 2016. [Online]. Available: https://www.britannica.com/science/joint-skeleton/Symphyses#ref470992.

[67] "desaturation", *TheFreeDictionary.com*, 2016. [Online]. Available: http://medical-dictionary.thefreedictionary.com/desaturation.